THESIS

PHYSIOLOGICAL RESPONSE OF THE CYANOBACTERIUM *SYNECHOCYSTIS SP*. PCC 6803 TO FLUCTUATING LIGHT

Submitted by

Matthew Thomas Youngblood

Department of Biology

In partial fulfillment of the requirements

For the Degree of Master of Science

Colorado State University

Fort Collins, Colorado

Summer 2015

Master's Committee:

Advisor: Graham Peers

Christie Peebles
Marinus Pilon

ABSTRACT

PHYSIOLOGICAL RESPONSE OF THE CYANOBACTERIUM *SYNECHOCYSTIS SP*. PCC 6803 TO FLUCTUATING LIGHT

Photosynthetic microbes are a promising feedstock for renewable biofuels, but the yields of industrial cultivation systems will need significant improvements if they are to be economically viable and succeed. One particular challenge faced by photosynthetic microbes in commercial production systems is the highly dynamic light environment created by vertical mixing within dense cultures. Rapid changes in light intensity make it difficult for these microbes to acclimate and utilize the available light efficiently. Attempts to identify targets for genetically improving photosynthetic microbes to flourish in these environments are hampered by a poor understanding of the physiological response to fluctuating light.

My thesis is focused on developing our fundamental understanding of the photophysiology and acclimation responses associated with light environments in industrial conditions. The aim is to eventually increase areal productivity in industrial cultivation systems by applying insights from physiological characterization into future strain engineering approaches.

The first chapter introduces the issues associated with industrial cultivation of photosynthetic microbes. I present some background on the need for biofuels, why there has been a focus on using photosynthetic microbes as a feedstock, and how photosynthetic microbes are cultivated industrially. I then present some of the physiological challenges faced by photosynthetic organisms in industrial cultivation, with particular focus on the challenge of a

dynamic light environments. I give a brief background on photosynthesis to explain some of the acclimation responses that can be altered in a fluctuating light environment.

Chapter 2 presents a proteomic and physiological comparison of the cyanobacterium *Synechocystis sp*. PCC6803 cultivated in a fluctuating light environment (30s light on/off) to a continuous light environment which had the same average photon flux density. We found that cultures in fluctuating light grew at half the exponential growth rate of continuous light cultures. Reduced growth did not appear to be due to photo-oxidative stress, as we detected reduced levels of reactive oxygen species and oxidative-stress responsive proteins in fluctuating light. We show evidence that reduced growth could be due to a partial shift to a respiratory state in fluctuating light. Reduced growth could also be due to increased dissipation of electrons, as suggested by the higher capacity for photosynthesis at light levels from 106-174 μmol photon m^{-2} s^{-1}. We found other surprising changes such as increases in some carbon concentration mechanism components and decreases in some others. These components were thought to be regulated by a similar mechanism due to their co-expression in high CO_2 to ambient CO_2 shift experiments. This suggesting some unusual signaling is occurring due to the fluctuating light. We also found a number of hypothetical and poorly characterized proteins were significantly different in fluctuating and continuous light.

In the appendix, I present the preliminary characterization of slr1719, a poorly characterized protein identified in the proteomic analysis of fluctuating and continuous light. This study generated a knock out of slr1719. We found that the Δslr1719 strain compared to a control strain grew much slower in low CO_2 conditions in saturating and sub saturating light conditions. However in replete CO_2 conditions, there was no difference in growth rate, regardless of light intensity tested in Δslr1719 versus the control. We argue that this finding, paired with evidence

from the literature, suggests slr1719 may participate in cyclic electron flow. Other roles suggested by the literature for this protein could have important roles in the acclimation to fluctuating light, and warrant further study.

ACKNOWLEDGEMENTS

I would like to thank my advisor Graham Peers and my committee members Christie Peebles and Marinus Pilon for their incredible patience, support and excellent scientific advice throughout this process. You all went above and beyond the call of duty in supporting me. I would also like to thank all the members of the Peers lab and in particular Mike Caballero, Michael Cantrell, Denis Jallet, and Nate Sindt for all their guidance, ideas, and support during data collection and editing of my thesis. Without their camaraderie I would not have been able to finish.

Chapter 2 would not have been possible without the sample preparation for proteomics by Mike Caballero, and proteomic data collection and processing by our collaborators Seijin Park and Ken Reardon. I would like to thank Lauren Cole for her help in data collection characterizing the slr1719 protein covered in the appendix. Her work was funded by the Colorado Center for Biorefining and Bioproducts (C2B2) NSF-REU fellowship (Research Experience for Undergraduates).

This project was funded by the National Science Foundation's Emerging Frontiers in Research and Innovation (NSF-EFRI) grant. My studies were additionally funded by the MAS bioenergy NSF-IGERT grant, and the Program for Molecular Plant Biology at Colorado State University.

Lastly, I would like to thank my friends and family for their unconditional love and support through this process. I have been so humbled by the outpouring of love you have given me.

TABLE OF CONTENTS

ABSTRACT ii

ACKNOWLEDGMENTS v

TABLE OF CONTENTS vi

CHAPTER 1: INTRODUCTION: BIOFUELS FROM PHOTOSYNTHETIC MICROBES, AND THE CHALLENGE OF CULTIVATION IN INDUSTRIAL CONDITONS 1

CHAPTER 2: PROTEOMIC AND PHOTOPHYSIOLOGICAL COMPARISON OF SYNECHOCYSTIS CULTURES ACCLIMATED TO CONTINUOUS VERSUS FLUCTUATING LIGHT 10

APPENDIX: ADDITIONAL OBSERVATIONS ABOUT SLR1719 97

CHAPTER 1:

INTRODUCTION: BIOFUELS FROM PHOTOSYNTHETIC MICROBES, AND THE CHALLENGE OF CULTIVATION IN INDUSTRIAL CONDITONS

Modern civilization is dependent on fossil fuel [1]. Despite recent advances in energy efficiency, the demand for fossil fuel energy has continued to increase [2]. As conventional oil reserves have started to decline, the petroleum industry has increasingly turned to using unconventional sources of oil such as hydraulic fracturing, shale oil and deep water drilling to meet demands [2, 3]. While these unconventional sources of oil stave off the reduction in fossil fuel supply, they come at a significant environmental cost [3]. An increased "energy return on investment" (EROI), meaning a reduced extraction of energy for the energy required to access a resource, paired with increased greenhouse gas production and water and land use requirements of these unconventional technologies result in greater environmental damage [4].

Various biofuel strategies have been proposed to meet the ever increasing energy demand in a way that minimizes environmental impact. So called "first-generation" biofuels, which use traditional crops like corn and soybeans to provide sugars for fermentation or oil for conversion into diesel, respectively, have been criticized for their limited greenhouse gas reduction and their use of land in a time when arable land for food production is becoming scarce [5]. As a response, a "second-generation" wave of technology has emerged to develop feedstock crops that can grow on marginal land, and to find ways to use the cellulosic portion of crops, so that agricultural waste can be used as a feedstock [6]. Although this is an improvement, the low areal yields of

second generation feedstocks makes complete replacement of the nations oil supply with biofuels impractical [7].

The use of photosynthetic microbes to produce biofuels has been proposed as a part of the so called “third generation” or “next-generation” wave of technology [7]. Photosynthetic microbes have several distinct advantages over land plants. They have higher predicted areal yields and algal ponds can be sited on low quality land [7]. An additional advantage of photosynthetic microbes over land plants is the relative ease and speed of genetically engineering them [8]. This allows faster strain engineering, but also makes complicated pathway development possible. For example *Synechocystis sp.* PCC6803 has been engineered to produce entirely new biofuel molecules such as isobutanol [9].

1. Cultivation of photosynthetic microbes for biofuels

Like plants, photosynthetic microbes utilize light energy to fix CO_2 into biomass. They are cultivated to a high density in open ponds or enclosed photobioreactors, and then harvested to extract a molecule of interest made by the microbes. Many photosynthetic microbes principally store their energy in the form of free lipids. These can be extracted and converted into biodiesels through trans-esterification [10]. However, because photosynthetic microbes can be rapidly genetically modified, there have been many other attempts to engineer them to produce drop in biofuels like isobutanol, and isoprene [11], a precursor to a broader class of molecules, isoprenoids, which have been suggested to be promising for biofuels [12].

A recent cost analysis of industrial cultivation strategies found that three aspects of cultivation had the largest bearing on final cost: areal biomass productivity, lipid content, and extraction efficiency [13]. While all of these are critical to the viability of biofuel strategies, my project is oriented towards increasing areal biomass productivity.

2. Improving photosynthetic productivity in industrial cultivation systems

Several aspects of industrial cultivation systems present unique challenges to improving biomass yields of photosynthetic microbes. Unlike controlled lab environments, where most research has been conducted, photosynthetic microbes in industrial ponds face a highly dynamic environment which can lower productivity in a variety of ways [14]. Seasonal and daily oscillations in temperature make it difficult to achieve optimal productivity [15, 16]. Photosynthetic microbes must also face competition/predation not faced in axenic lab cultures with controlled environments. Competition/predation can come from external sources of contamination [17], but genetically engineered strains can also genetically revert to a wild type form which can potentially outcompete the engineered strain [18].

Photosynthetic microbes in industrial cultivation systems also face variable light conditions not faced in most lab conditions. This consists of daily changes in solar irradiance and sporadic reductions in light intensity from cloud cover on the time scale of minutes to hours [19]. Additionally, vertical mixing throughout the water column can lead to fluctuations in light intensity on the scale of seconds (See Chapter 2 introduction for further discussion of this).

Several studies have attempted to recreate fluctuating light regimes in the lab with similar time scales as those induced by vertical mixing. These studies have found a decrease in productivity compared to a control receiving the same average light intensity but in continuous light [20-22]. The reduced growth in these simulated environments suggest that reduced yields in industrial cultivation systems could in part be due to this dynamic light environment.

3. Challenges faced by dynamic light environments

In order to appreciate why changes in light intensity are difficult for photosynthetic microbes to face the reader requires a basic understanding of photosynthesis. I will present a brief overview of photosynthesis in the following paragraphs.

This photochemical energy conversion process starts when light-derived excitation energy is captured or transferred to the reaction center chlorophylls of photosystem II (P680) [23]. This generates a strong reducing species ($P680^{*}$) which rapidly transfers an electron to a primary acceptor, thus separating positive and negative charged species [23]. The liberated electrons are further separated through a series of rapid transfer events between enzymatic cofactors and ultimately donated one at a time to the plastoquinone pool to form a plastoquinol (requiting two electrons). P680 is re-reduced by electrons removed through the oxidation of water [23]. Plastoquinols donate their electrons to the cytochrome b_6f complex. This complex pumps protons into the lumen, creating a trans-thylakoid proton gradient, and donates electrons to the soluble redox carriers plastocyanin and cytochrome c_6 [23]. The soluble redox carriers in turn reduce oxidized PSI. Solar energy captured by PSI creates a strong reducing species P700* which, through a series of electron transfer events, is used to reduce ferredoxin [23]. Ferredoxin then donates electrons to $NADP^+$ via the ferredoxin:$NADP^+$ reductase complex [23]. The proton gradient generated through linear electron flow is harnessed by ATP synthase to phosphorylate ADP to ATP. ATP and NADPH generated through this process are then used for carbon fixation in the Calvin cycle [23].

Natural light levels can far exceed the capacity of photosynthesis and carbon fixation [24]. If this is unchecked, several reactive oxygen species can form, which can cause cellular damage (For details see discussion section of Chapter 2) [25]. To protect against this,

photosynthetic microorganisms have a variety of energy dissipation strategies. In *Synechocystis* this occurs at the level of photon capture through thermal dissipation by the organic carotenoid protein [26]. However, they can also short circuit electron transport in a process called Alternative Electron Transport (AET), which consists of a variety of routes to transfer electrons in the electron transport chain to oxygen to form water [27]. Because these electrons are ultimately derived from water via water-splitting in photosystem II, the resulting process forms a futile cycle designed to dissipate excess energy.

When *Synechocystis* is cultivated in dim light, studies have shown some energy dissipation pathways are not necessary [28] or are deactivated [29]. To maximize photon capture, cells increase their pigment content [30]. However, if cells are then transferred to high light, these pigment complexes are down regulated, and energy dissipation mechanisms become necessary to prevent photo-oxidative damage [31, 32]. An additional acclimation state can occur if cells are fully transferred to the dark or below the compensation point. In this situation they can undergo a transition from photo-autotrophic metabolism to respiratory metabolism, in which they catabolize storage molecules such as glycogen to generate energy [33].

In order to properly acclimate to an appropriate light level, cells respond to a variety of signals that ultimately result from transitions in light flux [31]. These signals include changes in the redox state [34], acidification of the lumen [35], alterations in the oxidation state of $NADP^+$/NADPH [36], or direct signaling of light by phytochromes [37]. Because many of these processes are not fully understood, it is challenging to predict how fluctuating light would impact these signals, and the cellular response to them. Considering the role that fluctuating light could be playing in biomass reduction in industrial cultivation systems [21], more work needs to be put into understanding the physiological impact of fluctuating light on photosynthetic microbes.

4. Thesis overview

This thesis is focused on developing our fundamental understanding of the photophysiology and acclimation responses associated with light environments in industrial conditions. The aim of this characterization is to eventually increase areal productivity in industrial cultivation systems by applying insights from physiological characterization into future strain engineering approaches.

In chapter two I present an experiment that compares the growth of the cyanobacterium *Synechocystis sp.* PCC6803 in fluctuating light to continuous light having the same average photon exposure. This study used proteomics paired with photo-physiology, growth rates, and measurements of reactive oxygen species to examine the response to fluctuating light. From this study we identified several hypothetical and poorly characterized proteins that were altered in fluctuating light. In the appendix, I present the preliminary characterization of one of these poorly characterized proteins, slr1719. This study generated a knock out of slr1719 and compared growth in different light intensities and CO_2 levels.

REFERENCES

[1] M. Hambourger, G.F. Moore, D.M. Kramer, D. Gust, A.L. Moore, T.A. Moore, Biology and technology for photochemical fuel production, Chemical Society Reviews, 38 (2009) 25-35.

[2] P.M. Jackson, L.K. Smith, Exploring the undulating plateau: the future of global oil supply, Philosophical Transactions of the Royal Society of London A: Mathematical, Physical and Engineering Sciences, 372 (2013).

[3] K.J. Chew, The future of oil: unconventional fossil fuels, Philosophical Transactions of the Royal Society of London A: Mathematical, Physical and Engineering Sciences, 372 (2013).

[4] C.A.S. Hall, J.G. Lambert, S.B. Balogh, EROI of different fuels and the implications for society, Energy Policy, 64 (2014) 141-152.

[5] M.Q. Wang, J. Han, Z. Haq, W.E. Tyner, M. Wu, A. Elgowainy, Energy and greenhouse gas emission effects of corn and cellulosic ethanol with technology improvements and land use changes, Biomass and Bioenergy, 35 (2011) 1885-1896.

[6] H. Eggert, M. Greaker, Promoting Second Generation Biofuels: Does the First Generation Pave the Road?, Energies, 7 (2014) 4430-4445.

[7] P.G. Stephenson, C.M. Moore, M.J. Terry, M.V. Zubkov, T.S. Bibby, Improving photosynthesis for algal biofuels: toward a green revolution, Trends in biotechnology, 29 (2011) 615-623.

[8] D.C. Ducat, J.C. Way, P.A. Silver, Engineering cyanobacteria to generate high-value products, Trends in biotechnology, 29 (2011) 95-103.

[9] A.M. Varman, Y. Xiao, H.B. Pakrasi, Y.J. Tang, Metabolic Engineering of Synechocystis sp. Strain PCC 6803 for Isobutanol Production, Applied and environmental microbiology, 79 (2013) 908-914.

[10] D.E. Robertson, S.A. Jacobson, F. Morgan, D. Berry, G.M. Church, N.B. Afeyan, A new dawn for industrial photosynthesis, Photosynthesis research, 107 (2011) 269-277.

[11] P. Lindberg, S. Park, A. Melis, Engineering a platform for photosynthetic isoprene production in cyanobacteria, using Synechocystis as the model organism, Metabolic engineering, 12 (2010) 70-79.

[12] R. Radakovits, R.E. Jinkerson, A. Darzins, M.C. Posewitz, Genetic engineering of algae for enhanced biofuel production, Eukaryotic cell, 9 (2010) 486-501.

[13] J.N. Rogers, J.N. Rosenberg, B.J. Guzman, V.H. Oh, L.E. Mimbela, A. Ghassemi, M.J. Betenbaugh, G.A. Oyler, M.D. Donohue, A critical analysis of paddlewheel-driven raceway ponds for algal biofuel production at commercial scales, Algal Research, 4 (2014) 76-88.

[14] J.U. Grobbelaar, Mass Production of Microalgae at Optimal Photosynthetic Rates, 2013.

[15] B. Tamburic, S. Guruprasad, D.T. Radford, M. Szabo, R.M. Lilley, A.W. Larkum, J.B. Franklin, D.M. Kramer, S.I. Blackburn, J.A. Raven, M. Schliep, P.J. Ralph, The effect of Diel temperature and light cycles on the growth of nannochloropsis oculata in a photobioreactor matrix, PloS one, 9 (2014) e86047.

[16] A. Sukenik, J. Beardall, J.C. Kromkamp, J. Kopecký, J. Masojídek, S.v. Bergeijk, S. Gabai, E. Shaham, A. Yamshon, Photosynthetic performance of outdoor Nannochloropsis mass cultures under a wide range of environmental conditions, Aquatic Microbial Ecology, 56 (2009).

[17] S.P. Fulbright, M.K. Dean, G. Wardle, P.J. Lammers, S. Chisholm, Molecular diagnostics for monitoring contaminants in algal cultivation, Algal Research, 4 (2014) 41-51.

[18] J.J. Bull, S. Collins, Algae for Biofuels: Will the Evolution of Weeds Limit the Enterprise?, Evolution, 66 (2012) 2983-2987.

[19] P. Walsh, L. Legendre, Photosynthesis of natural phytoplankton under high frequency light fluctuations simulating those induced by sea surface waves, Limnology and Oceanography, 28 (1983) 688-697.

[20] M. Janssen, T.C. Kuijpers, B. Veldhoen, M.B. Ternbach, J. Tramper, L.R. Mur, R.H. Wijffels, Specific growth rate of Chlamydomonas reinhardtii and Chlorella sorokiniana under medium duration light/dark cycles: 13–87 s, Journal of Biotechnology, 70 (1999) 323-333.

[21] H. Takache, J. Pruvost, H. Marec, Investigation of light/dark cycles effects on the photosynthetic growth of Chlamydomonas reinhardtii in conditions representative of photobioreactor cultivation, Algal Research, 8 (2015) 192-204.

[22] H. Wagner, T. Jakob, C. Wilhelm, Balancing the energy flow from captured light to biomass under fluctuating light conditions, The New phytologist, 169 (2006) 95-108.

[23] P.G. Falkowski, J.A. Raven, Aquatic Photosynthesis, 2nd ed., Princeton University Press, Princeton, 2007.

[24] K.K. Niyogi, Safety valves for photosynthesis, Current opinion in plant biology, 3 (2000) 455-460.

[25] Y. Nishiyama, S.I. Allakhverdiev, N. Murata, Protein synthesis is the primary target of reactive oxygen species in the photoinhibition of photosystem II, Physiol Plant, 142 (2011) 35-46.

[26] A. Wilson, G. Ajlani, J.-M. Verbavatz, I. Vass, C.A. Kerfeld, D. Kirilovsky, A Soluble Carotenoid Protein Involved in Phycobilisome-Related Energy Dissipation in Cyanobacteria, The Plant cell, 18 (2006) 992-1007.

[27] C.W. Mullineaux, Electron transport and light-harvesting switches in cyanobacteria, Frontiers in plant science, 5 (2014) 7.

[28] Y. Allahverdiyeva, H. Mustila, M. Ermakova, L. Bersanini, P. Richaud, G. Ajlani, N. Battchikova, L. Cournac, E.-M. Aro, Flavodiiron proteins Flv1 and Flv3 enable cyanobacterial growth and photosynthesis under fluctuating light, Proceedings of the National Academy of Sciences, 110 (2013) 4111-4116.

[29] M. Gwizdala, A. Wilson, A. Omairi-Nasser, D. Kirilovsky, Characterization of the Synechocystis PCC 6803 Fluorescence Recovery Protein involved in photoprotection, Biochimica et biophysica acta, 1827 (2013) 348-354.

[30] H.L. MacIntyre, T.M. Kana, T. Anning, R.J. Geider, Photoacclimation of Photosynthesis Irradiance Reponse Curves and Photosynthetic Pigments in Microalgae and Cyanobacteria, Journal of Phycology, 38 (2002) 17-38.

[31] M. Muramatsu, Y. Hihara, Acclimation to high-light conditions in cyanobacteria: from gene expression to physiological responses, Journal of plant research, 125 (2012) 11-39.

[32] C. Hackenberg, A. Engelhardt, H.C. Matthijs, F. Wittink, H. Bauwe, A. Kaplan, M. Hagemann, Photorespiratory 2-phosphoglycolate metabolism and photoreduction of O2 cooperate in high-light acclimation of Synechocystis sp. strain PCC 6803, Planta, 230 (2009) 625-637.

[33] S. Díaz-Troya, L. López-Maury, A.M. Sánchez-Riego, M. Roldán, F.J. Florencio, Redox Regulation of Glycogen Biosynthesis in the Cyanobacterium Synechocystis sp. PCC 6803: Analysis of the AGP and Glycogen Synthases, Molecular Plant, 7 (2014) 87-100.

[34] J. Guo, A.Y. Nguyen, Z. Dai, D. Su, M.J. Gaffrey, R.J. Moore, J.M. Jacobs, M.E. Monroe, R.D. Smith, D.W. Koppenaal, H.B. Pakrasi, W.-J. Qian, Proteome-wide Light/Dark Modulation of Thiol Oxidation in Cyanobacteria Revealed by Quantitative Site-Specific Redox Proteomics, Molecular & Cellular Proteomics, (2014).

[35] C.E. Bratt, P.O. Arvidsson, M. Carlsson, H.E. Akerlund, Regulation of violaxanthin de-epoxidase activity by pH and ascorbate concentration, Photosynthesis research, 45 (1995) 169-175.

[36] J.W. Cooley, W.F. Vermaas, Succinate dehydrogenase and other respiratory pathways in thylakoid membranes of Synechocystis sp. strain PCC 6803: capacity comparisons and physiological function, Journal of bacteriology, 183 (2001) 4251-4258.

[37] T. Lamparter, B. Esteban, J. Hughes, Phytochrome Cph1 from the cyanobacterium Synechocystis PCC6803, European Journal of Biochemistry, 268 (2001) 4720-4730.

CHAPTER 2:

PROTEOMIC AND PHOTOPHYSIOLOGICAL COMPARISON OF SYNECHOCYSTIS CULTURES ACCLIMATED TO CONTINUOUS VERSUS FLUCTUATING LIGHT

Summary

There is a societal need for new sources of energy that are renewable and reduce greenhouse gas emission, yet do not use arable cropland. Photosynthetic microbes have been recognized as a promising biofuel feedstock, but will require increases in areal yields at scale to be economically viable. One particular environmental stress experienced by photosynthetic microbes growing in industrial cultivation systems is the dynamic light environment created by vertical mixing within dense cultures. The dynamic light environment makes it difficult for photosynthetic microbes to efficiently acclimate, leading to reduced growth and light use efficiency. Although many photosynthetic microbes can be genetically engineered quickly compared to land plants, targets for genetic improvements are difficult to identify due to the poor understanding of physiology in fluctuating light.

This study uses a systems approach to explore how physiology is altered in fluctuating light by comparing growth in a fluctuating light regime (30s on/off) to a continuous light environment receiving the same average number of photons. Cultures acclimated to fluctuating light grew at a nearly half the exponential growth rate. We measured reactive oxygen species generation in the two conditions and found that there was a reduced level of reactive oxygen species in fluctuating light, suggesting this was not the reason for reduced growth. This observation was reinforced by the finding that proteins associated with photo-oxidative stress

were less abundant in fluctuating light. The reduced levels of reactive oxygen species may be due to the increased abundance of catalase.

Frequent light-dark transitions could be triggering some aspects of the photo-autotrophic/respiratory transition process, leading to inefficiencies as pathways become suppressed. We observed a reduction of the Calvin cycle enzyme phosphoribulokinase, increases in a glucose responsive operon, and an increase in the respiratory succinate dehydrogenase in fluctuating light. A lower F_v/F_m in fluctuating light compared to continuous light acclimated cultures could be due an increased electron flow to the plastoquinone pool during dark acclimation. Reduced growth could also be due to increased dissipation of electrons, as suggested by the higher capacity for photosynthesis at light levels from 106-174 μmol photon m^{-2} s^{-1}.

Separate components of the carbon concentration mechanism, which in previous studies have shown concerted changes after a shift from ambient to low CO_2, were found to have contrasting responses in fluctuating versus continuous light. Carboxysome shell proteins were more abundant in fluctuating light, but low carbon inducible NDH-1 subunits were less abundant in fluctuating light. These two components are likely regulated by separate signals, such as NADPH/$NADP^+$ oxidation state or the plastoquinone pool redox state that normally are correlated. However the differential abundance of these in fluctuating light suggests an unsual signaling environment is created by the oscillations in light level.

Other surprising changes, such as decreases in protein levels that may be associated with aspartate degradation in fluctuating light compared to continuous light, and changes in abundance of several hypothetical proteins are not understood. Overall this study highlights our

cursory understanding of the physiological and systems response to rapidly fluctuating light regimes.

1. Introduction

Photosynthetic microorganisms are an attractive feedstock for the production of biofuels as they can be grown on non-arable land, produce higher areal yields than land-crops, and compared to land-crops can be more readily genetically engineered [1, 2]. The cyanobacterium *Synechocystis sp.* PCC6803 (hereafter Synechocystis) in particular has a well developed set of tools available for genetic analysis and manipulation [3]. Synechocystis is naturally competent and genes can be replaced by transgenes through a process of homologous recombination [4, 5]. Ease of genetic manipulation paired with numerous transcriptomic, proteomic, and metabolic flux studies have led to an expansive knowledgebase. However, there is still a critical gap in our knowledgebase that is hindering the engineering and optimization of strains for biofuel production. Although the behavior of photosynthetic microrganisms in highly controlled environments is reasonably well known, how they respond to dynamic conditions such as changes in temperature, O_2 and CO_2 concentrations, and in particular fluctuations in light intensity is still poorly understood [6].

Photosynthetic microbes experience fluctuations in light intensity across a wide range of time scales in natural outdoor conditions as reviewed by Walsh and Legendre (1983) [7]. Long term changes occur through diel changes in light intensity [8]. Medium term changes (hours) occur from cloud cover [9] and in natural environments via slow tidal changes [10]. Although adaptations to these slower changes in light intensity are reasonably well understood [11], we still do not understand the effect of more rapid changes on the scale of seconds to minutes. The

study presented here explores the physiological impact of these faster fluctuations on Synechocystis by simulating those conditions with a 30s on/off light regime.

1.1 Short scale fluctuations

Fluctuations in light intensity on the order of seconds to minutes can result from vertical mixing in the water column [7, 12, 13]. Two aspects of industrial cultivation can enhance the magnitude and frequency of these light fluctuations beyond what is typically experienced in nature. 1) Industrial production cultures are cultivated at higher cellular densities than found in nature in order to maximize the biomass collected from a harvest [14]. This practice of dense cultivation results in a steep gradient of light absorption in the water column which causes microbes to experience a larger change in light intensity with even small amounts of mixing [15, 16]. 2) In industrial cultivation cultures are actively mixed to incorporate CO_2 into ponds [17]. While this practice is necessary to prevent CO_2 limitation, it also increases the rate at which photosynthetic microbes are mixed throughout the water column, leading to more rapid changes in light intensity.

Only a handful of studies have previously examined photosynthetic microbes in fluctuating light on the timescale of second to minutes. We highlight one of the most recent studies as a representation of recent models being considered to explain the response to fluctuating light.

1.1.1 Growth in fluctuating light

Views in the literature about how photosynthetic microbes are predicted to respond to fluctuating light vary widely. This is highlighted by a recent paper by Takache et al. (2015) which compared experimentally measured biomass accumulation rates in fluctuating light to predicted biomass accumulation rates in two extreme case models. One model called “full

integration" holds that the organism does not respond to the light fluctuations at all, and is able to integrate the photons absorbed during the light phase during the dark phase [18]. Thus the organism would grow as if in the total average light intensity. This model was used by Martínez et al. (2011) to generate growth rate predictions for a recently isolated species of *Synechocystis sp.* [19]. The other extreme case that Takache et al. (2015) compared results to is called "response without integration," which assumes that there is an instantaneous transition from photo-autotrophic to a respiratory mode of growth upon transition of light to dark or vice-versa [18].

Takache et al. examined cultures of *Chlamydomonas reinhardtii* in light fluctuating between 220μmol photons m^{-2} s^{-1} and darkness across a wide range of durations (from 0.5s on/off to 6 min on/off). They found that with fluctuations longer than 12s on/off, cultures had biomass accumulation rates that very closely matched the "response without integration" model. However for fluctuations shorter than 12s on/off the cells showed a partial integration of the light: accumulating biomass faster than would be predicted by the response without integration, but still not coming close to matching the predictions of the full integration model [18]. In assuming an instantaneous switch to respiration in the "response without integration" model, the authors incorporated a biomass consumption factor that lowered their predicted growth rates. Although their experimental results are fairly close to this predicted growth rate, it is possible that other things besides biomass consumption would reduced the growth rate by a similar degree. For example a reduced efficiency of light utilization caused by an increase in energy dissipation could be at play, as suggested by the following studies.

1.1.2 Mutations in energy dissipation pathways display phenotypes in fluctuating light

Several other studies in Synechocystis have found that deletion of proteins involved in energy dissipation result in unique phenotypes in fluctuating light, or in sudden light-dark transitions. For example Allahverdiyeva et al. (2013) found a reduction in growth in fluctuating light when the flavodiiron proteins flv1 and flv3 were knocked out [20]. These proteins are able to short circuit the usual route of electron flow from PSI to the Calvin cycle by reducing O_2 to H_2O (without generating reactive oxygen species intermediates) using electrons from NADPH [20, 21]. This creates a futile cycle where electrons derived from water splitting at PSII are transferred to PSI and NADPH, and then ultimately are transferred back to water. Allahverdiyeva et al. found that in mutant lines with flv1 and flv3 knocked out, there was almost no growth in light fluctuating between 20 and 500 μmol photons m^{-2} s^{-1} for 5 minutes/30s, but robust growth in the WT control. In constant light at 50 μmol photons m^{-2} s^{-1} there was no difference in growth rate between the mutants and the WT. When the background illumination in fluctuating light was increased from 20 to 50 μmol photons m^{-2} s^{-1}, the mutants showed some growth (although still reduced when compared to WT). This suggests it is not only the duration of fluctuations but how dark the cultures become in between high light periods that effects growth. Thus, the reduction in growth rate in flv1/3 deletion mutants suggests this pathway for energy dissipation is involved in the response to fluctuating light.

Another route of energy dissipation is at the level of light energy harvesting. In cyanobacteria this occurs through a protein called the orange carotenoid protein (OCP). The OCP is activated by intense light in the blue spectrum, and once activated thermally dissipates a large fraction of captured photons [22]. In the patent filed by Peers (2015), he found that Synechocystis cultures accumulated more biomass in natural light, or in an artificially created

fluctuating light environment if components of the OCP were knocked out [23]. The fluctuating light environment had a background of 50 μmol photons m^{-2} s^{-1} with flashes of 2000 μmol photons m^{-2} s^{-1} every 2 minutes, which were programed to randomly last somewhere between 10s and 1 min [23]. This suggests that in WT cultures, the OCP is being activated with fluctuating light. Because deletion of OCP increases productivity in natural light and in fluctuating light, this suggests that in some cases the energy dissipation pathways employed in fluctuating light can limit growth.

Overall, these studies indicate that fluctuating light can limit growth, but the mechanism behind this is still poorly understood. A switch to respiration during dark periods, an increase in energy dissipation, or perhaps some other mechanism could be causing the reduced growth. To improve biomass yields in fluctuating light, targets similar to OCP need to be identified. However, a poor understanding of the physiological response to fluctuating light makes it difficult to identify new genetic targets. To address the knowledge-gap that exists for the response of photosynthetic microbes to fluctuating light, we conducted a study in the model cyanobacterium Synechocystis comparing growth in continuous light (100 μmol photons m^{-2} s^{-1}) to fluctuating light (200 μmol photons m^{-2} s^{-1} 30s on/ 30s off). The continuous light level was chosen so that both conditions would received the same average number of photons, but in different doses. Changes in cell density were monitored throughout and in late exponential growth, cells were harvested and assayed for proteomics, reactive oxygen species, and photophysiology. We found a reduced growth rate in the fluctuating light condition, and used a combination of proteomics and physiological data to explore a variety of possible causes. The evidence presented here suggests reduced growth rate is not due to photo-oxidative stress, but could be related to increased electron dissipation or dysregulation of respiratory/

photoautotrophic pathways caused by the frequent light/dark transitions. A number of other unusual findings in the physiological response are noted.

2. Materials and Methods

2.1 Culturing methods

Synechocystis cultures were grown in 900ml of BG-11 media in glass Roux flasks. Sampling port and air supply were provided by a custom made stopper constructed as follows: A standard size 5 silicone stopper (EW-06298-10 Cole-Parmer) had three holes bored into it with three tubes passing through made of PTFE 1/16in ID, 1/8in OD (06605-27 Cole-Parmer). One tube (~30cm long) was for sampling, and had a Clave Connector (ICU Medical) placed on top to provide a valve seal for sampling. The second tube (~30cm long) served as a bubbler by sealing the bottom end, and puncturing ~32 small slits with a 20G hypodermic needle. Care was taken to ensure that the slits were small enough to produce small bubbles, which aid in gas exchange with the media. The third tube was a shorter (~9cm) tube open at both ends for pressure release.

The cultures were bubbled with air filtered by a 0.45 μm polyethersulfone membrane (28145-505 VWR) at a volumetric flow rate of 1 liter of air per minute per liter of liquid culture as measured from the outlet. We found this air supply was sufficient to prevent changes in pH that could result from insufficient CO_2 supply for the photosynthetic consumption rate. The cultures were immersed in a clear plexiglass tank filled ~2/3rds with water and maintained at 30°C via a recirculating water bath (Fisher Scientific Isotemp 4100 R20). Roux flasks were held with a clamp stand at 45º angles to allow the bubbler to sit in the lower corner of the flask and evenly distribute air and prevent settling (Figure 1).

2.2 Growth Conditions

Two light regimes were applied to the cultures: continuous (100 μmol photons·m^{-2}·s^{-1}) and fluctuating (200 μmol photons·m^{-2}·s^{-1}, 30 s on/off cycles) with T5 cool-white fluorescent bulbs (GE Lighting). Light intensity was measured using a LICOR LI-250A light sensor at the center point between the two replicates in the "v" created between the two necks (Figure 1). Fluctuations in light were achieved by turning the power to the bulbs on and off every 30s using a digital recycle timer (Sentinel DRT-1). Light intensity was checked twice daily and bulbs were replaced if a bulb started flickering or losing intensity. Cultures were maintained in a semi-continuous manner by diluting them with fresh media before they reached stationary phase. Cultures were maintained in this way for at least 6 doublings before the start of the experiment.

2.3 Growth rates and harvest

Cell density was measured using a C6 BD Accuri flow cytometer. The flow cytometer was set to a flow rate of 14μl/min, and a core size of 10μm. For each determination 1 ml aliquots were measured for 90 seconds. Cell densities were natural log transformed and plotted against time in days to determine the exponential growth rate "k". This unit is the frequency of growing by a factor *e*, and can be used in the equation $f=i * e^{(k*t)}$ where f= final density, i= initial density, and t= time in days.

At a density of 16,000 cells·μl^{-1} ± 2,400 cells·μl^{-1}, which corresponded to late exponential growth phase, cells were harvested for proteomics, reactive oxygen species determination, and photophysiological assays.

2.4 Measurement of reactive oxide species

Reactive Oxygen Species (ROS) were measured using CellROX green (Invitrogen), a probe which has very little fluorescence in the reduced state but upon oxidation by ROS binds to DNA and exhibits bright green fluorescence with absorption/emission maxima of ~ 485/520 nm [24].

When cultures reached a density of 16,000 cells·μl^{-1} ± 2,400 cells·μl^{-1}, samples of the culture were collected, diluted 1:10 in 0.2μm filtered Millipore water in 1.5ml microcentrifuge tubes, and CellROX was added to a final concentration of 10μM. Samples were then either dark incubated or light incubated for 1 hour. For dark incubation, 3 technical replicates of a culture were placed in the dark at 30ºC for 20 minutes and then kept at ambient temperature in the dark for 40 minutes. For light incubation, three technical replicates were kept in a similar light regime as their growth condition for 20 minutes. This was achieved by floating the three technical replicates in the 30ºC water bath directly in front of the cultures, causing them to receive slightly higher light exposure than the cultures. For continuous light the samples received 118 μmol photons·m^{-2}·s^{-1}, for fluctuating light cultures the samples oscillated between 213 μmol photons·m^{-2}·s^{-1} and darkness in 30s intervals. After 20 minutes the light incubated samples were removed and held at ambient light and temperature for an additional 40 minutes. The relative amounts of ROS were quantified by measuring the fluorescence of the probe with a C6 BD Accuri flow cytometer at an emission and detection of 488nm and 533 ± 30 nm respectively. Samples were measured for 30 seconds at a flow rate of 14μl/min and a core size of 10μm. The mean fluorescence of the three technical replicates was averaged for each biological replicate. The values given in Table 1 are the difference in CellROX fluorescence after incubation in the light for 20 minutes and a control incubated in the dark for 20 minutes.

2.5 Chlorophyll fluorescence measurements

Chlorophyll fluorescence kinetics were measured using a Dual-PAM-100 (WALZ), and parameters were calculated using the equations described by Genty et al. (1989) [25]. Samples were prepared by collecting 5ml of culture, and adding 50µl of a 100mM $NaHCO_3$ solution for a final concentration of 1mM $NaHCO_3$ to provide the cells with inorganic carbon during the rapid light curve. Cells were then immediately placed in the dark and acclimated for 10 minutes. After dark acclimation, the cells were collected onto a 2µm pore glass fiber prefilter (Millipore AP2501300) to create an "artificial leaf" [26]. The filter was wrapped in a single layer of clear plastic wrap and clamped into the PAM's leaf clip. Two technical replicates were measured per culture and averaged together. All measurements were done within 1 hour of additional assays. Three biological replicates were measured for the continuous light cultures, and six biological replicates for the cultures cultivated under fluctuating light.

Chlorophyll fluorescence measurements were conducted using the light curve program of the WALZ Dual PAM (v1.11) software. After dark acclimation, a modulated beam was applied to determine the minimal fluorescence, F_o. This measurement assumes the plastoquinone pool is completely oxidized due to the dark acclimation, and all reaction centers are open. Then a saturating pulse of 10,000 µmol photons m^{-2} s^{-1} (λ=635nm) was delivered for 500ms to measure the F_m or maximum fluorescence yield. F_m assumes that any non-photochemical quenching mechanism are relaxed because of the dark acclimation. Using these measurements, we calculated the $F_v/F_m = (F_m-F_o)/F_m$, where F_v is the variable fluorescence.

Following the F_v/F_m determination, a rapid light curve was used to estimate the effective quantum yield, $YII=(F_m'-F)/ F_m'$ at several light intensities, where F_m' is the maximum quantum yield measured during a saturating pulse of cells acclimated to a given light intensity. F is the

fluorescence yield produced by the measuring light at that light intensity. Over the course of 5 minutes (in 30s intervals) an actinic light (λ=635nm) was applied with following intensities in μmol photons·m^{-2}·s^{-1} increasing step wise: 64, 71, 78, 106, 140, 174, 256, 390, 590, 908. After 30s of acclimation to a given actinic light, a saturating pulse was delivered to calculate F_m'. The measuring light used had a wavelength of 620nm, and an intensity of 64 μmol photons·m^{-2}·s^{-1} (intensity setting 10, block frequency MF-low 20, MF-high 10000).

2.6 Peptide Preparation

At harvest, cultures were centrifuged at 15,000 rcf for 300s at 4 °C. The supernatant was decanted, and cell pellets were massed. The cell pellets were resuspended 1:3 (μg:μl) in lysis buffer containing 50 mM TEAB (triethylammonium bicarbonate) and 2% SDS (sodium dodecyl sulfate). The cell suspension was sonicated three times with 15 s pulse, 60 s rest cycles (550 Sonic Dismembrator, Fisher Scientific). Centrifugation (15,000 rcf, 300 s, 4 °C) pelleted out cell debris. 1 ml of pre-chilled acetone was added to 200 μl of lysate, the sample was mixed gently, and incubated at -20 °C for 3 hours. Precipitated proteins were collected by centrifugation at 15,000 rcf for 300 s at 4 °C. The acetone was removed and the protein pellet was air-dried for 5 minutes. Then the pellet was reconstituted in 100 μl of 50 mM TEAB with limited water-bath sonication. Insoluble material was separated by centrifugation at 15,000 rcf for 300 s at 4 °C. Soluble protein was estimated with the BCA protein assay (Thermo Fisher Scientific). After determining the protein concentrations for each supernatant (Approximately 3.5-16 μg/μl), 20 μg of protein were brought to equal volumes with 50 mM TEAB and 10% (v/v) acetonitrile. Dithiothreitol (Thermo Fisher Scientific) and iodoacetamide (Thermo Fisher Scientific) added according to manufacturer's protocols. 1 μg Trypsin Gold (Promega) was added and allowed to digest overnight at 37 °C. Samples were then frozen at -80ºC until analysis.

2.7 LC/MS/MS Analysis

One μg of tryptic digest was loaded onto a column (C18, 75 μm ID, 150 mm length, 120 A, Eksigent Technologies) using NanoLC-Ultra-2D (Eksigent Technologies). A 2%~80% acetonitrile gradient with 0.1% formic acid (flow rate: 300 nL/min) was used for separation. Tandem MS (tripleTOF 5600, ABSciex) ran in data-dependent mode, in which the 50 most intense ions were selected for tandem MS. Default rolling collision energy was applied on mass and charge accordingly. The acquisition times of MS and tandem MS were 50 s and 20 s in the range of 400 ~ 1,800 *m/z*, respectively. The temperature of the interface was 120 °C and the electrospray voltage was 2,400 V.

2.8 Protein Identification, Label-free Quantification, and Statistical Analysis

Acquired MS data were converted into mzML format and used for protein identification followed by label-free quantification using PEAK 7.0 (BSI) software. PEAK 7.0 searched both MS and tandem MS spectra against the *Synechocystis* sp. PCC6803 database consisting of 3,672 protein entries (http://genome.kazusa.or.jp/cyanobase/Synechocystis). The following search parameters were used in the protein identification; 30 ppm of precursor mass error tolerance; 0.1 Da of fragment mass error; partial tryptic enzyme restraint; maximum of one missed tryptic cleavages; fixed carbamidomethylation of cysteine; variable oxidation of methionine; 1 % of false discovery rate (FDR). Peptide peak alignment and normalization was performed using the built-in algorithm of the PEAK 7.0 software (BSI). Ion intensities of corresponding peptides were compared for the label-free quantitation of proteins. Quantified values between light conditions were compared using a student's t-test (two-sample, assuming unequal variance) and filtered for significant differences ($p>0.05$ or $0.05\geq p>0.1$).

3. Results

3.1 Growth rate and reactive oxygen species are reduced in fluctuating light

The fluctuating light regime had a significantly reduced exponential growth rate when compared to continuous light ($p<0.05$ Table 1), despite receiving the same average number of photons. One possible cause of a reduced growth rate is the presence of more reactive oxygen species, which can lead to damage of the photosynthetic machinery and an increased metabolic demand to repair damaged proteins [27, 28]. To test if ROS levels were altered between cultures the intracellular dye CellROX green was used. Less CellROX fluorescence was detected in the fluctuating light cultures than the continuous light cultures in both the dark controls and the light incubated samples, indicating the fluctuating light regime results in lower reactive oxygen species levels (Table 1).

3.2 Photosynthetic capacity is lower after dark acclimation in fluctuating light, but increases at physiologically relevant light levels

Another possible cause of reduced growth rate is a reduced photosynthetic capacity. To test for this we measured the quantum yield of photosystem II in both cultures over the course of a rapid light curve (Figure 2). The first point on this curve was taken after 10 minutes of dark acclimation and represents the maximum quantum yield of photosystem II (F_v/F_m). The cultures cultivated in fluctuating light had a lower F_v/F_m than the continuous light cultures indicating a reduced maximal capacity for photosynthesis (Figure 2, Table 1). However, when we looked at the effective quantum yield (YII) across the rapid light curve spanning 64 to 908 μmol photons m^{-2} s^{-1} we saw a significant increase in YII in the fluctuating light condition at light intensities of 106, 140 and 174 μmol photons m^{-2} s^{-1}. This suggests that at the physiologically relevant light levels, the fluctuating light cultures actually have a higher capacity for photosynthesis.

3.3 Abundance of proteins in fluctuating and continuous light

Two biological replicates of cultures cultivated in each light condition, fluctuating or continuous, were harvested for proteomic analysis. The proteome of each biological replicate was measured in technical duplicate using shotgun proteomics. In total, 1066 proteins were identified with a peptide significance score $p<0.05$ (Figure 3). This represents a coverage of 34.8% of the hypothetical proteome. Other studies have been able to achieve a slightly higher coverage of 40-55% by using techniques such as fractionation, and using a specially designed long (65cm) reverse phase column [29]. Many of the membrane-bound proteins, which include many important elements of the photosynthetic apparatus, are underrepresented in proteomics [29, 30]. To estimate what percentage of our proteome was membrane bound, we used the online tool SOSUI which is described as a tool for the "classification and secondary structure prediction system for membrane proteins" (http://bp.nuap.nagoya-u.ac.jp/sosui) [31]. Running the entire predicted proteome of Synechocystis on SOSUI estimated 25.0% of proteins were membrane bound. Our data set was predicted to have 17.2% membrane bound proteins, suggesting a bias in our extraction technique against membrane proteins.

Of the 1066 total identified proteins, 582 were identified in both conditions, and 97 were significantly different ($p<0.1$) between the two conditions (Figure 3). The relative abundance of significantly different proteins ($p<0.05$) are listed in Table 2, and those that were significantly different using p values between 0.05 and 0.1 are listed in Supplementary Table 1. We found many proteins with similar functions and following similar trends with both the $p<0.05$ significance cutoff (Table 2) and with the expanded significance cut off using a p value between 0.05 and 0.1 (Supplementary Table 2), and therefore draw from both in our analysis.

Among proteins showing a significant difference, the majority of them (64/97) were less abundant in fluctuating light (Table 2, and Supplementary Table 1). We observed changes in several different clusters of proteins having a concerted function. For example we found several stress response proteins were less abundant in fluctuating light. Ribosomal proteins, and proteins involved in transcription/translation were also less abundant in fluctuating light. Several proteins involved in the NDH-1 complex were less abundant in fluctuating light. Proteins related to photosynthesis were in general less abundant as well. Additionally our analysis found significant differences in a large number of hypothetical or poorly characterized proteins. About half of the uncharacterized/hypothetical proteins were more abundant in fluctuating compared to continuous light.

Overall we found profound physiological changes in fluctuating light compared to continuous light. The growth rate was half the rate in continuous light. There were reduced levels of reactive oxygen species, a lower F_v/F_m, yet an increased capacity for photosynthesis at growth light levels, as indicated by the increased YII at these intensities. Adding to the diversity of this physiological response, we found close to 100 proteins of known and unknown function in several categories to be significantly different between the two conditions.

4. Discussion

This experiment sought to interrogate how the physiology of the cyanobacterium Synechocystis is altered when cultivated under a fluctuating light regime by using a combination of physiology and proteomics. We compared growth in a light regime of 200 μmol photons m^{-2} s^{-1} 30s on/ 30s off to a control culture growing in 100 μmol photons m^{-2} s^{-1}. Although this is likely a simplistic approximation of what photosynthetic microbes experience in an industrial scale raceway pond, the diverse physiological response suggest we still have much

to learn form this approximation. The state of the art technology used to predict the light regime experienced by photosynthetic microbes is the use of computational fluid dynamics (CFD) to model movement within a pond or photobioreactor. Although there have been several recent studies using CFD to model light fluctuations in tubular bioreactors or small scale raceway ponds [32, 33], so far none have estimated the light regime for large scale raceway ponds like those used in commercial endeavors.

4.1 Fluctuating light halves the growth rate

We observed that cultures in fluctuating light grew at half the rate of continuous light cultures, despite receiving the same number of photons (Table 1). As noted in the introduction, a similar reduction in growth was noted by Takache et al. (2015) and additionally by Janssen et al.(1999) in the green alga *Chlamydomonas* in fluctuating light [18, 34]. Although these studies found a reduction in growth, the mechanisms involved are not described. Several hypotheses could explain our observation of reduced growth in fluctuating light: Increased photo-oxidative damage [27], reduced efficiency of the Calvin cycle from frequent activation/deactivation [35], increased dissipation of photons [36], or increased dissipation of the electron transport chain [20]. Our physiology and proteomic dataset provides us the ability to consider all of these diverse hypothesies, however with the caveat that more directed physiology would be required for diffinitive proof.

4.2 Reduced reactive oxygen species abundance and proteins involved in photo-oxidative damage in fluctuating light compared to continuous light

One hypothesis for the decline in growth rate is that fluctuating light leads to the generation of more reactive oxygen species. Reactive oxygen species can lead to a decline in photosynthetic efficiency and an increased metabolic burden for the cells [28] which can slow

growth if reactive oxygen species are not detoxified [27]. There are several types of reactive oxygen species, and their production is an inevitable part of oxygenic photosynthesis. Singlet oxygen ($^1O_2$) is produced when photosensitized chlorophyll transfers energy to oxygen [37]. Another source of reactive oxygen species is through the Mehler reaction, which is caused by the transfer of electrons from PSI to oxygen rather than ferredoxin. This produces the extremely reactive superoxide anion (O_2^-) which can be converted into H_2O_2 and hydroxyl radical OH•. There is some debate about how common the Mehler reaction is in Synechocystis, given that the flavodiiron proteins are able to catalyze the same reaction without generating H_2O_2 [38]. Production of reactive oxygen species can be enhanced by the secondary effects of high light, such as the reduction of the PQ pool [39] or by acceptor side limitation of PSI, such as an inactive Calvin cycle [40]. Therefore, we hypothesized that the bursts of high photon flux in fluctuating light could lead to a reduced PQ pool or acceptor side limitation of PSI which could lead to increased reactive oxygen species generation, and to more photo-oxidative damage.

4.2.1 Fluctuating light has lower average ROS levels, possibly due to increased catalase

We tested the hypothesis that reduced growth in fluctuating light is due to an increase in photo-oxidative damage in two ways. One, we measured the relative amounts of ROS produced over the course of 20 minutes in continuous or fluctuating light cultures in their respective growth light conditions using the fluorescent dye CellROX. The manufacturer describes the dye as interacting with a broad range of ROS species, but does not provide specifics. H_2O_2 has been shown directly to trigger an increase in CellROX fluorescence [41]. Given the difficulty in detecting $^1O_2$ with other dyes, it is unlikely that CellROX is able to detect this particular species of reactive oxygen [42]. Thus differences in CellROX fluorescence likely indicate generation of O_2^-, H_2O_2 and OH•.

We found that the fluctuating light acclimated cultures had reduced reactive oxygen species levels (Table 1). This could be due to a more rapid elimination of ROS in fluctuating light. Evidence for this possibility comes from the increased abundance of the catalase katG (sll1987) (Supplementary Table 1). This enzyme is one of only two in Synechocystis that can catalyze the conversion of H_2O_2 into water and oxygen [43].

Considering how increased light fluence can lead to increased levels of ROS, the on/off nature of the fluctuating light could lead to transient bursts of ROS production, followed by relatively little ROS production in the dark. This could average out to an overall lower ROS level. Because our approach examines the average ROS levels, these short-term dynamics would escape our observation.

Future experiments could slightly modify our assay to differentiate between these possible causes of reduced ROS. If ROS is primarily reduced in fluctuating light due to the on/off nature of the light, then measuring ROS accumulation of continuous light acclimated cultures in a fluctuating light regime should show similar levels to fluctuating light acclimated cultures.

4.2.2 Fluctuating light has a reduced abundance of enzymes involved in the response to photo-oxidative damage

The potential for transient bursts of ROS production in fluctuating light raises the possibility that photo-oxidative damage could still be enhanced in fluctuating light, despite the reduced levels of ROS overall. Thus the second way we tested the hypothesis that reduced growth in fluctuating light is due to photo-oxidative damage was by examining proteins characteristic of this damage. There are several well-characterized heat shock proteins [44] that

increase in abundance in ROS generating conditions such as metal stress [45] and salt stress [46]. These proteins are involved in the removal and repair of damaged proteins.

We found that many of these heat shock proteins were less abundant in fluctuating light, suggesting that the reduced growth rate is not due to photo-oxidative damage. For example we found a reduced abundance of a clpB1 protease subunit (slr1641) [47] and oligopetidase A (slr0659) [44] (Supplementary Table 1, Table 2). These two proteins work in tandem with the heat shock protein dnaK2 (sll0170), which was also found to be less abundant in fluctuating light, to disaggregate damaged proteins, break them into smaller peptides, and degrade them [48-50] (Table 2). We also found a reduction in the NADPH-dependent glutathione peroxidase-like protein gpx1 (slr1171) (Supplementary Table 1). This enzyme is unable to directly catalyze the breakdown of H_2O_2 directly, but instead chemically reduces the targets of ROS mediated damage, such as lipid peroxides [51, 52].

Surprisingly, another commonly induced heat shock protein, the chaperonin groES (slr2075) [44], was more abundant in fluctuating light, which seems to contradict the observation that four other heat shock proteins are less abundant in fluctuating light (Table 2). The groESL complex helps damaged proteins refold by encapsulating them, providing an internal environment where partial unfolding can occur [53], and then allowing them to slowly refold [54]. It appears to have a complex regulation, and has several distinct regulatory elements that respond to different stresses [55]. One of these regulatory elements is called the “L-box” and responds to increases in light rather than other regulatory triggers such as redox state [55]. This same regulatory element does not exist in the promoter region of other heat shock proteins such as dnaK2 [55]. This suggests that perhaps differential expression of groES is due to the higher maximum light intensity (200uE) experienced in the fluctuating light regime, rather than as a

response to photo-oxidative damage. It is also important to note that the activity of groES is regulated by phosphorylation, so there may not be a direct correlation between protein abundance and activity [56].

To gain more direct evidence that there is reduced photo-oxidative damage in fluctuating light compared to continuous light, future experiments could directly measure the oxidation of the two main targets of reactive oxygen species damage: lipids or proteins. Kits to measure the oxidation of both of these are commercially available. For example the OxyBlot kit (Chemicon) measures protein oxidation by using a derivatization /western blot scheme to quantify carbonyl groups, which are characteristically added to protein side chains during oxidative damage. The lipid peroxidation (MDA) kit (Sigma) measures lipid oxidation by colorimetrically examining the formation of an adduct that results from the reaction of MDA a byproduct of lipid peroxidation, and thiobarbituric acid (TBA).

We hypothesized that reduced growth in fluctuating light could be due to photo-oxidative damage caused by increased ROS. However overall, we found reduced levels of ROS in fluctuating light, which is likely due to a combination of increased catalase katG, and reduced ROS generation during the dark periods. Additionally, we observed that many of the heat-shock proteins that are known to respond to increased photo-oxidative damage were less abundant in fluctuating light. Thus overall, our observations do not support the hypothesis that reduced growth rate in fluctuating light is due to photo-oxidative damage.

4.3 Reduced growth of fluctuating light cultures may be due to alterations in metabolism induced by dark/light transitions

Unlike eukaryotic algae and higher plants, cyanobacterial respiratory and photosynthetic pathways exist in the same membrane, and share many of the same components [57]. To avoid

crossover between these pathways, many of the respiratory enzymes are regulated indirectly by light levels through alterations in the redox state of cells [58-60]. We hypothesized that because of the frequent transitions between light and dark in the fluctuating light regime, some aspects of this system could be dysregulated and cause the reduced growth rate that we observed (Table 1) [61]. The mechanism for this could be through inefficiencies caused by the activation/deactivation of the Calvin cycle [62] or perhaps through alterations in the catabolism of storage products [63].

4.3.1 Overview of transition of photo-autotrophic growth to dark respiration in Synechocystis

When Synechocystis is switched from light to dark, a number of changes occur [64, 65]. The ferredoxin pool rapidly becomes oxidized as light driven electron donation from PSI ceases. In the light ferredoxin serves a crucial role as the donor of electrons to NADP+ via the Ferredoxin-NADPH reductase, which ultimately powers carbon fixation in the Calvin cycle. However, ferredoxin also serves as the electron donor to a set of molecules called thioredoxins via ferredoxin-thioredoxin reductase [60]. Thioredoxins have a broad regulatory role, which they accomplish by oxidizing or reducing disulfide bonds on many enzymes [66]. These changes in disulfide oxidation or reduction can activate or deactivate these enzymes [67]. These disulfide bonds can also be oxidized by hydrogen peroxide [67, 68]. Through the ferredoxin-thioredoxin system, a more oxidized redox state within the cells (caused by the transfer to the dark) causes a suppression of many of the Calvin cycle enzymes [66, 69], and deactivation of glycogen biosynthesis enzymes [59]. Additionally, alterations in NADP+/NADPH ratio that result from the transition to darkness, lead to the activation of the oxidative pentose phosphate pathway, which is an alternative pathway to glycolysis that provides NADPH, and ribose to the cells in the dark [70]. Two regulatory proteins, sigE or rre37, which are regulated by light [71], then induce

expression of glycogen catabolism genes [72, 73]. These alterations lead to a switch from photosynthetic carbon fixation to a heterotrophic-like degradation of stored glucose via the oxidative pentose phosphate pathway and ultimately by the TCA cycle. Through the TCA cycle enzyme succinate dehydrogenase (SDH), electrons from glucose are donated directly to the plastoquinone pool [74]. These electrons are ultimately consumed by the reduction of O_2 to H_2O by one of three terminal oxidases [75]. The time scales of this process are likely rapid, but are not precisely known, and how frequent dark/light transitions would influence these processes is also not known. Our physiology and proteomic observations suggest activation of a light-dark transition response, discussed in further detail below.

4.3.2 Transient deactivation of Calvin cycle

The initiation of this response in fluctuating light would begin with the rapid oxidation of the plastoquinone pool upon transition to darkness each cycle. Its is not clear how long the PQ would remain oxidized in this condition, as electrons from other sources could be passed into the plastoquinone pool via NDH [76] SDH [74] or possibly a recently identified L-Amino dehydrogenase [77]. If there are transient bursts of H_2O_2, as we suggested could occur in fluctuating light, a similar effect to oxidization could occur. Either of these routes would lead to a partial shutdown of the Calvin cycle. The deactivation rate of Calvin cycle enzymes has not been measured in cyanobacteria, but in soybeans, fructose 1,6 bisphosphatase was deactivated in 1-2 minutes of exposure to darkness, suggesting a fairly rapid response [78]. Although this rate is longer than the 30s of darkness Synechocystis cultures would be experiencing, the cumulative impact of many transitions into and out of darkness could affect the deactivation state of these enzymes. An experiment that compared Calvin cycle enzyme activity in soybeans cultivated under light fluctuating between 1s on/1-39s off compared to a continuous light with the same

mean PFD as the fluctuating light found partial deactivation of all enzymes tested [62]. While we did not directly measure the enzyme activities in our fluctuating light condition, this suggests it is reasonable that fluctuating light could impact the Calvin cycle.

We found a significantly reduced abundance of phosphoribulokinase (sll1525) in fluctuating light (Supplementary Table 1). This enzyme is unique to the Calvin cycle (not shared with glycolysis, or the oxidative pentose phosphate pathway) and is thought to act as a switch between activation of the Calvin cycle and the OPP pathway [35, 68, 79]. The reduced abundance could be a sign of a general suppression of Calvin cycle activation in fluctuating light compared to continuous light.

4.3.3 Increase in glycogen catabolism suggested by an increase of proteins encoded by a glucose responsive operon

Glycogen degradation begins by cleaving glucose monomers from branches of glycogen one sugar at a time until the branches are 4 sugars long [80]. These branches are then cleaved by glycogen isoamylase, which is encoded in Synechocystis by glgX [80, 81]. This enzyme is located on an operon called the icfG cluster which is made up of 10 other genes. All 10 genes are expressed together in the presence of glucose, but not in low CO_2 conditions [81, 82]. We did not find a significant difference in the abundance of glgX (Supplemental Table 2), but we did find a significant difference in three other proteins located on this gene cluster. These were all more abundant in fluctuating light, suggesting that glgX might also be more abundant in fluctuating light. However, potentially due to technical issues we did not see significant changes in glgX. One of the three icfG proteins found to be more abundant in fluctuating light was slr1856 (Table 2) [83]. This protein is located immediately upstream of glgX, and is a response regulator that is deactivated by the phosphatase icfG, for which this cluster is named. Deletion of icfG completely

stops growth in the presence of glucose, and low CO_2 [84]. A protein of unknown function slr1852 was also identified along with a poorly characterized protein with homology to a carboxymuconolactone hydrolase slr1853 (Table 2) [85]. Azuma et al. (2011) found changes in transcript abundance of glgX in a knock out of the sugar catabolism response regulator rre37 [72], suggesting this may be a part of a larger signal cascade.

4.3.4 Catabolism of glucose through glycolysis may be restricted by the regulator abr2

In fluctuating light we found a reduced abundance of the transcriptional regulator abrB2 (Table 2). This recently identified regulator appears to be important for activating glycolytic enzymes for catabolism of sugars in the light [63]. This study found that a knock out of the abrB2 led to an accumulation of metabolites in the early steps of glycolysis, suggesting an enzymatic blockage in glycolysis [63]. In our data set with reduced levels of abrB2 in fluctuating light, we found there was a reduced abundance of two enzymes to the later steps of glycolysis: sll0395, and slr1934 (Supplementary Table 1, Table 2). If there was reduced metabolite flow to the later steps of glycolysis, there would be less need for these enzymes, and thus they may be down regulated. sll0395 is a putative phosphoglycerate mutase, and slr1934 is a pyruvate dehydrogenase, which might be involved in incorporation of pyruvate into the TCA cycle.

In contrast to these two glycolytic enzymes that are less abundant, we found an increased abundance of glyceraldehyde 3-phosphate dehydrogenase gap2 (sll1342) in fluctuating light (Supplementary Table 1). This enzyme may play a more mysterious role during heterotrophic growth [86]. A proteomic study by Kurian et al. (2006) that looked at changes in protein composition after a shift from photoautotrophic to heterotrophic conditions found an increase in this enzyme [87]. It was initially thought that gap2 could perform a step in glycolysis, like its isoform gap1. However *in vivo* this activity was found to be inhibited by an unknown small

molecule, making it effectively only able to catalyze the reverse reaction in gluconeogenesis [86]. Kurian et al. found that gap2 became more abundant in heterotrophic conditions, yet cannot perform the enzymatic reaction thought to be involved in heterotrophic growth. Given this, it is not clear how to interpret the increased abundance we detected in fluctuating light.

We found two enzymes whose reduced abundance in fluctuating light would reduce the flux of glycolysis, perhaps as a response to the reduced levels of abrB2. If respiratory components are inadvertently being activated due to the fluctuating light regime, this may be a way to counteract that response. However, this response may result in reduced growth. Hanai et al.(2014) found that deletion of abrB2 led to a reduced growth rate when cultivated in 12hr light/dark cycles. It appeared from the glycogen content changes over several days that the reduced growth was due to the inability to regulate glycogen levels [63].

4.3.5 Reduction of the plastoquinone pool in the dark

The last step of this transition from photoautotrophic growth to respiration is donation of electrons derived from glycogen catabolism into the plastoquinone pool. These electrons will then ultimately be used to reduce O_2 into water via the terminal oxidases. In fluctuating light we see proteins and physiological changes that suggest that there is an enhanced electron flow from metabolites into the plastoquinone pool. For example in fluctuating light, we see a significantly increased abundance of an iron-sulfur cluster subunit of SDH: sll1625 (Table 2) which mediates the transfer of electrons into the plastoquinone pool [74]. NDH is also thought to act in respiration as a way to take reductant generated in the TCA cycle and transfer it to the plastoquinone pool [88]. Although we saw a reduction in several subunits of NDH-1 in fluctuating light, some of the specific subunits that were reduced are a part of a variant of NDH-1 that functions in the Carbon Concentrating Mechanism rather than respiration (see below for

further discussion), and thus may have some other role. Additionally we found an increased abundance in fluctuating light of the recently identified L-Amino dehydrogenase, slr0782 (Table 2). This enzyme, like SDH, is able to dehydrogenate certain amino acids, and donate the liberated electrons directly to the plastoquinone pool [77]. This enzyme was found to have *in vivo* activity with arginine [77]. Although this enzyme could have multiple substrates, considering that cyanobacteria store large amounts of arginine in the polymer cyanophycin (see below), this suggests metabolism of an alternative storage molecule in respiration may be possible [89].

In light of the above observations, a possible interpretation of the lower F_v/F_m that we found in fluctuating light (Table 1) is that this is due to an enhanced reduction of the plastoquinone pool in the dark. The increased abundance of SDH and the L-Amino dehydrogenase paired with the evidence that there could be more glycogen catabolism, would suggest that in the dark there would be a more rapid reduction of the plastoquinone pool. The intention of the dark acclimation given before measuring the F_v/F_m is to oxidize the plastoquinone pool. However, in cyanobacteria it is possible due to the shared nature of respiration and photosynthesis for these organisms to reduce their plastoquinone pools in the dark [90-92]. A reduced plastoquinone pool could result in a rise in F_o [91] which would lower the F_v/F_m, since the variable fluorescence is F_m-F_o [93]. A reduced plastoquinone pool could also reduce the F_v/F_m value by triggering a reorganization in the light harvesting apparatus to direct more energy to PSI [91]. This reorganization process is called a state 1 to state 2 transition [90, 92]. An alternative explanation for a reduced F_v/F_m is a lower F_m due to photoinhibition [93]. However, the reduced levels of ROS and evidence of less photo-oxidative damage in fluctuating light suggests enhanced photoinhibition is unlikely.

Future experiments could test whether the lower F_v/F_m is due to a reduced plastoquinone pool by providing a short period of low blue-light illumination prior to the saturating pulse. Blue-light, which is absorbed by chlorophyll but not strongly absorbed by phycobilisomes, is preferentially absorbed by PSI due to larger fraction of chlorophylls associated with PSI in cyanobacteria [94, 95]. This selectively excites PSI, leading an oxidation of the PQ pool [95]. If future experiments observe that the reduced F_v/F_m in fluctuating light goes away with blue-light oxidation, it would support this hypothesis.

In fluctuating light we have seen that, in principal, there could be some redox mediated down-regulation of the Calvin cycle either from an increase in H_2O_2 or from the exposure to darkness every 30s. Supporting this we saw reduced abundance of phophoribulokinase, a key enzyme of the Calvin cycle in fluctuating light. An oxidized redox state in a typical light-dark transition does not just shut the Calvin cycle down, but also activates glycolytic enzymes and through some unknown mechanism activates glycogen degradation genes [72, 73]. Supporting this, we found three proteins become more abundant in an operon that includes a glycogen degradation gene. This increased activation of glucose catabolism may be partially thwarted by the reduced abundance of abrB2, and the concomitant reduction in glycolytic enzymes. However, it seems there is at least a partial flow of metabolites to the TCA cycle, because we see an increase in the succinate dehydrogenase enzyme, and an enhanced reduction of the PQ in the dark.

4.4 Higher capacity for photosynthesis in fluctuating light suggests dissipation of electrons

Reduced growth in the fluctuating light could be due to a non-productive dissipation of energy. Energy dissipation through thermal dissipation at the level of photon capture [22], or as a purge valve in the electron transport chain through alternative electron transport [96] are

common mechanisms for photosynthetic microbes to protect themselves from excess light. Energy dissipation mechanisms reduce the energy available in order to reduce the probability that reactive oxygen species will be formed. However, in some conditions these energy dissipation mechanisms are activated, but are apparently unnecessary to maximize biomass accumulation. For example in the patent by Peers (2015), this study found an increase in Synechocystis biomass accumulation under a randomly fluctuating light regime when the Orange Carotenoid Protein was knocked out [23]. This protein has been shown to become activated by blue light, and once activated dissipates a large fraction of captured photons [22].

We observed that between light intensities of 106 and 174 μmol photons m^{-2} s^{-1} that the fluctuating light cultures had a significantly higher effective quantum yield of photosystem II (YII) (Figure 3). Although an increased YII means that more photons are used for charge separation and transfer of electrons to the electron transport chain, it does not necessarily mean that those electrons are used to fix CO_2. Modes of alternative electron transport that can dissipate these electrons such as terminal oxidases [75], or the reduction of oxygen via flavodiiron proteins [20], are possible ways to create a more oxidized electron transport chain, and have been shown to be necessary in fluctuating light. However, at the proteomic level we did not detect any of the terminal oxidases, and did not detect the flavodiiron proteins in both treatments (Supplemental Table 2), making it difficult to prove this is the mechanism behind reduced growth, and the increased YII.

Future experiments could use an inhibitor of terminal oxidases, KCN, to determine whether they are oxidizing the plastoquinone pool at higher light intensities in fluctuating light acclimated cultures. We would expect similar YIIs across the light curve for both cultures if KCN were added.

Enhanced transport to terminal oxidases would not necessarily need to be caused by an increase in terminal oxidase abundance. Liu et al. (2012) found that spatial arrangements can occur as a result of changes to the redox state of cells that places SDH and NDH-1 in closer proximity to terminal oxidases. This results in a larger fraction of electrons derived from storage molecules being dissipated through terminal oxidases rather than PSI [97].

4.5 Proteins involved in carbon concentrating mechanism show contrasting trends, suggesting different modes of induction

Cyanobacteria have a well-studied response to limiting CO_2 conditions known as the carbon concentrating mechanism (CCM) [98]. This involves increases in bicarbonate transporters, changes in the NDH-1 complex, which provides ATP to energize those transporters, and increases in carboxysomes, which concentrate RuBisCo and CO_2 into specialized compartments [99]. Although we did not observe changes in media pH, which is a good indicator of CO_2 limitation [100], in either fluctuating or continuous light cultures, surprisingly we observed significant changes in proteins involved in the CCM response. Also, components of CCM that have previously been shown to act in concert (increases in the NDH-1 MS complex, and increases in carboxysome shell proteins) displayed opposite trends in these conditions, suggesting some unusual regulation.

4.5.1 Subunits of NADPH dehydrogenase are less abundant in fluctuating light

The multisubunit NAD(P)H dehydrogenase complex (NDH-1) oxidizes NAD(P)H and reduces the plastoquinone pool [88]. This activity, called cyclic electron flow, allows electrons from NAD(P)H to be cycled back into the plastoquinone pool, leading to the generation of more ATP and altering the NAD(P)H/NAD(P)$^+$ ratios [74]. The overall ATP demand of the cell increases during stress, and when actively transporting inorganic carbon. As linear electron flow

can only produce a fixed ratio of NADPH/ATP, cyclic electron flow must be used to increase the amount of ATP [96]. Most NDH-1 subunits are always present, but a subset are interchangeable and lead to several types of NDH-1 complexes with distinct roles. For example NDH-1 complexes having subunits ndhD3/ndhF3/cupA form a complex called NDH-1MS which has been shown to be induced by low CO_2 conditions and leads to the generation of more ATP, which energizes the active transport of inorganic carbon [88].

This experiment found that two members of the NDH-1 MS complex: ndhD3 (sll1733), and cupA (sll1734) were less abundant in fluctuating light, suggesting less CO_2 stress (Supplementary Table 1). In addition, three other core subunits of the NDH-1 complex were less abundant in fluctuating light, ndhA, ndhH, and ndhN (sll0519, slr0261, sll1262 respectively) (Table 2, Supplementary Table 2). Battchikova et al. (2010) found all 5 of these proteins were more abundant after a shift from high CO_2 to ambient CO_2 conditions [101]. Curiously ndhF1 (slr0844) was not found in fluctuating light, but was abundant enough in continuous light to be considered significantly different (Supplementary Table 1). Unlike the other ndh proteins, Battchikova et al. did not find this protein to be significantly more abundant in their shift to low CO_2 [101]. The subunit ndhF1 is a part of the NDH-1L complex which is involved in respiration [102]. In addition a subunit of ATP synthase (atpI, sll1322) was upregulated, which may be associated with the increased need to generate ATP to energize CO_2 transport (Table 2). Although the NDH-1 complex becomes more abundant under low CO_2 conditions, it does not detect CO_2 levels directly. Instead, the NDH-1 complex is regulated by ccmR, which indirectly detects CO_2 levels through changes in $NADPH/NADH^+$ ratios and α-ketoglutarate levels [103].

4.5.2 Subunits of carboxysomes are more abundant in fluctuating light

In contrast to the finding that components of the NDH-1-MS complex were less abundant in fluctuating light, suggesting no CO_2 stress, we observed that components of the carboxysome shell: ccmK1 and ccmK2 (sll1029 and sll1028) are more abundant in fluctuating light (Table 2). These proteins have been shown to become more abundant under a shift to low CO_2, although their increase was mild compared to that of the NDH-1 MS subunits [101]. The ccmK proteins are a part of an operon containing several other carboxysome proteins: ccmKLMN. This cluster is not regulated by ccmR, as NDH-1 is, and it is suspected it may be constitutively regulated [99]. Considering we saw a fairly large magnitude increase in fluctuating light (6-8x), this suggests there is perhaps some other form of regulation that is being activated in the fluctuating light environment.

4.6 Changes in abundance of other classes of proteins reveal a complicated response to fluctuating light

Purine and DNA/RNA biosynthesis

Several enzymes involved in the synthesis of guanasine monophosphate (GMP) were less abundant in fluctuating light. These include purH, guaB, and guaA (slr0597, slr1722 and slr0213 respectively) (Table 2). GMP could have several functions. One possibility is that the GMP is used to synthesize GTP, which is necessary to energize specific enzymes such as the cell division protein ftsZ [104]. Another possibility is that GMP is used for the synthesis of DNA. Support for this possibility comes from an increased abundance in continuous light of a subunit of DNA polymerase III, dnaN (slr0965) (Table 2). A third possibility is that the GMP is used for the synthesis of various secondary messengers. Their role is poorly understood in cyanobacteria but secondary messengers are often used as the output domain of photoreceptors [105].

4.6.1 Cyanophycin utilization

Cyanobacteria accumulate a biopolymer called cyanophycin that is thought primarily to be a nitrogen reserve [106-108]. Cyanophycin is composed of a backbone of aspartate with branching arginine molecules [106]. Although the enzymes to catabolize cyanophycin to aspartate and arginine are well known [109], there remains considerable debate on how arginine and aspartate are further catabolized in cyanobacteria [77, 89, 107, 110]. Wegener et al. in their proteomic comparison found changes in cyanophycin catabolism in nearly all of the tested stress conditions [111], suggesting this pathway is important in the cyanobacterial response to stress.

Our analysis found that in continuous light there was an increased abundance of three enzymes that appear to use a cycle of arginine conversions to convert one of the breakdown products of cyanophycin, aspartate, into ammonium and fumarate, which can be used in the TCA cycle (Figure 4). The first enzyme (sll1336) was suggested by Schriek et al. (2007) to be arginine deiminase [89] (Table 2). This enzyme catalyzes the conversion of arginine to citrulline, releasing ammonium. Citrulline and aspartate are converted into argininosuccinate by argininosuccinate synthase, argG (slr0585) which was also more abundant in continuous light (Table 2). The third enzyme argininosuccinate lyase (sll1133) [112], was only detected in continuous light (Supplemental Table 2) and can recycle argininosuccinate back into arginine. This conversion releases fumarate, which could be utilized by the TCA cycle [107]. Taken together, these three enzymes perform a cycle similar to that proposed by Quintero et al. (2000) [107] that can utilize aspartate for the production of ammonium and fumarate. The only modification to the cycle described here from that originally proposed by Quintero et al. (2000) is the direct conversion of arginine to citrulline, rather than going through ornithine. This modification is supported by the observation that the proposed arginase enzymes were found *in*

vitro to not have arginase activity [110]. This increased abundance of enzymes in this proposed pathway is surprising because we would not expect there to be a need for degradation of aspartate in continuous light. As cyanophycin is made up of arginine and aspartate in a roughly 1:1 ratio, there may also be enhanced degradation of arginine in the continuous light that was not detected by our proteomic assay. It is likely that arginine would be catabolized by the arginine deiminase pathway, or the arginine dehydrogenase pathway [89]. Given that several stress conditions showed changes in arginine degradation, and that in continuous light we saw evidence for greater photo-oxidative stress, perhaps this pathway somehow provides rapid energy or carbon skeletons for the repair of protein damage.

4.6.2 Several hypothetical proteins were significantly different in the fluctuating light regime

Of the 97 proteins that were significantly different between fluctuating and continuous light, about 20% of them were annotated as hypothetical, putative, or unknown (Table 2, Supplementary Table 1). Given that the only difference in the treatment of our two conditions was how the light was delivered, significant changes in these proteins suggest they may have an important role in photosynthesis and the adaptation to fluctuating light.

A number of these hypothetical proteins are particularly interesting. For example, slr1702, which was less abundant in fluctuating light, interacts with sigE, a regulatory element for transcription involved in activating sugar metabolism [113]. Although sigE responds to light, the signaling mechanism is not completely understood, and the gene product of slr1702 was suggested as a candidate to post- translationally activate sigE [71].

Another hypothetical protein slr1590, which was also less abundant in fluctuating light was found to comigrate with a band of small CAB-like proteins (scpB, or hliC) [114]. This class of proteins has similarity to the light harvesting complex proteins of eukaryotic algae, and has

been suggested to be involved in the response to stress [114]. Recently another CAB-like protein hliD was suggested to be able to thermally dissipate light energy [115].

In fluctuating light there was an increased abundance of sll0872. This is a membrane bound protein that was more abundant in five different stress conditions tested (Nitrogen starvation, hexane, butane, ethanol, and salt stress) [116]. These three hypothetical proteins were chosen to represent the potential diversity of acclimation responses that these hypothetical proteins could be involved in, and which could inform our understanding of the response to fluctuating light.

5. Conclusion

This experiment sought to explore the physiological response of Synechocystis to fluctuating light, which is a particularly poorly understood environmental factor associated with growth in industrial cultivation systems. Our data demonstrates that a very different physiological state exists when cultures are cultivated in fluctuating light rather than the continuous light conditions that are often used in the laboratory. Our observations offer new lines of inquiry to pursue on factors that could limit growth in fluctuating light. These include the role of energy dissipation, photo-autotrophic/respiration transitions, and reduced efficiency of the Calvin cycle due to redox regulation. Furthermore, the surprising changes in CCM components and ROS generation, along with changes in a number of hypothetical proteins provide more pieces to integrate into the emerging conceptual understanding of fluctuating light conditions.

REFERENCES

[1] G.C. Dismukes, D. Carrieri, N. Bennette, G.M. Ananyev, M.C. Posewitz, Aquatic phototrophs: efficient alternatives to land-based crops for biofuels, Current opinion in biotechnology, 19 (2008) 235-240.

[2] D.C. Ducat, J.C. Way, P.A. Silver, Engineering cyanobacteria to generate high-value products, Trends in biotechnology, 29 (2011) 95-103.

[3] M. Ikeuchi, S. Tabata, Synechocystis sp. PCC 6803 — a useful tool in the study of the genetics of cyanobacteria, Photosynthesis research, 70 (2001) 73-83.

[4] X. Zang, B. Liu, S. Liu, K.K.I.U. Arunakumara, X. Zhang, Optimum conditions for transformation of Synechocystis sp. PCC 6803.pdf, The Journal of Microbiology, 45 (2007) 241-245.

[5] J.J. Eaton-Rye, The construction of gene knockouts in the cyanobacterium Synechocystis sp. PCC 6803.pdf, Methods in Molecular Biology, 274 (2004) 309-324.

[6] G. Peers, Increasing algal photosynthetic productivity by integrating ecophysiology with systems biology, Trends in biotechnology, 32 (2014) 551-555.

[7] P. Walsh, L. Legendre, Photosynthesis of natural phytoplankton under high frequency light fluctuations simulating those induced by sea surface waves, Limnology and Oceanography, 28 (1983) 688-697.

[8] A. Sournia, Circadian Periodicities in Natural Populations of Marine Phytoplankton, in: S.R. Frederick, Y. Maurice (Eds.) Advances in Marine Biology, Academic Press1975, pp. 325-389.

[9] C.L. Gallegos, G.M. Hornberger, M.G. Kelly, Photosynthesis—light relationships of a mixed culture of phytoplankton in fluctuating light, Limnology and Oceanography, 25 (1980) 1082-1092.

[10] M. Fréchette, L. Legendre, Phytoplankton photosynthetic response to light in an internal tide dominated environment, Estuaries, 5 (1982) 287-293.

[11] M. Muramatsu, Y. Hihara, Acclimation to high-light conditions in cyanobacteria: from gene expression to physiological responses, Journal of plant research, 125 (2012) 11-39.

[12] H. Schubert, H.C.P. Matthijs, L.R. Mur, U. Schiewer, Blooming of cyanobacteria in turbulent water with steep light gradients: The effect of intermittent light and dark periods on the oxygen evolution capacity of Synechocystis sp. PCC 6803, FEMS Microbiology Ecology, 18 (1995) 237-245.

[13] H. Schubert, S. Sagert, R.M. Forster, Evaluation of the different levels of variability in the underwater light field of a shallow estuary, Helgol Mar Res, 55 (2001) 12-22.

[14] R. Davis, A. Aden, P.T. Pienkos, Techno-economic analysis of autotrophic microalgae for fuel production, Applied Energy, 88 (2011) 3524-3531.

[15] C.-G. Lee, Calculation of light penetration depth in photobioreactors, Biotechnol. Bioprocess Eng., 4 (1999) 78-81.

[16] B.D. Fernandes, G.M. Dragone, J.A. Teixeira, A.A. Vicente, Light regime characterization in an airlift photobioreactor for production of microalgae with high starch content, Applied biochemistry and biotechnology, 161 (2010) 218-226.

[17] L. Brennan, P. Owende, Biofuels from microalgae—A review of technologies for production, processing, and extractions of biofuels and co-products, Renewable and Sustainable Energy Reviews, 14 (2010) 557-577.

[18] H. Takache, J. Pruvost, H. Marec, Investigation of light/dark cycles effects on the photosynthetic growth of Chlamydomonas reinhardtii in conditions representative of photobioreactor cultivation, Algal Research, 8 (2015) 192-204.

[19] L. Martínez, A. Morán, A.I. García, Effect of light on Synechocystis sp. and modelling of its growth rate as a response to average irradiance, Journal of Applied Phycology, 24 (2011) 125-134.

[20] Y. Allahverdiyeva, H. Mustila, M. Ermakova, L. Bersanini, P. Richaud, G. Ajlani, N. Battchikova, L. Cournac, E.-M. Aro, Flavodiiron proteins Flv1 and Flv3 enable cyanobacterial growth and photosynthesis under fluctuating light, Proceedings of the National Academy of Sciences, 110 (2013) 4111-4116.

[21] Y. Helman, D. Tchernov, L. Reinhold, M. Shibata, T. Ogawa, R. Schwarz, I. Ohad, A. Kaplan, Genes encoding A-type flavoproteins are essential for photoreduction of O2 in cyanobacteria, Current biology : CB, 13 (2003) 230-235.

[22] D. Kirilovsky, C.A. Kerfeld, The orange carotenoid protein in photoprotection of photosystem II in cyanobacteria, Biochimica et biophysica acta, 1817 (2012) 158-166.

[23] G. Peers, Enhancement of biomass production by disruption of light energy dissipation pathways, Google Patents, ExxonMobil Research and Engineering Company, Annandale, NJ, United States, 2015.

[24] J. Anfelt, B. Hallström, J. Nielsen, M. Uhlén, E.P. Hudson, Using Transcriptomics To Improve Butanol Tolerance of Synechocystis sp. Strain PCC 6803, Applied and environmental microbiology, 79 (2013) 7419-7427.

[25] B. Genty, J.-M. Briantais, N.R. Baker, The relationship between the quantum yield of photosynthetic electron transport and quenching of chlorophyll fluorescence, Biochimica et Biophysica Acta (BBA) - General Subjects, 990 (1989) 87-92.

[26] H. Qiao, X. Fan, D. Xu, N. Ye, J. Wang, S. Cao, Artificial leaf aids analysis of chlorophyll fluorescence and P700 absorbance in studies involving microalgae, Phycological Research, 63 (2015) 72-76.

[27] M.B. Pascual, A. Mata-Cabana, F.J. Florencio, M. Lindahl, F.J. Cejudo, Overoxidation of 2-Cys Peroxiredoxin in Prokaryotes: Cyanobacterial 2-Cys Peroxiredoxins sensitve to Oxidative stress, The Journal of biological chemistry, 285 (2010) 34485-34492.

[28] Y. Nishiyama, S.I. Allakhverdiev, N. Murata, Protein synthesis is the primary target of reactive oxygen species in the photoinhibition of photosystem II, Physiol Plant, 142 (2011) 35-46.

[29] L. Gao, J. Wang, H. Ge, L. Fang, Y. Zhang, X. Huang, Y. Wang, Toward the complete proteome of Synechocystis sp. PCC 6803, Photosynthesis research, (2015).

[30] N. Battchikova, M. Angeleri, E.-M. Aro, Proteomic approaches in research of cyanobacterial photosynthesis, Photosynthesis research, (2014) 1-24.

[31] T. Hirokawa, S. Boon-Chieng, S. Mitaku, SOSUI: classification and secondary structure prediction system for membrane proteins, Bioinformatics, 14 (1998) 378-379.

[32] B. Xu, P. Li, P. Waller, M. Huesemann, Evaluation of flow mixing in an ARID-HV algal raceway using statistics of temporal and spatial distribution of fluid particles, Algal Research, 9 (2015) 27-39.

[33] A. Soman, Y. Shastri, Optimization of novel photobioreactor design using computational fluid dynamics, Applied Energy, 140 (2015) 246-255.

[34] M. Janssen, T.C. Kuijpers, B. Veldhoen, M.B. Ternbach, J. Tramper, L.R. Mur, R.H. Wijffels, Specific growth rate of Chlamydomonas reinhardtii and Chlorella sorokiniana under medium duration light/dark cycles: 13–87 s, Journal of Biotechnology, 70 (1999) 323-333.

[35] M. Tamoi, T. Miyazaki, T. Fukamizo, S. Shigeoka, The Calvin cycle in cyanobacteria is regulated by CP12 via the NAD(H)/NADP(H) ratio under light/dark conditions, The Plant Journal, 42 (2005) 504-513.

[36] G. Peers, Enhancement of biomass production by disruption of light energy dissipation pathways, Google Patents, 2012.

[37] A. Latifi, M. Ruiz, C.-C. Zhang, Oxidative stress in cyanobacteria, 2009.

[38] Y. Allahverdiyeva, J. Isojärvi, P. Zhang, E.-M. Aro, Cyanobacterial Oxygenic Photosynthesis is Protected by Flavodiiron Proteins, Life, 5 (2015) 716-743.

[39] C. Fufezan, C.M. Gross, M. Sjodin, A.W. Rutherford, A. Krieger-Liszkay, D. Kirilovsky, Influence of the redox potential of the primary quinone electron acceptor on photoinhibition in photosystem II, The Journal of biological chemistry, 282 (2007) 12492-12502.

[40] A. Makino, C. Miyake, A. Yokota, Physiological Functions of the Water–Water Cycle (Mehler Reaction) and the Cyclic Electron Flow around PSI in Rice Leaves, Plant and Cell Physiology, 43 (2002) 1017-1026.

[41] G. Cheloni, C. Cosio, V.I. Slaveykova, Antagonistic and synergistic effects of light irradiation on the effects of copper on Chlamydomonas reinhardtii, Aquatic toxicology (Amsterdam, Netherlands), 155 (2014) 275-282.

[42] B.B. Fischer, E. Hideg, A. Krieger-Liszkay, Production, detection, and signaling of singlet oxygen in photosynthetic organisms, Antioxidants & redox signaling, 18 (2013) 2145-2162.

[43] M. Tichy, W. Vermaas, In vivo role of catalase-peroxidase in synechocystis sp. strain PCC 6803, Journal of bacteriology, 181 (1999) 1875-1882.

[44] A.R. Slabas, I. Suzuki, N. Murata, W.J. Simon, J.J. Hall, Proteomic analysis of the heat shock response in Synechocystis PCC6803 and a thermally tolerant knockout strain lacking the histidine kinase 34 gene, Proteomics, 6 (2006) 845-864.

[45] O. Castielli, B. De la Cerda, J.A. Navarro, M. Hervás, M.A. De la Rosa, Proteomic analyses of the response of cyanobacteria to different stress conditions, FEBS letters, 583 (2009) 1753-1758.

[46] S. Fulda, S. Mikkat, F. Huang, J. Huckauf, K. Marin, B. Norling, M. Hagemann, Proteome analysis of salt stress response in the cyanobacterium Synechocystis sp. strain PCC 6803, Proteomics, 6 (2006) 2733-2745.

[47] C.R. Gonzalez-Esquer, W.F.J. Vermaas, ClpB1 Overproduction in Synechocystis sp. Strain PCC 6803 Increases Tolerance to Rapid Heat Shock, Applied and environmental microbiology, 79 (2013) 6220-6227.

[48] Y. Oguchi, E. Kummer, F. Seyffer, M. Berynskyy, B. Anstett, R. Zahn, R.C. Wade, A. Mogk, B. Bukau, A tightly regulated molecular toggle controls AAA+ disaggregase, Nat Struct Mol Biol, 19 (2012) 1338-1346.

[49] J. Winter, K. Linke, A. Jatzek, U. Jakob, Severe oxidative stress causes inactivation of DnaK and activation of the redox-regulated chaperone Hsp33, Molecular cell, 17 (2005) 381-392.

[50] R. Jain, M.K. Chan, Support for a potential role of E. coli oligopeptidase A in protein degradation, Biochem Biophys Res Commun, 359 (2007) 486-490.

[51] A. Gaber, M. Tamoi, T. Takeda, Y. Nakano, S. Shigeoka, NADPH-dependent glutathione peroxidase-like proteins (Gpx-1, Gpx-2) reduce unsaturated fatty acid hydroperoxides in Synechocystis PCC 6803, FEBS letters, 499 (2001) 32-36.

[52] M. Bernroitner, M. Zamocky, P.G. Furtmüller, G.A. Peschek, C. Obinger, Occurrence, phylogeny, structure, and function of catalases and peroxidases in cyanobacteria, Journal of experimental botany, 60 (2009) 423-440.

[53] S. Sharma, K. Chakraborty, B.K. Müller, N. Astola, Y.-C. Tang, D.C. Lamb, M. Hayer-Hartl, F.U. Hartl, Monitoring Protein Conformation along the Pathway of Chaperonin-Assisted Folding, Cell, 133 142-153.

[54] F.U. Hartl, A. Bracher, M. Hayer-Hartl, Molecular chaperones in protein folding and proteostasis, Nature, 475 (2011) 324-332.

[55] K. Kojima, H. Nakamoto, A novel light- and heat-responsive regulation of the groE transcription in the absence of HrcA or CIRCE in cyanobacteria, FEBS letters, 581 (2007) 1871-1880.

[56] A.A. Zorina, V.S. Bedbenov, G.V. Novikova, V.B. Panichkin, D.A. Los', Involvement of serine/threonine protein kinases in the cold stress response in the cyanobacterium Synechocystis sp. PCC 6803: Functional characterization of SpkE protein kinase, Mol Biol, 48 (2014) 390-398.

[57] C.W. Mullineaux, Co-existence of photosynthetic and respiratory activities in cyanobacterial thylakoid membranes, Biochimica et biophysica acta, 1837 (2014) 503-511.

[58] S. Díaz-Troya, L. López-Maury, A.M. Sánchez-Riego, M. Roldán, F.J. Florencio, Redox Regulation of Glycogen Biosynthesis in the Cyanobacterium Synechocystis sp. PCC 6803: Analysis of the AGP and Glycogen Synthases, Molecular Plant, 7 (2014) 87-100.

[59] M. Lindahl, F.J. Florencio, Thioredoxin-linked processes in cyanobacteria are as numerous as in chloroplasts, but targets are different, Proceedings of the National Academy of Sciences, 100 (2003) 16107-16112.

[60] F.J. Florencio, M.E. Perez-Perez, L. Lopez-Maury, A. Mata-Cabana, M. Lindahl, The diversity and complexity of the cyanobacterial thioredoxin systems, Photosynthesis research, 89 (2006) 157-171.

[61] L. Nikkanen, E. Rintamaki, Thioredoxin-dependent regulatory networks in chloroplasts under fluctuating light conditions, Philosophical transactions of the Royal Society of London. Series B, Biological sciences, 369 (2014) 20130224.

[62] G.F. Sassenrath-Cole, R.W. Pearcy, S. Steinmaus, The role of enzyme activation state in limiting carbon assimilation under variable light conditions, Photosynthesis research, 41 (1994) 295-302.

[63] M. Hanai, Y. Sato, A. Miyagi, M. Kawai-Yamada, K. Tanaka, Y. Kaneko, Y. Nishiyama, Y. Hihara, The Effects of Dark Incubation on Cellular Metabolism of the Wild Type Cyanobacterium Synechocystis sp. PCC 6803 and a Mutant Lacking the Transcriptional Regulator cyAbrB2, Life, 4 (2014) 770-787.

[64] R.T. Gill, E. Katsoulakis, W. Schmitt, G. Taroncher-Oldenburg, J. Misra, G. Stephanopoulos, Genome-Wide Dynamic Transcriptional Profiling of the Light-to-Dark Transition in Synechocystis sp. Strain PCC 6803, Journal of bacteriology, 184 (2002) 3671-3681.

[65] C. Ansong, N.C. Sadler, E.A. Hill, M.P. Lewis, E.M. Zink, R.D. Smith, A.S. Beliaev, A.E. Konopka, A.T. Wright, Characterization of protein redox dynamics induced during light-to-dark transitions and nutrient limitation in cyanobacteria, Frontiers in microbiology, 5 (2014) 325.

[66] J. Guo, A.Y. Nguyen, Z. Dai, D. Su, M.J. Gaffrey, R.J. Moore, J.M. Jacobs, M.E. Monroe, R.D. Smith, D.W. Koppenaal, H.B. Pakrasi, W.-J. Qian, Proteome-wide Light/Dark Modulation of Thiol Oxidation in Cyanobacteria Revealed by Quantitative Site-Specific Redox Proteomics, Molecular & Cellular Proteomics, (2014).

[67] M. Balsera, E. Uberegui, P. Schurmann, B.B. Buchanan, Evolutionary development of redox regulation in chloroplasts, Antioxidants & redox signaling, 21 (2014) 1327-1355.

[68] W. Kaiser, Reversible inhibition of the calvin cycle and activation of oxidative pentose phosphate cycle in isolated intact chloroplasts by hydrogen peroxide, Planta, 145 (1979) 377-382.

[69] H. MacIntyre, T. Sharkey, R. Geider, Activation and deactivation of ribulose-1,5-bisphosphate carboxylase/oxygenase (Rubisco) in three marine microalgae, Photosynthesis research, 51 (1997) 93-106.

[70] A. Grossman, R.E. McGowan, Regulation of glucose 6-phosphate dehydrogenase in blue-green algae, Plant physiology, 55 (1975) 658-662.

[71] T. Osanai, M. Imashimizu, A. Seki, S. Sato, S. Tabata, S. Imamura, M. Asayama, M. Ikeuchi, K. Tanaka, ChlH, the H subunit of the Mg-chelatase, is an anti-sigma factor for SigE in Synechocystis sp. PCC 6803, Proceedings of the National Academy of Sciences, 106 (2009) 6860-6865.

[72] M. Azuma, T. Osanai, M.Y. Hirai, K. Tanaka, A response regulator Rre37 and an RNA polymerase sigma factor SigE represent two parallel pathways to activate sugar catabolism in a cyanobacterium Synechocystis sp. PCC 6803, Plant & cell physiology, 52 (2011) 404-412.

[73] T. Osanai, A. Oikawa, K. Numata, A. Kuwahara, H. Iijima, Y. Doi, K. Saito, M.Y. Hirai, Pathway-level acceleration of glycogen catabolism by a response regulator in the cyanobacterium Synechocystis species PCC 6803, Plant physiology, 164 (2014) 1831-1841.

[74] J.W. Cooley, W.F. Vermaas, Succinate dehydrogenase and other respiratory pathways in thylakoid membranes of Synechocystis sp. strain PCC 6803: capacity comparisons and physiological function, Journal of bacteriology, 183 (2001) 4251-4258.

[75] D.J. Lea-Smith, N. Ross, M. Zori, D.S. Bendall, J.S. Dennis, S.A. Scott, A.G. Smith, C.J. Howe, Thylakoid terminal oxidases are essential for the cyanobacterium Synechocystis sp. PCC 6803 to survive rapidly changing light intensities, Plant physiology, 162 (2013) 484-495.

[76] G. Bernat, J. Appel, T. Ogawa, M. Rogner, Distinct roles of multiple NDH-1 complexes in the cyanobacterial electron transport network as revealed by kinetic analysis of P700+ reduction in various Ndh-deficient mutants of Synechocystis sp. strain PCC6803, Journal of bacteriology, 193 (2011) 292-295.

[77] S. Schriek, U. Kahmann, D. Staiger, E.K. Pistorius, K.-P. Michel, Detection of an L-amino acid dehydrogenase activity in Synechocystis sp. PCC 6803, Journal of experimental botany, 60 (2009) 1035-1046.

[78] G.F. Sassenrath-Cole, R.W. Pearcy, Regulation of Photosynthetic Induction State by the Magnitude and Duration of Low Light Exposure, Plant physiology, 105 (1994) 1115-1123.

[79] N. Wedel, J. Soll, Evolutionary conserved light regulation of Calvin cycle activity by NADPH-mediated reversible phosphoribulokinase/CP12/ glyceraldehyde-3-phosphate dehydrogenase complex dissociation, Proceedings of the National Academy of Sciences, 95 (1998) 9699-9704.

[80] Y. Zilliges, Glycogen, a Dynamic Cellular Sink and Reservoir for Carbon, in: E. Flores, A. Herrero (Eds.) The Cell Biology of Cyanobacteria, Caister Academic Press, Seville, Spain, 2014, pp. 211-219.

[81] E. Suzuki, K. Umeda, S. Nihei, K. Moriya, H. Ohkawa, S. Fujiwara, M. Tsuzuki, Y. Nakamura, Role of the GlgX protein in glycogen metabolism of the cyanobacterium, Synechococcus elongatus PCC 7942, Biochimica et Biophysica Acta (BBA) - General Subjects, 1770 (2007) 763-773.

[82] H.L. Wang, B.L. Postier, R.L. Burnap, Alterations in global patterns of gene expression in Synechocystis sp. PCC 6803 in response to inorganic carbon limitation and the inactivation of ndhR, a LysR family regulator, The Journal of biological chemistry, 279 (2004) 5739-5751.

[83] L. SHI, K.M. BISCHOFF, P.J. KENNELLY, The icfG Gene Cluster of Synechocystis sp. Strain PCC 6803 Encodes an Rsb/Spo-Like Protein Kinase, Protein Phosphatase, and Two Phosphoproteins, Journal of bacteriology, 181 (1999) 4761–4767.

[84] L. Beuf, S. Bédu, M.-C. Durand, F. Joset, A protein involved in coordinated regulation of inorganic carbon and glucose metabolism in the facultative photoautotrophic cyanobacterium Synechocystis PCC6803, Plant Mol Biol, 25 (1994) 855-864.

[85] E.V. Koonin, Genome sequences: Genome sequence of a model prokaryote, Current Biology, 7 (1997) R656-R659.

[86] O. Koksharova, M. Schubert, S. Shestakov, R. Cerff, Genetic and biochemical evidence for distinct key functions of two highly divergent GAPDH genes in catabolic and anabolic carbon flow of the cyanobacterium Synechocystis sp. PCC 6803, Plant Mol Biol, 36 (1998) 183-194.

[87] D. Kurian, T. Jansèn, P. Mäenpää, Proteomic analysis of heterotrophy in Synechocystis sp. PCC 6803, Proteomics, 6 (2006) 1483-1494.

[88] N. Battchikova, M. Eisenhut, E.M. Aro, Cyanobacterial NDH-1 complexes: novel insights and remaining puzzles, Biochimica et biophysica acta, 1807 (2011) 935-944.

[89] S. Schriek, C. Rückert, D. Staiger, E.K. Pistorius, K.-P. Michel, Bioinformatic evaluation of L-arginine catabolic pathways in 24 cyanobacteria and transcriptional analysis of genes encoding

enzymes of L-arginine catabolism in the cyanobacterium Synechocystis sp. PCC 6803, BMC Genomics, 8 (2007) 437-437.

[90] C.W. Mullineaux, J.F. Allen, The state 2 transition in the cyanobacterium Synechococcus 6301 can be driven by respiratory electron flow into the plastoquinone pool, FEBS letters, 205 (1986) 155-160.

[91] M.J. Behrenfeld, Widespread Iron Limitation of Phytoplankton in the South Pacific Ocean, Science, 283 (1999) 840-843.

[92] Y.V. Bolychevtseva, F.I. Kuzminov, I.V. Elanskaya, M.Y. Gorbunov, N.V. Karapetyan, Photosystem activity and state transitions of the photosynthetic apparatus in cyanobacterium Synechocystis PCC 6803 mutants with different redox state of the plastoquinone pool, Biochemistry (Moscow), 80 (2015) 50-60.

[93] D. Campbell, V. Hurry, A.K. Clarke, P. Gustafsson, G. Öquist, Chlorophyll Fluorescence Analysis of Cyanobacterial Photosynthesis and Acclimation, Microbiology and Molecular Biology Reviews, 62 (1998) 667-683.

[94] G. Shen, S. Boussiba, W.F. Vermaas, Synechocystis sp PCC 6803 strains lacking photosystem I and phycobilisome function, The Plant cell, 5 (1993) 1853-1863.

[95] U. Schreiber, T. Endo, H. Mi, K. Asada, Quenching Analysis of Chlorophyll Fluorescence by the Saturation Pulse Method: Particular Aspects Relating to the Study of Eukaryotic Algae and Cyanobacteria, Plant and Cell Physiology, 36 (1995) 873-882.

[96] J. Nogales, S. Gudmundsson, E.M. Knight, B.O. Palsson, I. Thiele, Detailing the optimality of photosynthesis in cyanobacteria through systems biology analysis, Proceedings of the National Academy of Sciences, 109 (2012) 2678-2683.

[97] L.-N. Liu, S.J. Bryan, F. Huang, J. Yu, P.J. Nixon, P.R. Rich, C.W. Mullineaux, Control of electron transport routes through redox-regulated redistribution of respiratory complexes, Proceedings of the National Academy of Sciences, 109 (2012) 11431-11436.

[98] M.R. Badger, G.D. Price, CO2 concentrating mechanisms in cyanobacteria: molecular components, their diversity and evolution, Journal of experimental botany, 54 (2003) 609-622.

[99] G.D. Price, M.R. Badger, F.J. Woodger, B.M. Long, Advances in understanding the cyanobacterial CO2-concentrating-mechanism (CCM): functional components, Ci transporters, diversity, genetic regulation and prospects for engineering into plants, Journal of experimental botany, 59 (2008) 1441-1461.

[100] J.C. Goldman, Bioengineering aspects of inorganic carbon supply to mass algal cultures, Third Ann. Biomass Conf. Energy Biomass, Golden Colorado, SERI/TP-33-285, US Dept Energy, 1979, pp. 25-32.

[101] N. Battchikova, J.P. Vainonen, N. Vorontsova, M. Keränen, D. Carmel, E.-M. Aro, Dynamic Changes in the Proteome of Synechocystis 6803 in Response to CO2 Limitation Revealed by Quantitative Proteomics, Journal of Proteome Research, 9 (2010) 5896-5912.

[102] H. Ohkawa, H.B. Pakrasi, T. Ogawa, Two types of functionally distinct NAD(P)H dehydrogenases in Synechocystis sp. strain PCC6803, The Journal of biological chemistry, 275 (2000) 31630-31634.

[103] S.M.E. Daley, A.D. Kappell, M.J. Carrick, R.L. Burnap, Regulation of the Cyanobacterial CO2 Concentrating Mechanism Involves Internal Sensing of NADP+ and α-Ketogutarate Levels by Transcription Factor CcmR, PloS one, 7 (2012) e41286.

[104] P. de Boer, R. Crossley, L. Rothfield, The essential bacterial cell-division protein FtsZ is a GTPase, Nature, 359 (1992) 254-256.

[105] M. Agostoni, B.J. Koestler, C.M. Waters, B.L. Williams, B.L. Montgomery, Occurrence of cyclic di-GMP-modulating output domains in cyanobacteria: an illuminating perspective, mBio, 4 (2013).

[106] R.D. Simon, Cyanophycin Granules from the Blue-Green Alga Anabaena cylindrica: A Reserve Material Consisting of Copolymers of Aspartic Acid and Arginine, Proceedings of the National Academy of Sciences of the United States of America, 68 (1971) 265-267.

[107] M.J. Quintero, A.M. Muro-Pastor, A. Herrero, E. Flores, Arginine Catabolism in the Cyanobacterium Synechocystis sp. Strain PCC 6803 Involves the Urea Cycle and Arginase Pathway, Journal of bacteriology, 182 (2000) 1008-1015.

[108] A. Herrero, M. Burnat, Cyanophycin, a Cellular Nitrogen Reserve Material, in: E. Flores, A. Herrero (Eds.) The Cell Biology of Cyanobacteria, Caister Academic Press, Seville, Spain, 2014, pp. 211-219.

[109] R. Richter, M. Hejazi, R. Kraft, K. Ziegler, W. Lockau, Cyanophycinase, a peptidase degrading the cyanobacterial reserve material multi-L-arginyl-poly-L-aspartic acid (cyanophycin): molecular cloning of the gene of Synechocystis sp. PCC 6803, expression in Escherichia coli, and biochemical characterization of the purified enzyme, European journal of biochemistry / FEBS, 263 (1999) 163-169.

[110] A. Sekowska, A. Danchin, J.L. Risler, Phylogeny of related functions: the case of polyamine biosynthetic enzymes, Microbiology, 146 (Pt 8) (2000) 1815-1828.

[111] K.M. Wegener, A.K. Singh, J.M. Jacobs, T. Elvitigala, E.A. Welsh, N. Keren, M.A. Gritsenko, B.K. Ghosh, D.G. Camp, 2nd, R.D. Smith, H.B. Pakrasi, Global proteomics reveal an atypical strategy for carbon/nitrogen assimilation by a cyanobacterium under diverse environmental perturbations, Molecular & cellular proteomics : MCP, 9 (2010) 2678-2689.

[112] O. Troshina, A. Hansel, P. Lindblad, Cloning, Characterization, and Functional Expression in Escherichia coli of argH Encoding Argininosuccinate Lyase in the Cyanobacterium Nostoc sp. Strain PCC 73102, Current microbiology, 43 (2001) 260-264.

[113] S. Sato, Y. Shimoda, A. Muraki, M. Kohara, Y. Nakamura, S. Tabata, A Large-scale Protein–protein Interaction Analysis in Synechocystis sp. PCC6803, DNA Research, 14 (2007) 207-216.

[114] G. Kufryk, M. Hernandez-Prieto, T. Kieselbach, H. Miranda, W. Vermaas, C. Funk, Association of small CAB-like proteins (SCPs) of Synechocystis sp. PCC 6803 with Photosystem II, Photosynthesis research, 95 (2008) 135-145.

[115] H. Staleva, J. Komenda, M.K. Shukla, V. Šlouf, R. Kaňa, T. Polívka, R. Sobotka, Mechanism of photoprotection in the cyanobacterial ancestor of plant antenna proteins, Nature chemical biology, 11 (2015) 287-291.

[116] J. Qiao, M. Shao, L. Chen, J. Wang, G. Wu, X. Tian, J. Liu, S. Huang, W. Zhang, Systematic characterization of hypothetical proteins in Synechocystis sp. PCC 6803 reveals proteins functionally relevant to stress responses, Gene, 512 (2013) 6-15.

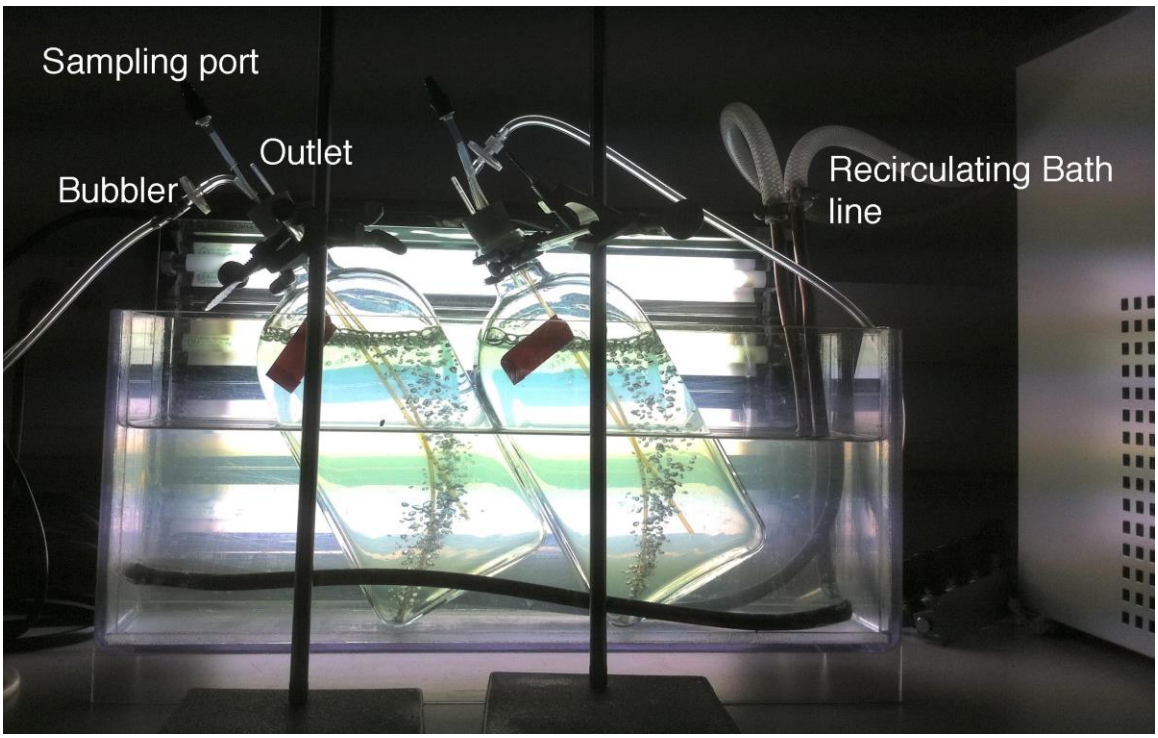

Figure 1: Cyanobacteria growth set up. Two biological replicates were grown at a time. Cultures were held at an angle as shown to evenly distribute gas. A light, shown here in the background provided either continuous or fluctuating illumination to the cultures.

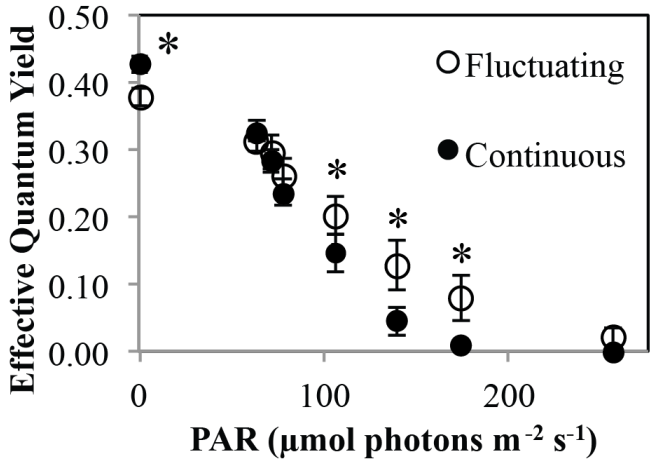

Figure 2: At light intensities of 106-174 µmol photon m^{-2} s^{-1} cultures cultivated in fluctuating light have a higher capacity for photosynthesis, as shown by a graph of the effective quantum yield of PSII (YII) measured across a rapid light curve. Points at 390, 590, and 908 µmol photon m^{-2} s^{-1} had a YII of 0 and are omitted from this graph. Values represent the mean of biological replicates with error bars ± 1 standard deviation. n=3 continuous, n=6 fluctuating. The average of two technical replicates is taken for each biological replicate. *= significant difference using a students t-test ($p<0.05$).

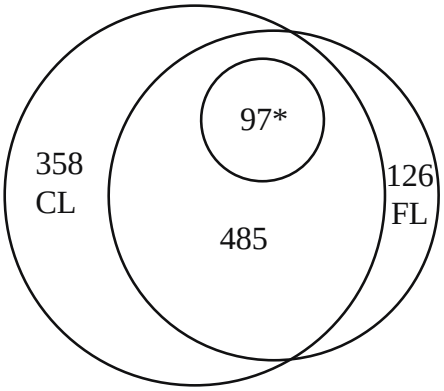

Figure 3: Distribution of identified proteins under 2 light conditions: CL: Continuous Light FL: Fluctuating Light. *= Proteins with a significantly different abundance between the two conditions ($p<0.1$) In total identified 1066 proteins of 3673 in *Synechocystis sp.* PCC6803 genome.

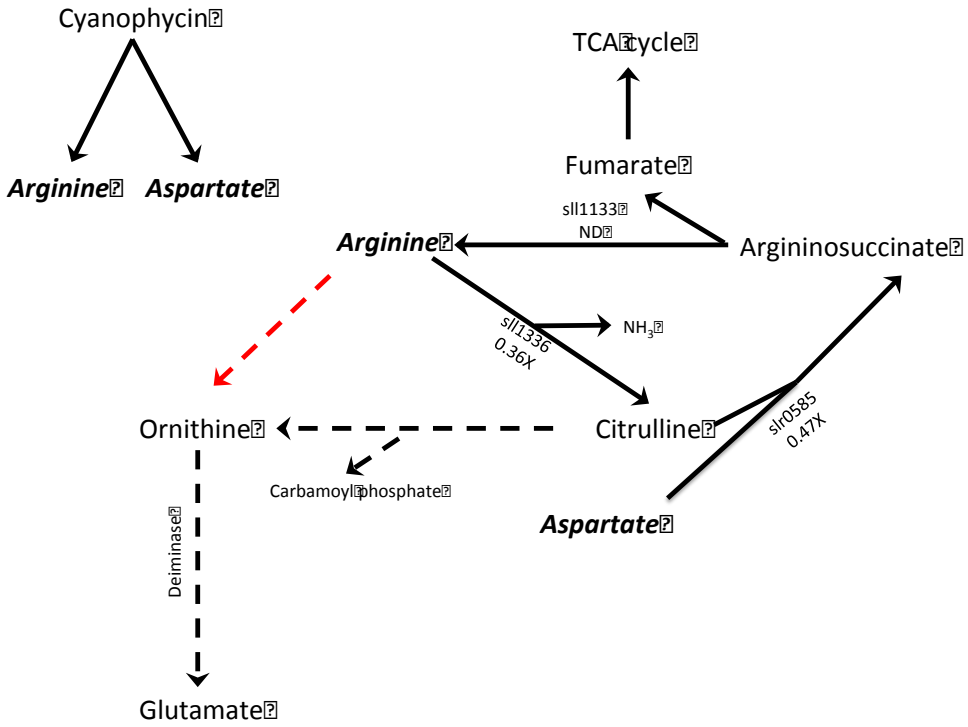

Figure 4: Based on recent findings in the literature, and our proteomic results, we propose a modification of the cycle originally proposed by Quintero et al. (2000) for the degradation of the components of cyanophycin: aspartate and arginine [107]. The cycle from arginine to citrulline to argininosuccinate is shown in solid lines. A possible route of arginine degradation is shown in dotted lines. The dehydrogenation of arginine to ornithine (shown in red) was demonstrated by Sekowkska et al. (2000) to not be catalyzed by any of the proposed enzymes, suggesting this step may not occur [110]. This cycle uses modifications to arginine to ultimately break aspartate into NH_3 and fumarate, which can be further catabolized in the TCA cycle. We found two of the three enzymes involved in this pathway were significantly reduced in fluctuating light, and one was not present in fluctuating light.

Table 1: *Differences in growth, photosynthetic efficiency (F_v/F_m) and reactive oxygen species generation (CellROX) observed in Synechocystis cultures growing in fluctuating light versus continuous light*

Treatment	Exponential growth rate (day^{-1})[a]	CellROX RFU/cell[b]	F_v/F_m[c]
Continuous Light	3.0 ± 0.2	1044 ± 51	0.43 ± 0.01
Fluctuating Light	1.6 ± 0.4	828 ± 43	0.38 ± 0.01

a. Data represent the mean ± 1 standard deviation of biological replicates: n=3 continuous, n=6 fluctuating. Growth rates were significantly different using a students t-test ($p<0.05$).

b. Higher relative fluorescence units (RFU) per cell of the intracellular dye CellROX green represent more reactive oxygen species. Data represent the mean ± 1 standard deviation of biological replicates: n=3 continuous, n=4 fluctuating. Levels were significantly different using a students t-test ($p<0.05$).

c. Data represent the mean ± 1 standard deviation of biological replicates: n=3 continuous, n=6 fluctuating. Each biological replicate is the average of 2 F_v/F_m technical replicates. F_v/F_m was significantly different using a Student's t-test ($p<0.05$)

Table 2. *Subset of differentially abundant* Synechocystis *proteins in fluctuating (FL) vs continuous light (CL) with significance p<0.05*
Abundance was determined by label-free quantification using Peaks 7.0. Proteins were filtered for a peptide significance of p<0.05 and an abundance signficance of p<0.05. Values are based on 2 biological replicates. Locus ID, gene symbol and annotation are derived from

Locus ID	Gene Symbol	Annotation	Ratio (FL/CL)	p value
sll0170	dnaK2	DnaK protein 2 heat shock protein 70 molecular chaperone	0.41	0.004
sll0172		periplasmic protein function unknown	4.84	0.012
sll0199	petE	plastocyanin	3.14	0.014
sll0258	psbV	cytochrome c550	3.10	0.025
sll0379	lpxA	acyl-[acyl-carrier-protein]--UDP-N-acetylglucosamine o-acyltransferase	0.20	0.003
sll0448		unknown protein	3.87	0.047
sll0480	dapL	probable aminotransferase	0.22	0.021
sll0519	ndhA	NADH dehydrogenase subunit 1	0.18	0.030
sll0588		unknown protein	**only in FL**	0.008
sll0822	abrB2	AbrB-like transcriptional regulator	0.43	0.044
sll0849	psbD	photosystem II reaction center D2 protein	0.39	0.004
sll0872		unknown protein	4.77	0.012
sll1028	ccmK2	carbon dioxide concentrating mechanism protein CcmK	8.63	0.000
sll1029	ccmK1	carbon dioxide concentrating mechanism protein CcmK	6.44	0.002
sll1043	pnp	polyribonucleotide nucleotidyltransferase	0.37	0.035
sll1069	fabF	3-oxoacyl-[acyl-carrier-protein] synthase II	2.08	0.022
sll1185	hemF	coproporphyrinogen III oxidase aerobic (oxygen-dependent)	2.16	0.005
sll1214	ycf59	magnesium-protoporphyrin IX monomethyl ester cyclase	0.18	0.046
sll1262	ndhN	NadhN	0.26	0.027
sll1322	atpI	ATP synthase A chain of CF(0)	0.25	0.026
sll1336		putative L-arginine deiminase	0.36	0.004
sll1471	cpcG2	phycobilisome rod-core linker polypeptide	0.07	0.016
sll1553	pheT	phenylalanyl-tRNA synthetase	0.20	0.014
sll1625	sdhB	succinate dehydrogenase iron- sulphur protein subunit	9.45	0.039
sll1694	pilA1	pilin polypeptide PilA1	3.62	0.045
sll1769		hypothetical protein	4.09	0.039
sll1784		periplasmic protein function unknown	2.68	0.008
sll1804	rps3	30S ribosomal protein S3	0.09	0.002
sll1817	rps11	30S ribosomal protein S11	0.14	0.040
sll1822	rps9	30S ribosomal protein S9	0.19	0.004

Table 2. Continued

Locus ID	Gene Symbol	Annotation	Ratio (FL/CL)	p value
sll1910	zam	protein conferring resistance to acetazolamide Zam	0.11	0.006
sll1945	dxs	1-deoxyxylulose-5-phosphate synthase	0.33	0.016
slr0001		hypothetical protein	0.15	0.002
slr0213	guaA	GMP synthetase	0.25	0.003
slr0455		hypothetical protein	2.08	0.022
slr0552		hypothetical protein	0.39	0.010
slr0585	argG	argininosuccinate synthetase	0.47	0.031
slr0597	purH	phosphoribosyl aminoimidazole carboxy formyl formyltransferase/inosinemonophosphate cyclohydrolase (PUR-H(J))	0.09	0.033
slr0659	prlC, opdA	oligopeptidase A	0.33	0.016
slr0739	crtE	geranylgeranyl pyrophosphate synthase	0.38	0.009
slr0782		putative flavin-containing monoamine oxidase	6.31	0.006
slr0879	gcvH	glycine decarboxylase complex H-protein	2.17	0.026
slr0899	cynS	cyanate lyase	**only in FL**	0.017
slr0965	dnaN	DNA polymerase III beta subunit	0.17	0.001
slr1265	rpoC1	RNA polymerase gamma-subunit	0.31	0.024
slr1295	futA1	iron transport system substrate-binding protein	2.08	0.011
slr1299		UDP-glucose dehydrogenase	0.15	0.045
slr1342		hypothetical protein	0.28	0.043
slr1471	yidC	hypothetical protein	3.14	0.015
slr1590		hypothetical protein	0.27	0.024
slr1645	psb27,psbZ	photosystem II 11 kD protein	0.24	0.001
slr1722	guaB, gnaB	inosine-5'-monophosphate dehydrogenase	0.30	0.004
slr1835	psaB	P700 apoprotein subunit Ib	0.43	0.021
slr1842	cysK	cysteine synthase	3.38	0.048
slr1852		unknown protein	3.98	0.011
slr1853		carboxymuconolactone decarboxylase	5.65	0.043
slr1856		phosphoprotein substrate of icfG gene cluster	6.85	0.034
slr1934	pdhA	pyruvate dehydrogenase E1 component alpha subunit	0.15	0.032
slr2075	groES	10kD chaperonin	2.75	0.012
ssl1426	rpl35	50S ribosomal protein L35	0.56	0.024
ssr0482	rps16	30S ribosomal protein S16	0.26	0.005

Supplemental Table 1. *Subset of differentially abundant* Synechocystis *proteins in fluctuating (FL) vs continuous light (CL) with significance of 0.05<p<0.1*
Abundance was determined by label-free quantification using Peaks 7.0. Proteins were filtered for a peptide significance of p<0.05 and an abundance signficance of 0.05<p<0.1. Values are based on 2 biological replicates. Locus ID, gene symbol and annotation are derived from cyanobase.

Locus ID	Gene Symbol	Annotation	Ratio (FL/CL)	p value
sll0064		periplasmic protein putative polar amino acid transport system substrate-binding protein	4.79	0.082
sll0271	nusB	N utilization substance protein B homolog	0.03	0.063
sll0359		hypothetical protein	0.20	0.068
sll0395		phosphoglycerate mutase	0.06	0.082
sll1021		hypothetical protein	0.11	0.064
sll1180	hlyB	toxin secretion ABC transporter ATP-binding protein	0.25	0.080
sll1260	rps2	30S ribosomal protein S2	0.28	0.079
sll1342	gap2	NAD(P)-dependent glyceraldehyde-3-phosphate dehydrogenase	4.21	0.076
sll1398	psb28	photosystem II reaction center 13 kDa protein	4.15	0.057
sll1525	prk	phosphoribulokinase	0.39	0.083
sll1536	moeB	molybdopterin biosynthesis MoeB protein	0.21	0.053
sll1733	ndhD3	NADH dehydrogenase subunit 4 (involved in low CO2-inducible high affinity CO2 uptake	0.12	0.089
sll1734	cupA	protein involved in low CO2-inducible high affinity CO2 uptake	0.10	0.084
sll1789	rpoC2	RNA polymerase beta prime subunit	0.23	0.053
sll1812	rps5	30S ribosomal protein S5	0.42	0.077
sll1987	katG	catalase peroxidase	2.15	0.071
sll2010	murD	UDP-N-acetylmuramoylalanine--D-glutamate ligase	0.19	0.052
slr0261	ndhH	NADH dehydrogenase subunit 7	0.33	0.051
slr0452	ilvD	dihydroxyacid dehydratase	4.68	0.058
slr0469	rps4	30S ribosomal protein S4	0.17	0.067
slr0844	ndhF1	NADH dehydrogenase subunit 5	**only in CL**	0.094
slr0906	psbB	photosystem II core light harvesting protein	0.28	0.091
slr0947	rpaB	response regulator for energy transfer from phycobilisomes to photosystems	0.18	0.066
slr0984	rfbG	CDP-glucose 4 6-dehydratase	7.96	0.060
slr1098		hypothetical protein	3.09	0.081
slr1165	met3, sopT, sat	sulfate adenylyltransferase	0.34	0.077
slr1171	gpx1	glutathione peroxidase-like NADPH peroxidase glutathione peroxidase	0.25	0.054
slr1517	leuB	3-isopropylmalate dehydrogenase	0.24	0.061
slr1641	clpB1	ClpB protein	0.29	0.074

Supplemental Table 1. Continued

Locus ID	Gene Symbol	Annotation	Ratio (FL/CL)	p value
slr1702		hypothetical protein	0.14	0.084
slr1761	ytfC	FKBP-type peptidyl-prolyl cis-trans isomerase periplasmic protein	4.58	0.099
slr1763		probable methyltransferase	0.31	0.075
slr1841		probable porin; major outer membrane protein	0.17	0.051
slr5112		unknown protein	1.41	0.094
slr7023		hypothetical protein	**only in FL**	0.071
ssl3445	rpl31	50S ribosomal protein L31	4.17	0.076

Supplemental Table 2. *All proteins identified with a peptide significance of p<0.05 in one or both biological replicates of Continuous or Fluctuating light cultures*
0: not identified, one: identified in one of the biological repliates, Both: Identified in both biological replicates, yes: identified in all samples and their biological replicates

Locus ID	Annotation	Continuous Light	Fluctuating Light	All samples?
sll0558	hypothetical protein YCF53	**BOTH**	0	
sll1214	hypothetical protein YCF59	**BOTH**	**BOTH**	**Yes**
sll1213	GDP-fucose synthetase	**BOTH**	**BOTH**	**Yes**
sll1212	GDP-mannose 4,6-dehydratase	**BOTH**	one	
slr1311	photosystem II D1 protein	**BOTH**	**BOTH**	**Yes**
slr1492	iron(III) dicitrate transport system substrate-binding protein	one	0	
sll1401	unknown protein	one	0	
sll1398	photosystem II reaction center 13 kDa protein	**BOTH**	**BOTH**	**Yes**
slr1495	hypothetical protein	one	0	
sll1393	glycogen (starch) synthase	**BOTH**	0	
ssr1853	unknown protein	**BOTH**	**BOTH**	**Yes**
sll1059	adenylate kinase	one	0	
sll1058	dihydrodipicolinate reductase	**BOTH**	one	
sll1056	phosphoribosylformyl glycinamidine synthetase II	**BOTH**	0	
sll1054	hypothetical protein	0	**BOTH**	
sll1053	hypothetical protein	**BOTH**	0	
slr1124	phosphoglycerate mutase	**BOTH**	**BOTH**	**Yes**
sll1049	hypothetical protein	one	0	
slr1128	hypothetical protein	**BOTH**	one	
slr1129	ribonuclease E	**BOTH**	0	
sll1043	polyribonucleotide nucleotidyltransferase	**BOTH**	**BOTH**	**Yes**
slr0721	malic enzyme	**BOTH**	0	
sll0712	cysteine synthase	**BOTH**	**BOTH**	**Yes**
slr0728	hypothetical protein	one	0	
slr0729	hypothetical protein	**BOTH**	**BOTH**	**Yes**
slr0731	hypothetical protein	one	0	
slr0737	photosystem I subunit II	**BOTH**	**BOTH**	**Yes**
slr0738	anthranilate synthetase alpha-subunit	one	0	
slr0739	geranylgeranyl pyrophosphate synthase	**BOTH**	0	
slr0740	hypothetical protein	one	0	
slr0743	similar to N utilization substance protein	**BOTH**	**BOTH**	**Yes**

Supplemental Table 2. Continued

Locus ID	Annotation	Continuous Light	Fluctuating Light	All samples?
slr0744	translation initiation factor IF-2	**BOTH**	**BOTH**	**Yes**
slr0242	bacterioferritin comigratory protein homolog	**BOTH**	**BOTH**	**Yes**
sll0230	hypothetical protein	0	one	
slr0244	hypothetical protein	**BOTH**	**BOTH**	**Yes**
sll0228	arginase	one	**BOTH**	
sll0227	peptidyl-prolyl cis-trans isomerase B, periplasmic protein	**BOTH**	**BOTH**	**Yes**
sll0224	amino-acid ABC transporter binding protein	**BOTH**	**BOTH**	**Yes**
slr0250	hypothetical protein	0	one	
ssr0390	photosystem I reaction center subunit X	**BOTH**	**BOTH**	**Yes**
sll0220	L-glutamine:D-fructose-6-P amidotransferase	**BOTH**	0	
sll0219	flavoprotein	0	one	
sll1327	ATP synthase gamma chain	**BOTH**	**BOTH**	**Yes**
sll1326	ATP synthase alpha chain	**BOTH**	**BOTH**	**Yes**
sll1325	ATP synthase delta chain of CF(1)	**BOTH**	**BOTH**	**Yes**
sll1324	ATP synthase B chain (subunit I) of CF(0)	one	**BOTH**	
sll1323	ATP synthase subunit b' of CF(0)	**BOTH**	**BOTH**	**Yes**
ssl2615	ATP synthase C chain of CF(0)	one	0	
sll1322	ATP synthase A chain of CF(0)	**BOTH**	**BOTH**	**Yes**
slr1096	dihydrolipoamide dehydrogenase	**BOTH**	**BOTH**	**Yes**
slr1097	hypothetical protein	**BOTH**	**BOTH**	**Yes**
slr1098	hypothetical protein	one	0	
slr1105	GTP-binding protein TypA/BipA homolog	**BOTH**	**BOTH**	**Yes**
ssl2009	hypothetical protein	one	**BOTH**	
sll1035	uracil phosphoribosyltransferase	**BOTH**	one	
slr1106	prohibitin	one	0	
sll1033	probable protein phosphatase	**BOTH**	one	
sll1031	carbon dioxide concentrating mechanism protein CcmM, putative carboxysome structural protein	**BOTH**	**BOTH**	**Yes**
sll1029	carbon dioxide concentrating mechanism protein CcmK	**BOTH**	**BOTH**	**Yes**
sll1028	carbon dioxide concentrating mechanism protein CcmK	**BOTH**	**BOTH**	**Yes**
sll1027	NADH-dependent glutamate synthase small subunit	**BOTH**	one	
slr1777	magnesium protoporphyrin IX chelatase subunit D	0	one	
sll1682	alanine dehydrogenase	one	0	

Supplemental Table 2. Continued

Locus ID	Annotation	Continuous Light	Fluctuating Light	All samples?
slr1780	hypothetical protein YCF54	**BOTH**	**BOTH**	**Yes**
sll1681	unknown protein	one	0	
sll1680	hypothetical protein	**BOTH**	0	
sll1679	periplasmic protease HhoA	**BOTH**	0	
slr1783	two-component response regulator NarL subfamily	**BOTH**	**BOTH**	**Yes**
slr1784	biliverdin reductase	0	one	
sll1676	4-alpha-glucanotransferase	**BOTH**	0	
slr1789	unknown protein	0	one	
sll1670	heat-inducible transcription repressor HrcA homolog	0	one	
sll1669	shikimate kinase	**BOTH**	0	
slr1793	transaldolase	**BOTH**	**BOTH**	**Yes**
ssr2998	hypothetical protein	**BOTH**	**BOTH**	**Yes**
slr1794	probable anion transporting ATPase	**BOTH**	0	
slr1796	hypothetical protein	**BOTH**	0	
sll1665	unknown protein	**BOTH**	**BOTH**	**Yes**
sll1663	phycocyanin alpha phycocyanobilin lyase related protein	**BOTH**	**BOTH**	**Yes**
slr1800	hypothetical protein	**BOTH**	0	
sll1656	hypothetical protein	one	0	
sll1654	hypothetical protein	**BOTH**	**BOTH**	**Yes**
slr1289	isocitrate dehydrogenase (NADP+)	**BOTH**	one	
slr1295	iron transport system substrate-binding protein	**BOTH**	**BOTH**	**Yes**
sll1198	tRNA (guanine-N1)-methyltransferase	0	one	
sll1194	photosystem II 12 kDa extrinsic protein	**BOTH**	**BOTH**	**Yes**
slr1299	UDP-glucose dehydrogenase	**BOTH**	one	
slr1301	hypothetical protein	**BOTH**	**BOTH**	**Yes**
sll1189	glycolate oxidase subunit GlcE	one	0	
sll1188	hypothetical protein	**BOTH**	**BOTH**	**Yes**
sll1185	coproporphyrinogen III oxidase, aerobic (oxygen-dependent)	**BOTH**	**BOTH**	**Yes**
sll1184	heme oxygenase	**BOTH**	**BOTH**	**Yes**
slr1307	hypothetical protein	0	**BOTH**	
ssr1604	50S ribosomal protein L28	**BOTH**	**BOTH**	**Yes**
slr0962	unknown protein	one	0	
slr0963	ferredoxin-sulfite reductase	**BOTH**	**BOTH**	**Yes**

Supplemental Table 2. Continued

Locus ID	Annotation	Continuous Light	Fluctuating Light	All samples?
slr0965	DNA polymerase III beta subunit	**BOTH**	0	
slr0966	tryptophan synthase alpha chain	**BOTH**	**BOTH**	**Yes**
sll0936	putative oxidoreductase	one	0	
slr0969	precorrin methylase	one	**BOTH**	
sll0934	carboxysome formation protein CcmA	**BOTH**	**BOTH**	**Yes**
sll0931	hypothetical protein	one	0	
sll0928	allophycocyanin-B	**BOTH**	**BOTH**	**Yes**
sll0927	S-adenosylmethionine synthetase	**BOTH**	**BOTH**	**Yes**
slr0974	initiation factor IF-3	**BOTH**	**BOTH**	**Yes**
slr0977	ABC transporter, permease component	one	**BOTH**	
slr0978	hypothetical protein	one	0	
slr0984	CDP-glucose 4,6-dehydratase	one	**BOTH**	
slr1610	putative C-3 methyl transferase	0	one	
slr1618	unknown protein	**BOTH**	0	
slr1619	hypothetical protein	**BOTH**	**BOTH**	**Yes**
slr1074	unknown protein	one	one	
ssr1765	hypothetical protein	**BOTH**	0	
ssl1972	hypothetical protein	**BOTH**	**BOTH**	**Yes**
sll1023	succinyl-CoA synthetase beta chain	**BOTH**	0	
sll1021	hypothetical protein	**BOTH**	one	
slr0670	hypothetical protein	**BOTH**	0	
slr0676	adenylylsulfate kinase	**BOTH**	**BOTH**	**Yes**
slr0678	biopolymer transport ExbD like protein	0	one	
slr0679	sun protein	one	0	
sll0646	guanylyl cyclase	one	0	
sll0634	photosystem I biogenesis protein BtpA	one	0	
slr0695	hypothetical protein	**BOTH**	0	
slr1590	hypothetical protein	**BOTH**	0	
sll1516	hypothetical protein	one	0	
slr1596	a protein in the cytoplasmic membrane involved in light-induced proton extrusion.	0	one	
sll1514	16.6 kDa small heat shock protein, molecular chaperone	**BOTH**	0	
sll1509	hypothetical protein YCF20	0	one	

Supplemental Table 2. Continued

Locus ID	Annotation	Continuous Light	Fluctuating Light	All samples?
slr1600	hypothetical protein	**BOTH**	**BOTH**	**Yes**
slr1604	cell division protein FtsH	**BOTH**	**BOTH**	**Yes**
sll1502	NADH-dependent glutamate synthase large subunit	**BOTH**	**BOTH**	**Yes**
slr1609	long-chain-fatty-acid CoA ligase	**BOTH**	one	
slr1042	two-component response regulator CheY subfamily	**BOTH**	**BOTH**	**Yes**
slr1043	similar to chemotaxis protein CheW	**BOTH**	**BOTH**	**Yes**
slr1044	methyl-accepting chemotaxis protein, required for the biogenesis of thick pilli	one	0	
slr1048	hypothetical protein	0	one	
ssr1736	50S ribosomal protein L32	**BOTH**	**BOTH**	**Yes**
slr1051	enoyl-[acyl-carrier-protein] reductase	**BOTH**	one	
slr1053	unknown protein	one	0	
slr1055	magnesium protoporphyrin IX chelatase subunit H	**BOTH**	0	
ssl1918	hypothetical protein	**BOTH**	0	
slr1755	NAD+ dependent glycerol-3-phosphate dehydrogenase	one	0	
slr1756	glutamate--ammonia ligase	**BOTH**	**BOTH**	**Yes**
slr1761	FKBP-type peptidyl-prolyl cis-trans isomerase, periplasmic protein	**BOTH**	**BOTH**	**Yes**
slr1763	probable methyltransferase	**BOTH**	one	
sll1641	glutamate decarboxylase	**BOTH**	0	
sll1638	hypothetical protein	**BOTH**	**BOTH**	**Yes**
sll1635	Thy1 protein homolog	one	0	
ssr3122	hypothetical protein	**BOTH**	**BOTH**	**Yes**
slr1847	hypothetical protein	**BOTH**	**BOTH**	**Yes**
slr1848	histidinol dehydrogenase	**BOTH**	**BOTH**	**Yes**
slr1849	probable mercuric reductase	one	0	
sll1750	urease alpha subunit	**BOTH**	one	
slr2032	hypothetical protein YCF23	**BOTH**	**BOTH**	**Yes**
sll1945	1-deoxyxylulose-5-phosphate synthase	**BOTH**	**BOTH**	**Yes**
slr2033	membrane-associated rubredoxin, essential for photosystem I assembly	**BOTH**	**BOTH**	**Yes**
slr2034	putative homolog of plant HCF136, which is essential for stability or assembly of photosystem II	**BOTH**	**BOTH**	**Yes**
ssr3451	cytochrome b559 alpha subunit	**BOTH**	**BOTH**	**Yes**
smr0006	cytochrome b559 b subunit	**BOTH**	**BOTH**	**Yes**
sll1941	DNA gyrase A subunit	one	one	
slr2041	probable two-component response regulator	one	0	

Supplemental Table 2. Continued

Locus ID	Annotation	Continuous Light	Fluctuating Light	All samples?
sll1940	hypothetical protein	0	one	
sll1938	hypothetical protein	one	**BOTH**	
slr2043	zinc transport system substrate-binding protein	one	0	
slr2049	hypothetical protein YCF58	one	**BOTH**	
slr2051	phycobilisome rod-core linker polypeptide	**BOTH**	**BOTH**	**Yes**
sll1932	DnaK protein	**BOTH**	one	
sll1931	serine hydroxymethyltransferase	**BOTH**	**BOTH**	**Yes**
slr1908	probable porin; major outer membrane protein	0	**BOTH**	
slr1909	two-component response regulator NarL subfamily	**BOTH**	**BOTH**	**Yes**
sll1837	periplasmic protein, function unknown	0	**BOTH**	
slr1913	hypothetical protein	0	one	
sll1835	periplasmic protein, function unknown	**BOTH**	**BOTH**	**Yes**
sll1830	unknown protein	**BOTH**	**BOTH**	**Yes**
sll0998	LysR family transcriptional regulator	**BOTH**	0	
slr1020	sulfolipid biosynthesis protein SqdB	**BOTH**	**BOTH**	**Yes**
sll0993	potassium channel	0	one	
slr1022	N-acetylornithine aminotransferase	**BOTH**	**BOTH**	**Yes**
slr1030	magnesium protoporphyrin IX chelatase subunit I	**BOTH**	**BOTH**	**Yes**
slr1031	tyrosyl tRNA synthetase	**BOTH**	0	
slr1034	hypothetical protein YCF41	**BOTH**	**BOTH**	**Yes**
sll0985	unknown protein	0	one	
sll0982	unknown protein	**BOTH**	**BOTH**	**Yes**
sll1298	putative carboxymethylenebutenolidase	**BOTH**	**BOTH**	**Yes**
sll1294	methyl-accepting chemotaxis protein	**BOTH**	one	
sll1292	two-component response regulator CheY subfamily	**BOTH**	0	
sll1289	hypothetical protein	**BOTH**	**BOTH**	**Yes**
slr1390	cell division protein FtsH	**BOTH**	0	
slr1393	phytochrome-like protein, two-component sensor histidine kinase	**BOTH**	**BOTH**	**Yes**
sll1283	similar to stage II sporulation protein D	one	0	
sll1583	unknown protein	**BOTH**	**BOTH**	**Yes**
sll1582	unknown protein	**BOTH**	**BOTH**	**Yes**
slr1702	hypothetical protein	**BOTH**	one	
slr1703	seryl-tRNA synthetase	**BOTH**	**BOTH**	**Yes**

Supplemental Table 2. Continued

Locus ID	Annotation	Continuous Light	Fluctuating Light	All samples?
ssl3093	phycobilisome small rod linker polypeptide	**BOTH**	**BOTH**	**Yes**
sll1580	phycobilisome rod linker polypeptide	**BOTH**	**BOTH**	**Yes**
sll1579	phycobilisome rod linker polypeptide	**BOTH**	**BOTH**	**Yes**
sll1578	phycocyanin alpha subunit	**BOTH**	**BOTH**	**Yes**
sll1577	phycocyanin beta subunit	**BOTH**	**BOTH**	**Yes**
slr1704	hypothetical protein	**BOTH**	0	
ssr2857	mercuric transport protein periplasmic component precursor	**BOTH**	**BOTH**	**Yes**
slr1708	probable peptidase	**BOTH**	0	
sll1568	fibrillin	one	0	
slr2005	periplasmic protein, function unknown	**BOTH**	0	
slr2023	malonyl coenzyme A-acyl carrier protein transacylase	one	one	
slr2024	two-component response regulator CheY subfamily	**BOTH**	**BOTH**	**Yes**
sll1911	hypothetical protein	0	**BOTH**	
sll1910	protein conferring resistance to acetazolamide Zam	**BOTH**	0	
slr2030	hypothetical protein	one	0	
slr1133	L-argininosuccinate lyase	**BOTH**	0	
slr1135	unknown protein	one	one	
sll1084	hypothetical protein	one	0	
slr1139	thioredoxin	0	one	
slr1140	DegT/DnrJ/EryC1/StrS family protein	**BOTH**	**BOTH**	**Yes**
sll1076	cation-transporting ATPase PacL	0	**BOTH**	
sll1074	leucyl-tRNA synthetase	**BOTH**	one	
sml0011	hypothetical protein	**BOTH**	one	
sll1070	transketolase	**BOTH**	**BOTH**	**Yes**
sll1069	3-oxoacyl-[acyl-carrier-protein] synthase II	**BOTH**	**BOTH**	**Yes**
ssl2084	acyl carrier protein	**BOTH**	**BOTH**	**Yes**
ssl3451	hypothetical protein	0	one	
slr1890	bacterioferritin	**BOTH**	**BOTH**	**Yes**
sll1824	50S ribosomal protein L25	one	0	
sll1823	adenylosuccinate synthetase	**BOTH**	**BOTH**	**Yes**
ssl3445	50S ribosomal protein L31	**BOTH**	**BOTH**	**Yes**
sll1822	30S ribosomal protein S9	**BOTH**	**BOTH**	**Yes**
sll1821	50S ribosomal protein L13	**BOTH**	**BOTH**	**Yes**

Supplemental Table 2. Continued

Locus ID	Annotation	Continuous Light	Fluctuating Light	All samples?
sll1819	50S ribosomal protein L17	**BOTH**	**BOTH**	**Yes**
sll1818	RNA polymerase alpha subunit	**BOTH**	**BOTH**	**Yes**
sll1817	30S ribosomal protein S11	**BOTH**	**BOTH**	**Yes**
sll1816	30S ribosomal protein S13	**BOTH**	**BOTH**	**Yes**
ssl3441	initiation factor IF-1	**BOTH**	**BOTH**	**Yes**
sll1815	adenylate kinase	**BOTH**	**BOTH**	**Yes**
sll1814	preprotein translocase SecY subunit	**BOTH**	0	
sll1813	50S ribosomal protein L15	**BOTH**	**BOTH**	**Yes**
sll1812	30S ribosomal protein S5	**BOTH**	**BOTH**	**Yes**
sll1811	50S ribosomal protein L18	**BOTH**	**BOTH**	**Yes**
sll1810	50S ribosomal protein L6	**BOTH**	**BOTH**	**Yes**
sll1809	30S ribosomal protein S8	**BOTH**	**BOTH**	**Yes**
sll1808	50S ribosomal protein L5	**BOTH**	**BOTH**	**Yes**
sll1807	50S ribosomal protein L24	one	**BOTH**	
sll1806	50S ribosomal protein L14	**BOTH**	**BOTH**	**Yes**
ssl3437	30S ribosomal protein S17	**BOTH**	0	
ssl3436	50S ribosomal protein L29	**BOTH**	**BOTH**	**Yes**
sll1805	50S ribosomal protein L16	**BOTH**	**BOTH**	**Yes**
sll1804	30S ribosomal protein S3	**BOTH**	**BOTH**	**Yes**
sll1803	50S ribosomal protein L22	**BOTH**	**BOTH**	**Yes**
ssl3432	30S ribosomal protein S19	**BOTH**	**BOTH**	**Yes**
sll1802	50S ribosomal protein L2	**BOTH**	**BOTH**	**Yes**
sll1801	50S ribosomal protein L23	**BOTH**	**BOTH**	**Yes**
sll1800	50S ribosomal protein L4	**BOTH**	**BOTH**	**Yes**
sll1799	50S ribosomal protein L3	**BOTH**	**BOTH**	**Yes**
slr1894	probable DNA-binding stress protein	**BOTH**	**BOTH**	**Yes**
sll1796	cytochrome c553	**BOTH**	**BOTH**	**Yes**
slr1898	N-acetylglutamate kinase	one	one	
slr1900	hypothetical protein	**BOTH**	**BOTH**	**Yes**
sll1789	RNA polymerase beta prime subunit	**BOTH**	**BOTH**	**Yes**
sll1787	RNA polymerase beta subunit	**BOTH**	**BOTH**	**Yes**
sll1786	putative deoxyribonuclease, tatD homolog	0	**BOTH**	
ssl2233	30S ribosomal protein S20	**BOTH**	**BOTH**	**Yes**

Supplemental Table 2. Continued

Locus ID	Annotation	Continuous Light	Fluctuating Light	All samples?
slr1194	hypothetical protein	**BOTH**	0	
slr1196	periplasmic protein, function unknown	one	one	
slr1198	antioxidant protein	**BOTH**	**BOTH**	**Yes**
slr1199	DNA mismatch repair protein MutL	one	0	
slr1204	protease	one	0	
slr1205	similar to chlorobenzene dioxygenase, ferredoxin component	**BOTH**	**BOTH**	**Yes**
slr1208	probable oxidoreductase	one	one	
slr1211	cobalt-chelatase subunit CobN	**BOTH**	0	
sll1971	probable hexosyltransferase	one	0	
slr2072	L-threonine deaminase	one	0	
slr2073	hypothetical protein YCF50	**BOTH**	**BOTH**	**Yes**
slr2075	10kD chaperonin	**BOTH**	**BOTH**	**Yes**
slr2076	60kD chaperonin	**BOTH**	**BOTH**	**Yes**
sll1747	chorismate synthase	**BOTH**	**BOTH**	**Yes**
sll1746	50S ribosomal protein L12	**BOTH**	**BOTH**	**Yes**
sll1745	50S ribosomal protein L10	**BOTH**	**BOTH**	**Yes**
sll1744	50S ribosomal protein L1	**BOTH**	**BOTH**	**Yes**
sll1743	50S ribosomal protein L11	**BOTH**	**BOTH**	**Yes**
sll1742	transcription antitermination protein NusG	**BOTH**	**BOTH**	**Yes**
sll1740	50S ribosomal protein L19	**BOTH**	**BOTH**	**Yes**
sll1737	hypothetical protein YCF60	one	0	
slr1828	ferredoxin, petF-like protein	one	**BOTH**	
sll1735	hypothetical protein	**BOTH**	**BOTH**	**Yes**
sll1734	protein involved in low CO2-inducible, high affinity CO2 uptake	**BOTH**	0	
sll1733	NADH dehydrogenase subunit 4 (involved in low CO2-inducible, high affinity CO2 uptake)	**BOTH**	0	
slr1834	P700 apoprotein subunit Ia	**BOTH**	**BOTH**	**Yes**
slr1835	P700 apoprotein subunit Ib	**BOTH**	**BOTH**	**Yes**
sll1723	probable glycosyltransferase	0	one	
sll1721	pyruvate dehydrogenase E1 component, beta subunit	**BOTH**	**BOTH**	**Yes**
slr1838	carbon dioxide concentrating mechanism protein CcmK homolog 3, putative carboxysome assembly protein	one	0	
slr1839	carbon dioxide concentrating mechanism protein CcmK homolog 4, putative carboxysome assembly protein	**BOTH**	one	
slr1841	probable porin; major outer membrane protein	**BOTH**	**BOTH**	**Yes**

Supplemental Table 2. Continued

Locus ID	Annotation	Continuous Light	Fluctuating Light	All samples?
slr1842	cysteine synthase	**BOTH**	**BOTH**	**Yes**
slr1843	glucose 6-phosphate dehydrogenase	**BOTH**	0	
sll1712	DNA binding protein HU	**BOTH**	**BOTH**	**Yes**
slr1537	unknown protein	one	0	
slr1540	mRNA-binding protein	**BOTH**	one	
slr1542	2-C-methyl-D-erythritol 2,4-cyclodiphosphate synthase	one	**BOTH**	
sll1463	cell division protein FtsH	**BOTH**	**BOTH**	**Yes**
slr1549	polypeptide deformylase	**BOTH**	**BOTH**	**Yes**
slr1550	lysyl-tRNA synthetase	**BOTH**	0	
sll1457	probable glycosyltransferase	**BOTH**	0	
sll1456	unknown protein	one	0	
sll1454	ferredoxin-nitrate reductase	one	0	
sll1453	nitrate/nitrite transport system ATP-binding protein	**BOTH**	0	
sll1452	nitrate/nitrite transport system ATP-binding protein	**BOTH**	0	
sll1451	nitrate/nitrite transport system permease protein	**BOTH**	0	
sll1450	nitrate/nitrite transport system substrate-binding protein	one	**BOTH**	
sll1633	cell division protein FtsZ	**BOTH**	**BOTH**	**Yes**
slr1751	periplasmic carboxyl-terminal protease	**BOTH**	**BOTH**	**Yes**
slr1220	hypothetical protein	**BOTH**	**BOTH**	**Yes**
sll1143	ATP-dependent helicase PcrA	0	one	
slr1223	hypothetical protein	**BOTH**	0	
slr1226	phosphoribosyl aminoidazole succinocarboxamide synthetase	**BOTH**	one	
slr1228	peptide-chain-release factor 3	one	0	
ssr2047	hypothetical protein	0	one	
ssr2049	unknown protein	0	**BOTH**	
slr1234	protein kinase C inhibitor	**BOTH**	**BOTH**	**Yes**
sll1130	unknown protein	**BOTH**	**BOTH**	**Yes**
ssl2245	unknown protein	**BOTH**	**BOTH**	**Yes**
ssr2061	glutaredoxin	**BOTH**	0	
slr1238	glutathione synthetase	**BOTH**	0	
slr1239	pyridine nucleotide transhydrogenase alpha subunit	**BOTH**	one	
slr1434	pyridine nucleotide transhydrogenase beta subunit	one	0	
slr1435	PmbA protein homolog	one	0	

Supplemental Table 2. Continued

Locus ID	Annotation	Continuous Light	Fluctuating Light	All samples?
sll1362	isoleucyl-tRNA synthetase	**BOTH**	0	
sll1359	unknown protein	**BOTH**	**BOTH**	**Yes**
sll1358	putative oxalate decarboxylase, periplasmic protein	0	**BOTH**	
slr1356	30S ribosomal protein S1	**BOTH**	**BOTH**	**Yes**
sll1276	ATP-binding protein of ABC transporter	**BOTH**	0	
sll1275	pyruvate kinase 2	**BOTH**	**BOTH**	**Yes**
slr1364	biotin synthetase	**BOTH**	0	
sll1270	periplasmic substrate-binding and integral membrane protein of the ABC-type Bgt permease for basic amino acids and glutamine BgtB	one	0	
slr1367	glycogen phosphorylase	**BOTH**	one	
sll1267	unknown protein	**BOTH**	0	
slr0876	hypothetical protein	**BOTH**	0	
ssr1480	putative RNA-binding protein	**BOTH**	**BOTH**	**Yes**
slr0877	glutamyl-tRNA(Gln) amidotransferase subunit A	**BOTH**	**BOTH**	**Yes**
slr0879	glycine decarboxylase complex H-protein	**BOTH**	**BOTH**	**Yes**
sll0872	unknown protein	**BOTH**	**BOTH**	**Yes**
slr0884	glyceraldehyde 3-phosphate dehydrogenase 1 (NAD+)	**BOTH**	**BOTH**	**Yes**
sll0868	lipoic acid synthetase	one	0	
slr0886	3-oxoacyl-[acyl-carrier protein] reductase	**BOTH**	**BOTH**	**Yes**
sll0861	hypothetical protein	one	one	
sll0860	hypothetical protein	one	**BOTH**	
sll1317	apocytochrome f, component of cytochrome b6/f complex	**BOTH**	**BOTH**	**Yes**
sll1316	cytochrome b6-f complex iron-sulfur subunit (Rieske iron sulfur protein)	**BOTH**	**BOTH**	**Yes**
ssl2598	photosystem II PsbH protein	**BOTH**	**BOTH**	**Yes**
ssl2595	hypothetical protein	**BOTH**	**BOTH**	**Yes**
slr1403	unknown protein	0	one	
slr1406	periplasmic protein, function unknown	0	one	
slr1407	unknown protein	0	one	
slr1409	periplasmic WD-repeat protein	one	one	
slr1410	periplasmic WD-repeat protein	0	one	
sll1307	periplasmic protein, function unknown	0	one	
sll1305	probable hydrolase	one	0	
sll1304	unknown protein	0	one	

Supplemental Table 2. Continued

Locus ID	Annotation	Continuous Light	Fluctuating Light	All samples?
sll1785	periplasmic protein, function unknown	**BOTH**	**BOTH**	**Yes**
sll1784	periplasmic protein, function unknown	**BOTH**	**BOTH**	**Yes**
sll1783	hypothetical protein	**BOTH**	**BOTH**	**Yes**
slr1852	unknown protein	**BOTH**	**BOTH**	**Yes**
slr1853	carboxymuconolactone decarboxylase	**BOTH**	**BOTH**	**Yes**
slr1854	unknown protein	**BOTH**	**BOTH**	**Yes**
slr1855	unknown protein	**BOTH**	**BOTH**	**Yes**
slr1856	phosphoprotein substrate of icfG gene cluster	**BOTH**	**BOTH**	**Yes**
slr1857	isoamylase	**BOTH**	**BOTH**	**Yes**
slr1859	anti-sigma f factor antagonist	**BOTH**	**BOTH**	**Yes**
slr1867	anthranilate phosphoribosyltransferase	**BOTH**	0	
sll1774	hypothetical protein	**BOTH**	**BOTH**	**Yes**
slr1871	transcriptional regulator	one	0	
sll1771	protein serin-threonin phosphatase	**BOTH**	**BOTH**	**Yes**
sll1770	hypothetical protein	**BOTH**	0	
sll1769	hypothetical protein	**BOTH**	**BOTH**	**Yes**
slr1874	D-alanine--D-alanine ligase	**BOTH**	**BOTH**	**Yes**
sll1767	30S ribosomal protein S6	**BOTH**	0	
slr1877	2-hydroxyhepta-2,4-diene-1,7-dioate isomerase	**BOTH**	one	
sll1763	unknown protein	one	0	
sll1762	periplasmic protein, putative polar amino acid transport system substrate-binding protein	**BOTH**	**BOTH**	**Yes**
sll1760	homoserine kinase	one	0	
sll1757	hypothetical protein	**BOTH**	**BOTH**	**Yes**
ssr3188	hypothetical protein	one	0	
ssl3364	CP12 polypeptide	**BOTH**	**BOTH**	**Yes**
slr1884	tryptophanyl-tRNA synthetase	**BOTH**	0	
slr1887	porphobilinogen deaminase (hydroxymethylbilane synthase, preuroporphyrinogen synthase)	**BOTH**	**BOTH**	**Yes**
slr1888	4-hydroxybutyrate coenzyme A transferase.	0	one	
sll2010	UDP-N-acetylmuramoylalanine--D-glutamate ligase	**BOTH**	0	
sll2008	processing protease	one	0	
slr2136	GcpE protein homolog	**BOTH**	**BOTH**	**Yes**
sll2005	DNA gyrase B subunit [Contains: Ssp gyrB intein]	**BOTH**	0	
slr2141	hypothetical protein	**BOTH**	0	

Supplemental Table 2. Continued

Locus ID	Annotation	Continuous Light	Fluctuating Light	All samples?
slr2143	L-cysteine/cystine lyase	one	**BOTH**	
sll2002	hypothetical protein	**BOTH**	0	
slr2144	periplasmic protein, function unknown	**BOTH**	**BOTH**	**Yes**
sll1709	3-ketoacyl-acyl carrier protein reductase	**BOTH**	0	
sll1708	two-component response regulator NarL subfamily	0	one	
slr1805	two-component sensor histidine kinase	one	0	
slr1807	hypothetical protein	**BOTH**	0	
slr1808	transfer RNA-Gln reductase	**BOTH**	0	
slr1815	hypothetical protein	0	**BOTH**	
sll1696	hypothetical protein	one	0	
sll1694	pilin polypeptide PilA1	**BOTH**	**BOTH**	**Yes**
sll1693	hypothetical protein	**BOTH**	0	
sll1688	threonine synthase	**BOTH**	**BOTH**	**Yes**
sll1628	hypothetical protein	one	0	
slr1734	glucose 6-phosphate dehydrogenase assembly protein	**BOTH**	one	
slr1735	ATP-binding subunit of the ABC-type Bgt permease for basic amino acids and glutamine	one	one	
sll1626	LexA repressor	**BOTH**	**BOTH**	**Yes**
sll1625	succinate dehydrogenase iron- sulphur protein subunit	0	**BOTH**	
sll1621	AhpC/TSA family protein	**BOTH**	**BOTH**	**Yes**
slr1740	oligopeptide binding protein of ABC transporter	one	**BOTH**	
sll1618	hypothetical protein	one	**BOTH**	
slr1744	N-acetylmuramoyl-L-alanine amidase, periplasmic protein	**BOTH**	one	
slr0854	DNA photolyase	one	0	
sll0854	hypothetical protein	one	0	
sll0853	hypothetical protein	**BOTH**	**BOTH**	**Yes**
sll0851	photosystem II CP43 protein	**BOTH**	**BOTH**	**Yes**
sll0849	photosystem II reaction center D2 protein	**BOTH**	**BOTH**	**Yes**
slr0861	glycinamide ribonucleotide transformylase	**BOTH**	0	
sll0837	periplasmic protein, function unknown	**BOTH**	**BOTH**	**Yes**
sll1165	DNA mismatch repair protein	**BOTH**	**BOTH**	**Yes**
slr1243	unknown protein	0	one	
sll1161	probable adenylate cyclase	one	0	
slr1251	peptidyl-prolyl cis-trans isomerase	**BOTH**	**BOTH**	**Yes**

Supplemental Table 2. Continued

Locus ID	Annotation	Continuous Light	Fluctuating Light	All samples?
ssl2296	pterin-4a-carbinolamine dehydratase	**BOTH**	0	
sll1151	unknown protein	0	one	
slr1254	phytoene dehydrogenase (phytoene desaturase)	**BOTH**	0	
slr1256	urease gamma subunit	one	0	
slr1259	hypothetical protein	**BOTH**	0	
slr1261	hypothetical protein	**BOTH**	0	
slr1263	hypothetical protein	one	0	
sll1961	hypothetical protein	**BOTH**	one	
sll1958	histidinol phosphate aminotransferase	**BOTH**	**BOTH**	**Yes**
sll1957	transcriptional regulator	**BOTH**	**BOTH**	**Yes**
slr2058	DNA topoisomerase I	**BOTH**	0	
slr2060	hypothetical protein	0	one	
sll1951	unknown protein	**BOTH**	**BOTH**	**Yes**
slr2067	allophycocyanin alpha subunit	**BOTH**	**BOTH**	**Yes**
slr1986	allophycocyanin beta subunit	**BOTH**	**BOTH**	**Yes**
ssr3383	phycobilisome small core linker polypeptide	**BOTH**	**BOTH**	**Yes**
sll1908	D-3-phosphoglycerate dehydrogenase	**BOTH**	**BOTH**	**Yes**
slr1992	glutathione peroxidase-like NADPH peroxidase	**BOTH**	**BOTH**	**Yes**
slr1993	PHA-specific beta-ketothiolase	one	one	
slr1994	PHA-specific acetoacetyl-CoA reductase	one	0	
sll1905	two-component hybrid sensor and regulator	0	one	
slr2001	cyanophycinase	**BOTH**	**BOTH**	**Yes**
slr2002	cyanophycin synthetase	**BOTH**	**BOTH**	**Yes**
ssr3402	unknown protein	0	**BOTH**	
slr1712	hypothetical protein	one	**BOTH**	
sll1612	folylpolyglutamate synthase	one	one	
slr1717	hypothetical protein	one	one	
slr1718	hypothetical protein	**BOTH**	0	
slr1719	DrgA protein homolog	**BOTH**	**BOTH**	**Yes**
slr1720	aspartyl-tRNA synthetase	**BOTH**	one	
slr1722	inosine-5'-monophosphate dehydrogenase	**BOTH**	**BOTH**	**Yes**
slr1724	hypothetical protein	**BOTH**	one	
sll1594	ndhF3 operon transcriptional regulator, LysR family protein	**BOTH**	0	

Supplemental Table 2. Continued

Locus ID	Annotation	Continuous Light	Fluctuating Light	All samples?
slr1727	Na+/H+ antiporter	one	0	
sll1590	two-component sensor histidine kinase	one	0	
slr0260	cob(I)alamin adenosyltransferase	**BOTH**	0	
ssl0467	unknown protein	**BOTH**	**BOTH**	**Yes**
slr0261	NADH dehydrogenase subunit 7	**BOTH**	**BOTH**	**Yes**
ssl0461	hypothetical protein	**BOTH**	**BOTH**	**Yes**
sll0248	flavodoxin	**BOTH**	0	
sll0245	probable GTP binding protein	**BOTH**	**BOTH**	**Yes**
sll0241	unknown protein	**BOTH**	one	
sll0236	unknown protein	one	0	
sll1987	catalase peroxidase	**BOTH**	**BOTH**	**Yes**
slr2088	acetohydroxy acid synthase	**BOTH**	**BOTH**	**Yes**
slr2089	squalene-hopene-cyclase	one	one	
sll1981	acetolactate synthase	one	0	
sll1979	hypothetical protein	**BOTH**	**BOTH**	**Yes**
slr2094	fructose-1,6-/sedoheptulose-1,7-bisphosphatase	**BOTH**	**BOTH**	**Yes**
slr2098	two-component hybrid sensor and regulator	0	one	
slr2102	cell division protein FtsY	one	0	
sll1430	adenine phosphoribosyltransferase	**BOTH**	one	
sll1427	protease	one	0	
sll1425	proline-tRNA ligase	**BOTH**	one	
slr1505	unknown protein	**BOTH**	0	
sll1423	global nitrogen regulator	one	0	
ssl2781	hypothetical protein	**BOTH**	**BOTH**	**Yes**
slr1506	hypothetical protein	**BOTH**	one	
slr1507	hypothetical protein	**BOTH**	0	
slr1510	fatty acid/phospholipid synthesis protein PlsX	**BOTH**	0	
slr1511	3-oxoacyl-[acyl-carrier-protein] synthase III	one	0	
sll1418	photosystem II oxygen-evolving complex 23K protein PsbP homolog	**BOTH**	**BOTH**	**Yes**
slr1512	sodium-dependent bicarbonate transporter	**BOTH**	0	
slr1513	periplasmic protein, function unknown	one	**BOTH**	
sll1414	hypothetical protein	**BOTH**	**BOTH**	**Yes**
slr1516	superoxide dismutase	**BOTH**	**BOTH**	**Yes**

Supplemental Table 2. Continued

Locus ID	Annotation	Continuous Light	Fluctuating Light	All samples?
slr1517	3-isopropylmalate dehydrogenase	**BOTH**	0	
ssr2554	hypothetical protein	0	one	
sll2001	leucine aminopeptidase	**BOTH**	**BOTH**	**Yes**
slr2122	hypothetical protein	one	0	
slr2123	similar to D-3-phosphoglycerate dehydrogenase	one	0	
sll1994	porphobilinogen synthase (5-aminolevulinate dehydratase)	**BOTH**	**BOTH**	**Yes**
sll1239	unknown protein	**BOTH**	0	
slr1322	putative modulator of DNA gyrase; TldD	**BOTH**	**BOTH**	**Yes**
ssr2194	unknown protein	one	0	
sll1234	adenosylhomocysteinase	**BOTH**	**BOTH**	**Yes**
sll1229	two-component hybrid sensor and regulator	one	0	
slr1329	ATP synthase beta subunit	**BOTH**	**BOTH**	**Yes**
slr1330	ATP synthase epsilon chain of CF(1)	**BOTH**	**BOTH**	**Yes**
sll1226	hydrogenase subunit of the bidirectional hydrogenase	one	0	
sll1224	hydrogenase subunit of the bidirectional hydrogenase	**BOTH**	0	
slr1334	phosphoglucomutase/phosphomannomutase	one	0	
sll1218	hypothetical protein YCF39	**BOTH**	0	
slr0806	hypothetical protein	**BOTH**	0	
sml0008	photosystem I subunit IX	**BOTH**	**BOTH**	**Yes**
sll0819	photosystem I reaction center subunit III precursor (PSI-F), plastocyanin (cyt c553) docking prot	**BOTH**	**BOTH**	**Yes**
slr0809	dTDP-glucose 4,6-dehydratase	**BOTH**	0	
sll0817	tRNA delta-2-isopentenylpyrophosphate (IPP) transferase	**BOTH**	**BOTH**	**Yes**
slr0821	hypothetical protein	**BOTH**	**BOTH**	**Yes**
sll0807	pentose-5-phosphate-3-epimerase	**BOTH**	**BOTH**	**Yes**
slr0823	photosystem I assembly related protein	**BOTH**	**BOTH**	**Yes**
sll1262	hypothetical protein	**BOTH**	one	
sll1261	elongation factor TS	**BOTH**	**BOTH**	**Yes**
sll1260	30S ribosomal protein S2	**BOTH**	**BOTH**	**Yes**
slr1342	hypothetical protein	**BOTH**	0	
sll1251	hypothetical protein	0	**BOTH**	
sll1249	pantothenate synthetase/cytidylate kinase	**BOTH**	one	
slr1347	beta-type carbonic anhydrase localized in the carboxysome	**BOTH**	**BOTH**	**Yes**
slr1349	glucose-6-phosphate isomerase	**BOTH**	**BOTH**	**Yes**

Supplemental Table 2. Continued

Locus ID	Annotation	Continuous Light	Fluctuating Light	All samples?
slr1350	acyl-lipid desaturase (delta 12)	one	0	
slr1351	UDP-N-acetylmuramoylalanyl-D-glutamyl-2 6-diaminopimelate--D-alanyl-D-alanine ligase	**BOTH**	0	
sll1244	50S ribosomal protein L9	**BOTH**	**BOTH**	**Yes**
sll1242	hypothetical protein	0	one	
slr1963	water-soluble carotenoid protein	**BOTH**	**BOTH**	**Yes**
slr1964	hypothetical protein	one	0	
sll1891	unknown protein	**BOTH**	**BOTH**	**Yes**
slr1969	two-component sensor histidine kinase	0	one	
slr1970	hypothetical protein	**BOTH**	**BOTH**	**Yes**
slr1971	hypothetical protein	**BOTH**	0	
slr1974	GTP binding protein	one	0	
sll1883	arginine biosynthesis bifunctional protein ArgJ	**BOTH**	0	
slr1975	N-acylglucosamine 2-epimerase	**BOTH**	0	
sll1873	unknown protein	**BOTH**	**BOTH**	**Yes**
sll1872	transcriptional regulator	0	one	
slr1982	two-component response regulator CheY subfamily	0	**BOTH**	
slr1984	nucleic acid-binding protein, 30S ribosomal protein S1 homolog	**BOTH**	**BOTH**	**Yes**
sll1867	photosystem II D1 protein	**BOTH**	**BOTH**	**Yes**
sll1390	hypothetical protein	one	0	
ssl2717	hypothetical protein	**BOTH**	**BOTH**	**Yes**
slr1471	hypothetical protein	**BOTH**	**BOTH**	**Yes**
slr1472	hypothetical protein	one	**BOTH**	
sll1384	similar to DnaJ protein	**BOTH**	0	
sll1382	ferredoxin, petF-like protein	**BOTH**	**BOTH**	**Yes**
sll1380	periplasmic protein, function unknown	**BOTH**	0	
slr1478	hypothetical protein	0	one	
sll1374	probable sugar transporter	one	0	
sll1370	mannose-1-phosphate guanylyltransferase	one	0	
sll1181	similar to hemolysin secretion protein	**BOTH**	0	
sll1180	toxin secretion ABC transporter ATP-binding protein	**BOTH**	0	
slr1265	RNA polymerase gamma-subunit	**BOTH**	**BOTH**	**Yes**
slr1266	hypothetical protein	**BOTH**	**BOTH**	**Yes**
slr1271	probable UDP-N-acetyl-D-mannosaminuronic acid transferase	one	0	

Supplemental Table 2. Continued

Locus ID	Annotation	Continuous Light	Fluctuating Light	All samples?
slr1272	probable porin; major outer membrane protein	0	**BOTH**	
slr1273	hypothetical protein	**BOTH**	**BOTH**	**Yes**
slr1274	probable fimbrial assembly protein PilM, required for motility	**BOTH**	**BOTH**	**Yes**
slr1275	hypothetical protein	**BOTH**	0	
slr1276	hypothetical protein	one	**BOTH**	
slr1277	pilus assembly protein homologous to general secretion pathway protein D	one	0	
sll1173	hypothetical protein	one	0	
sll1172	threonine synthase	**BOTH**	**BOTH**	**Yes**
slr1280	NADH dehydrogenase subunit NdhK	**BOTH**	0	
slr1281	NADH dehydrogenase subunit I	**BOTH**	**BOTH**	**Yes**
ssr2130	hypothetical protein	0	one	
sll1444	3-isopropylmalate dehydratase small subunit	**BOTH**	one	
sll1443	CTP synthetase	**BOTH**	0	
slr1531	signal recognition particle protein	**BOTH**	0	
sll1435	glutamyl-tRNA(Gln) amidotransferase subunit B	**BOTH**	**BOTH**	**Yes**
sll1434	penicillin-binding protein	one	0	
slr1533	hypothetical protein	**BOTH**	0	
sll1101	30S ribosomal protein S10	**BOTH**	**BOTH**	**Yes**
sll1099	elongation factor Tu	**BOTH**	**BOTH**	**Yes**
sll1098	elongation factor EF-G	**BOTH**	**BOTH**	**Yes**
sll1097	30S ribosomal protein S7	**BOTH**	**BOTH**	**Yes**
sll1096	30S ribosomal protein S12	**BOTH**	**BOTH**	**Yes**
slr1159	glycinamide ribonucleotide synthetase	**BOTH**	**BOTH**	**Yes**
slr1160	periplasmic protein, function unknown	**BOTH**	**BOTH**	**Yes**
slr1161	hypothetical protein	one	0	
slr1165	sulfate adenylyltransferase	**BOTH**	**BOTH**	**Yes**
sll1091	geranylgeranyl hydrogenase	**BOTH**	**BOTH**	**Yes**
slr1171	glutathione peroxidase-like NADPH peroxidase,glutathione peroxidase	**BOTH**	0	
sll1089	periplasmic protein, function unknown	0	**BOTH**	
sll1087	similar to sodium/glucose cotransporter	0	one	
ssr1951	hypothetical protein	**BOTH**	one	
sll1566	glucosylglycerolphosphate synthase	one	0	
slr1670	unknown protein	0	one	

Supplemental Table 2. Continued

Locus ID	Annotation	Continuous Light	Fluctuating Light	All samples?
slr1677	hypothetical protein	0	one	
slr1678	50S ribosomal protein L21	**BOTH**	**BOTH**	**Yes**
ssr2799	50S ribosomal protein L27	**BOTH**	**BOTH**	**Yes**
sll1561	proline oxidase	**BOTH**	0	
sll1559	soluble hydrogenase 42 kD subunit	**BOTH**	**BOTH**	**Yes**
ssl3044	probable ferredoxin	**BOTH**	**BOTH**	**Yes**
ssr2831	photosystem I subunit IV	**BOTH**	**BOTH**	**Yes**
slr1694	expression activator appA homolog	one	0	
sll1553	phenylalanyl-tRNA synthetase	**BOTH**	**BOTH**	**Yes**
sll0921	two-component response regulator NarL subfamily	**BOTH**	0	
sll0920	phosphoenolpyruvate carboxylase	**BOTH**	one	
ssl1762	hypothetical protein	0	one	
slr0936	nicotinate-nucleotide pyrophosphorylase	0	one	
slr0938	probable UDP-N-acetylmuramyl tripeptide synthetase	one	one	
sll0915	periplasmic protease	one	0	
slr0940	zeta-carotene desaturase	**BOTH**	0	
slr0941	hypothetical protein	one	0	
slr0942	alcohol dehydrogenase [NADP+]	**BOTH**	**BOTH**	**Yes**
slr0947	response regulator for energy transfer from phycobilisomes to photosystems	**BOTH**	**BOTH**	**Yes**
sll0912	ABC transporter ATP binding protein	one	0	
sll0911	unknown protein	**BOTH**	0	
slr0952	fructose-1,6-bisphosphatase	one	0	
ssr1600	similar to anti-sigma f factor antagonist	**BOTH**	**BOTH**	**Yes**
slr0955	probable tRNA/rRNA methyltransferase	**BOTH**	0	
slr0957	hypothetical protein	one	0	
slr0958	cysteinyl-tRNA synthetase	0	one	
slr1622	soluble inorganic pyrophosphatase	**BOTH**	**BOTH**	**Yes**
slr1624	hypothetical protein	**BOTH**	**BOTH**	**Yes**
slr1626	dihydroneopterin aldolase	**BOTH**	one	
sll1536	molybdopterin biosynthesis MoeB protein	**BOTH**	**BOTH**	**Yes**
slr1628	hypothetical protein	0	**BOTH**	
slr1629	ribosomal large subunit pseudouridine synthase D	0	**BOTH**	
sll1533	twitching mobility protein	one	one	

Supplemental Table 2. Continued

Locus ID	Annotation	Continuous Light	Fluctuating Light	All samples?
ssl2982	probable DNA-directed RNA polymerase omega subunit	**BOTH**	**BOTH**	**Yes**
sll1530	unknown protein	**BOTH**	0	
sll1528	unknown protein	**BOTH**	0	
sll1526	hypothetical protein	**BOTH**	one	
slr1641	ClpB protein	**BOTH**	0	
sll1525	phosphoribulokinase	**BOTH**	**BOTH**	**Yes**
slr1643	ferredoxin-NADP oxidoreductase	**BOTH**	**BOTH**	**Yes**
slr1645	photosystem II 11 kD protein	**BOTH**	**BOTH**	**Yes**
slr1649	hypothetical protein	**BOTH**	**BOTH**	**Yes**
sll0427	photosystem II manganese-stabilizing polypeptide	**BOTH**	**BOTH**	**Yes**
slr0443	hypothetical protein	**BOTH**	**BOTH**	**Yes**
slr0444	3-phosphoshikimate 1-carboxyvinyltransferase	one	0	
sll0422	asparaginase	**BOTH**	one	
sll0421	adenylosuccinate lyase	**BOTH**	0	
sll0420	urease beta subunit	0	one	
slr0447	periplasmic protein, ABC-type urea transport system substrate-binding protein	**BOTH**	**BOTH**	**Yes**
slr0448	DNA repair protein RadA	one	**BOTH**	
sll0274	hypothetical protein	**BOTH**	**BOTH**	**Yes**
sll0272	hypothetical protein	**BOTH**	**BOTH**	**Yes**
sll0271	N utilization substance protein B homolog	**BOTH**	0	
sll0270	primosomal protein N'	one	0	
sll0267	unknown protein	one	0	
ssr0482	30S ribosomal protein S16	**BOTH**	**BOTH**	**Yes**
slr0287	hypothetical protein	**BOTH**	one	
slr0288	glutamate--ammonia ligase	**BOTH**	**BOTH**	**Yes**
sll0258	cytochrome c550	**BOTH**	**BOTH**	**Yes**
slr0292	hypothetical protein	one	0	
slr0293	glycine dehydrogenase	**BOTH**	0	
slr0392	unknown protein	one	0	
slr0394	phosphoglycerate kinase	**BOTH**	**BOTH**	**Yes**
sll0362	alanyl-tRNA synthetase	**BOTH**	one	
sll0359	hypothetical protein	**BOTH**	**BOTH**	**Yes**
slr0397	hypothetical protein	0	one	

Supplemental Table 2. Continued

Locus ID	Annotation	Continuous Light	Fluctuating Light	All samples?
slr0398	unknown protein	**BOTH**	**BOTH**	**Yes**
slr0399	chaperon-like protein for quinone binding in photosystem II	one	0	
ssl0707	nitrogen regulatory protein P-II	**BOTH**	**BOTH**	**Yes**
slr0404	hypothetical protein	**BOTH**	0	
slr0146	hypothetical protein	0	**BOTH**	
slr0147	hypothetical protein	0	one	
slr0148	hypothetical protein	**BOTH**	**BOTH**	**Yes**
slr0149	hypothetical protein	one	0	
slr0151	unknown protein	one	0	
sll0149	hypothetical protein	one	0	
sll0148	hypothetical protein	0	**BOTH**	
sll0145	ribosome releasing factor	**BOTH**	**BOTH**	**Yes**
sll0144	uridine monophosphate kinase	**BOTH**	0	
ssl0259	hypothetical protein	0	one	
slr0156	ClpB protein	**BOTH**	0	
sll0141	hypothetical protein	one	one	
slr0161	twitching motility protein PilT	**BOTH**	0	
slr0163	a part of pilC, pilin biogenesis protein, required for twitching motility	**BOTH**	0	
slr0164	ATP-dependent Clp protease proteolytic subunit	**BOTH**	**BOTH**	**Yes**
slr0165	ATP-dependent Clp protease proteolytic subunit	**BOTH**	**BOTH**	**Yes**
sll0136	aminopeptidase P	one	0	
ssl0242	hypothetical protein	**BOTH**	**BOTH**	**Yes**
slr1923	hypothetical protein	**BOTH**	0	
slr1926	hypothetical protein	**BOTH**	0	
slr1934	pyruvate dehydrogenase E1 component, alpha subunit	**BOTH**	**BOTH**	**Yes**
sll1854	exodeoxyribonuclease III	0	one	
sll1852	nucleoside diphosphate kinase	**BOTH**	**BOTH**	**Yes**
slr1938	putative translation initiation factor EIF-2b subunit 1	**BOTH**	0	
slr1939	unknown protein	one	0	
slr1940	periplasmic protein, function unknown	one	0	
slr1942	circadian clock protein KaiC homolog	one	0	
slr1944	periplasmic protein, function unknown	one	0	
slr1945	2,3-bisphosphoglycerate-independent phosphoglycerate mutase	one	0	

Supplemental Table 2. Continued

Locus ID	Annotation	Continuous Light	Fluctuating Light	All samples?
sll1841	pyruvate dehydrogenase dihydrolipoamide acetyltransferase component (E2)	**BOTH**	**BOTH**	**Yes**
slr0990	hypothetical protein	one	0	
slr0992	probable tRNA/rRNA methyltransferase	one	0	
slr0993	putative peptidase	one	0	
sll0947	light repressed protein A homolog	**BOTH**	**BOTH**	**Yes**
sll0945	glycogen synthase	**BOTH**	one	
slr0321	GTP-binding protein ERA homolog	**BOTH**	0	
slr0322	two-component hybrid sensor and regulator	**BOTH**	**BOTH**	**Yes**
sll0301	hypothetical protein	**BOTH**	**BOTH**	**Yes**
slr0326	hypothetical protein	0	**BOTH**	
ssl0563	photosystem I subunit VII	**BOTH**	**BOTH**	**Yes**
slr0331	NADH dehydrogenase subunit 4 (involved in photosystem-1 cyclic electron flow)	one	0	
slr0333	unknown protein	one	**BOTH**	
slr0335	phycobilisome core-membrane linker polypeptide	**BOTH**	**BOTH**	**Yes**
slr0171	photosystem I assembly related protein Ycf37	**BOTH**	0	
slr0172	hypothetical protein	**BOTH**	**BOTH**	**Yes**
sll0173	virginiamycin B hydrolase, periplasmic protein	**BOTH**	**BOTH**	**Yes**
sll0172	periplasmic protein, function unknown	one	**BOTH**	
sll0170	DnaK protein 2, heat shock protein 70, molecular chaperone	**BOTH**	**BOTH**	**Yes**
sll0169	cell division protein Ftn2 homolog	one	**BOTH**	
sll0162	hypothetical protein	**BOTH**	**BOTH**	**Yes**
slr0179	hypothetical protein	0	one	
ssl0294	hypothetical protein	**BOTH**	one	
sll0158	1,4-alpha-glucan branching enzyme	**BOTH**	**BOTH**	**Yes**
slr0185	orotate phosphoribosyltransferase	**BOTH**	0	
sll0154	hypothetical protein	0	one	
slr0186	2-isopropylmalate synthase	**BOTH**	0	
slr0359	hypothetical protein	0	one	
slr0364	hypothetical protein	one	one	
slr0369	RND multidrug efflux transporter	one	0	
slr0370	succinate-semialdehyde dehydrogenase (NADP+)	0	**BOTH**	
sll0336	acetyl-CoA carboxylase beta subunit	**BOTH**	0	
slr0378	similar to 7-beta-(4-carbaxybutanamido)cephalosporanic acid acylase	0	one	

Supplemental Table 2. Continued

Locus ID	Annotation	Continuous Light	Fluctuating Light	All samples?
slr0381	lactoylglutathione lyase	one	**BOTH**	
sll0330	sepiapterine reductase	one	0	
slr0384	sulfoquinovosyldiacylglycerol biosynthesis protein SqdX	one	0	
sll0329	6-phosphogluconate dehydrogenase	**BOTH**	**BOTH**	**Yes**
slr0769	hypothetical protein	0	one	
slr0774	protein-export membrane protein SecD	**BOTH**	one	
slr0776	UDP-3-o-[3-hydroxymyristoyl] glucosamine n-acyltransferase	one	0	
sll0767	50S ribosomal protein L20	**BOTH**	**BOTH**	**Yes**
ssl1426	50S ribosomal protein L35	0	**BOTH**	
sll0766	DNA repair protein RadC	one	**BOTH**	
sll0764	urea transport system ATP-binding protein	one	0	
sll0759	ABC transporter ATP-binding protein	**BOTH**	0	
sll0757	amidophosphoribosyltransferase	**BOTH**	**BOTH**	**Yes**
sll0756	unknown protein	0	**BOTH**	
sll0755	thioredoxin peroxidase	one	one	
sll0754	ribosome binding factor A	**BOTH**	**BOTH**	**Yes**
sll0753	FolD bifunctional protein	**BOTH**	0	
sll0752	hypothetical protein	one	0	
slr0782	putative flavin-containing monoamine oxidase	0	**BOTH**	
slr0783	triosephosphate isomerase	**BOTH**	**BOTH**	**Yes**
slr0342	cytochrome b6	**BOTH**	**BOTH**	**Yes**
sll0321	unknown protein	**BOTH**	0	
sll0320	probable ribonuclease D	**BOTH**	0	
sll0319	periplasmic protein, function unknown	**BOTH**	0	
slr0348	hypothetical protein	**BOTH**	0	
sll0314	periplasmic protein, function unknown	**BOTH**	0	
ssl0601	30S ribosomal protein S21	**BOTH**	**BOTH**	**Yes**
slr0355	hypothetical protein	**BOTH**	**BOTH**	**Yes**
slr0357	histidyl-tRNA synthetase	**BOTH**	0	
slr0001	hypothetical protein	one	**BOTH**	
sll0020	ATP-dependent Clp protease ATPase subunit	**BOTH**	**BOTH**	**Yes**
sll0019	1-deoxy-d-xylulose 5-phosphate reductoisomerase	**BOTH**	**BOTH**	**Yes**
sll0018	fructose-bisphosphate aldolase, class II	**BOTH**	**BOTH**	**Yes**

Supplemental Table 2. Continued

Locus ID	Annotation	Continuous Light	Fluctuating Light	All samples?
sll0017	glutamate-1-semialdehyde aminomutase	**BOTH**	**BOTH**	**Yes**
slr0009	ribulose bisphosphate carboxylase large subunit	**BOTH**	**BOTH**	**Yes**
slr0012	ribulose bisphosphate carboxylase small subunit	**BOTH**	**BOTH**	**Yes**
slr0013	hypothetical protein	**BOTH**	**BOTH**	**Yes**
ssl0020	ferredoxin I, essential for growth	**BOTH**	**BOTH**	**Yes**
slr0017	UDP-N-acetylglucosamine 1-carboxyvinyltransferase	**BOTH**	**BOTH**	**Yes**
sll0006	putative aminotransferase	one	one	
slr0213	GMP synthetase	**BOTH**	0	
sll0209	hypothetical protein	one	0	
sll0208	hypothetical protein	**BOTH**	**BOTH**	**Yes**
slr0220	glycyl-tRNA synthetase beta chain	**BOTH**	one	
slr0222	two-component hybrid sensor and regulator	one	one	
sll0199	plastocyanin	**BOTH**	**BOTH**	**Yes**
slr0228	cell division protein FtsH	**BOTH**	**BOTH**	**Yes**
sll0195	probable ATP-dependent protease	one	0	
sll0416	60 kDa chaperonin 2, GroEL2, molecular chaperone	**BOTH**	**BOTH**	**Yes**
sll0415	ATP-binding protein of ABC transporter	one	0	
sll0414	hypothetical protein	one	0	
sll0413	hypothetical protein	one	0	
sll0408	peptidyl-prolyl cis-trans isomerase	**BOTH**	**BOTH**	**Yes**
slr0434	elongation factor P	**BOTH**	**BOTH**	**Yes**
slr0435	biotin carboxyl carrier protein of acetyl-CoA carboxylase	**BOTH**	**BOTH**	**Yes**
slr0436	carbon dioxide concentrating mechanism protein CcmO	one	0	
sll0402	aspartate aminotransferase	**BOTH**	0	
sll0401	citrate synthase	**BOTH**	0	
slr0049	hypothetical protein	**BOTH**	0	
sll0067	glutathione S-transferase	**BOTH**	0	
sll0065	acetolactate synthase small subunit	**BOTH**	**BOTH**	**Yes**
sll0064	periplasmic protein, putative polar amino acid transport system substrate-binding protein	**BOTH**	**BOTH**	**Yes**
slr0058	hypothetical protein	**BOTH**	0	
sll0058	DnaK protein 1, heat shock protein 70, molecular chaperone	**BOTH**	**BOTH**	**Yes**
sll0057	heat shock protein GrpE	**BOTH**	**BOTH**	**Yes**
slr0063	pilus biogenesis protein homologous to general secretion pathway protein E	**BOTH**	0	

Supplemental Table 2. Continued

Locus ID	Annotation	Continuous Light	Fluctuating Light	All samples?
slr0067	MRP protein homolog	**BOTH**	0	
sll0053	biotin carboxylase	**BOTH**	0	
slr0469	30S ribosomal protein S4	**BOTH**	**BOTH**	**Yes**
slr0476	unknown protein	**BOTH**	**BOTH**	**Yes**
slr0479	hypothetical protein	0	one	
slr0483	hypothetical protein	**BOTH**	**BOTH**	**Yes**
sll0455	homoserine dehydrogenase	**BOTH**	**BOTH**	**Yes**
sll0454	phenylalanyl-tRNA synthetase alpha chain	**BOTH**	one	
sll0689	Na+/H+ antiporter	**BOTH**	one	
sll0680	phosphate-binding periplasmic protein precursor (PBP)	**BOTH**	0	
slr0719	unknown protein	**BOTH**	one	
slr0628	30S ribosomal protein S14	**BOTH**	**BOTH**	**Yes**
sll0617	plasma membrane protein essential for thylakoid formation	**BOTH**	**BOTH**	**Yes**
sll0616	preprotein translocase SecA subunit	**BOTH**	**BOTH**	**Yes**
slr0633	thiamine biosynthesis protein ThiG	**BOTH**	0	
slr0635	hypothetical protein	one	0	
sll0611	hypothetical protein	**BOTH**	one	
slr0637	hypothetical protein	**BOTH**	0	
slr0638	glycyl-tRNA synthetase alpha chain	**BOTH**	one	
slr0642	hypothetical protein	one	one	
sll0601	nitrilase homolog	one	0	
slr0649	methionyl-tRNA synthetase	**BOTH**	one	
slr0650	hypothetical protein	**BOTH**	0	
sll0395	phosphoglycerate mutase	**BOTH**	**BOTH**	**Yes**
slr0416	unknown protein	one	0	
slr0417	DNA gyrase subunit A	**BOTH**	**BOTH**	**Yes**
sll0381	hypothetical protein	0	**BOTH**	
sll0379	acyl-[acyl-carrier-protein]--UDP-N-acetylglucosamine o-acyltransferase	**BOTH**	0	
sll0373	gamma-glutamyl phosphate reductase	**BOTH**	0	
sll0370	carbamoyl-phosphate synthase, pyrimidine-specific, large chain	**BOTH**	**BOTH**	**Yes**
slr0426	GTP cyclohydrolase I	**BOTH**	**BOTH**	**Yes**
slr0427	putative competence-damage protein	one	**BOTH**	
slr0193	RNA-binding protein	**BOTH**	**BOTH**	**Yes**

Supplemental Table 2. Continued

Locus ID	Annotation	Continuous Light	Fluctuating Light	All samples?
slr0194	ribose 5-phosphate isomerase	**BOTH**	**BOTH**	**Yes**
sll0185	hypothetical protein	**BOTH**	**BOTH**	**Yes**
slr0201	heterodisulfide reductase subunit B	one	one	
ssl0352	hypothetical protein	**BOTH**	**BOTH**	**Yes**
sll0180	hypothetical protein	**BOTH**	one	
sll0179	glutamyl-tRNA synthetase	**BOTH**	0	
slr0208	hypothetical protein	**BOTH**	one	
ssr0330	ferredoxin-thioredoxin reductase, variable chain	**BOTH**	**BOTH**	**Yes**
slr0209	unknown protein	one	0	
ssr0332	hypothetical protein	**BOTH**	0	
slr0212	5-methyltetrahydrofolate--homocysteine methyltransferase	**BOTH**	**BOTH**	**Yes**
ssr0335	unknown protein	**BOTH**	**BOTH**	**Yes**
sll0887	putative modulator of DNA gyrase; PmbA homolog	**BOTH**	**BOTH**	**Yes**
slr0897	probable endoglucanase	0	one	
slr0898	ferredoxin--nitrite reductase	**BOTH**	**BOTH**	**Yes**
slr0899	cyanate lyase	0	**BOTH**	
ssr1528	hypothetical protein	**BOTH**	**BOTH**	**Yes**
slr0906	photosystem II core light harvesting protein	**BOTH**	**BOTH**	**Yes**
slr0907	unknown protein	**BOTH**	0	
slr0909	unknown protein	**BOTH**	0	
slr0912	unknown protein	**BOTH**	**BOTH**	**Yes**
ssl1690	hypothetical protein	**BOTH**	**BOTH**	**Yes**
slr0923	hypothetical protein YCF65	**BOTH**	**BOTH**	**Yes**
slr0924	periplasmic protein, function unknown	**BOTH**	**BOTH**	**Yes**
slr0559	periplasmic binding protein of ABC transporter for natural amino acids	0	**BOTH**	
sll0554	ferredoxin-thioredoxin reductase, catalytic chain	**BOTH**	**BOTH**	**Yes**
sll0553	hypothetical protein	**BOTH**	0	
slr0565	hypothetical protein	**BOTH**	**BOTH**	**Yes**
sll0550	flavoprotein	**BOTH**	0	
sll0542	acetyl-coenzyme A synthetase	**BOTH**	0	
slr0582	unknown protein	0	one	
slr0583	similar to GDP-fucose synthetase	**BOTH**	0	
ssr1398	50S ribosomal protein L33	**BOTH**	0	

Supplemental Table 2. Continued

Locus ID	Annotation	Continuous Light	Fluctuating Light	All samples?
ssr1399	30S ribosomal protein S18	**BOTH**	**BOTH**	**Yes**
slr0829	unknown protein	0	one	
slr0835	MoxR protein homolog	one	0	
sll0830	elongation factor EF-G	0	one	
slr0838	phosphoribosyl formylglycinamidine cyclo-ligase	one	0	
slr0839	ferrochelatase	**BOTH**	one	
slr0841	periplasmic protein, function unknown	**BOTH**	**BOTH**	**Yes**
slr0844	NADH dehydrogenase subunit 5	**BOTH**	0	
sll0822	hypothetical protein	**BOTH**	**BOTH**	**Yes**
slr0848	hypothetical protein	**BOTH**	**BOTH**	**Yes**
slr0073	two-component sensor histidine kinase	one	one	
slr0074	ABC transporter subunit	**BOTH**	**BOTH**	**Yes**
slr0075	ABC transporter ATP-binding protein	**BOTH**	**BOTH**	**Yes**
slr0076	hypothetical protein	**BOTH**	0	
slr0077	cysteine desulfurase	0	**BOTH**	
sll0086	putative arsenical pump-driving ATPase	**BOTH**	one	
sll0085	unknown protein	0	**BOTH**	
slr0082	hypothetical protein	one	0	
slr0083	RNA helicase Light	**BOTH**	one	
sll0080	N-acetyl-gamma-glutamyl-phosphate reductase	**BOTH**	one	
sll0078	threonyl-tRNA synthetase	**BOTH**	one	
slr0086	similar to DnaK protein	**BOTH**	0	
sll0489	ATP-binding protein of ABC transporter	one	0	
slr0502	cobalamin synthesis protein cobW homolog	**BOTH**	0	
slr0506	light-dependent NADPH-protochlorophyllide oxidoreductase	**BOTH**	**BOTH**	**Yes**
sll0480	probable aminotransferase	**BOTH**	**BOTH**	**Yes**
slr0510	hypothetical protein	one	0	
sll0477	putative biopolymer transport ExbB-like protein	one	0	
slr0513	iron transport system substrate-binding protein, periplasmic protein	**BOTH**	**BOTH**	**Yes**
slr0516	hypothetical protein	one	**BOTH**	
slr0520	phosphoribosyl formylglycinamidine synthase	**BOTH**	0	
sll0470	hypothetical protein	**BOTH**	0	
sll0469	ribose-phosphate pyrophosphokinase	**BOTH**	0	

Supplemental Table 2. Continued

Locus ID	Annotation	Continuous Light	Fluctuating Light	All samples?
slr0523	similar to dethiobiotin synthetase	one	0	
sll0588	unknown protein	0	one	
slr0623	thioredoxin	**BOTH**	**BOTH**	**Yes**
slr0626	probable glycosyltransferase	**BOTH**	0	
sll0108	ammonium/methylammonium permease	**BOTH**	**BOTH**	**Yes**
slr0110	hypothetical protein	one	0	
slr0111	unknown protein	0	**BOTH**	
slr0118	thiamine biosynthesis protein ThiC	**BOTH**	**BOTH**	**Yes**
sll0289	septum site-determining protein MinD	**BOTH**	**BOTH**	**Yes**
slr0298	FraH protein homolog	one	0	
slr0306	unknown protein	0	one	
slr0309	probable methyltransferase	one	0	
slr0319	beta-lactamase	0	one	
sll0789	two-component response regulator OmpR subfamily	one	0	
sll0783	unknown protein	0	one	
sll0779	unknown protein	**BOTH**	**BOTH**	**Yes**
sll0777	putative carboxypeptidase	one	0	
sll0672	cation-transporting p-type ATPase PacL	one	0	
slr0708	periplasmic protein, function unknown	**BOTH**	**BOTH**	**Yes**
slr0709	hypothetical protein	**BOTH**	**BOTH**	**Yes**
slr0710	glutamate dehydrogenase (NADP+)	**BOTH**	**BOTH**	**Yes**
slr0711	hypothetical protein	one	**BOTH**	
sll0048	unknown protein	**BOTH**	0	
sll0043	positive phototaxis protein, homologous to chemotaxis protein CheA, two-component hybrid histidine kinase	0	one	
sll0041	phytochrome-like photoreceptor protein for positive phototaxis; homologous to methyl-accepting chemotaxis protein	**BOTH**	**BOTH**	**Yes**
sll0039	positive phototaxis protein, two-component response regulator CheY subfamily	**BOTH**	**BOTH**	**Yes**
slr0032	probable branched-chain amino acid aminotransferase	**BOTH**	**BOTH**	**Yes**
slr0033	glutamyl-tRNA(Gln) amidotransferase subunit C	**BOTH**	**BOTH**	**Yes**
sll0037	hypothetical protein	one	0	
sll0036	hypothetical protein	0	one	
sll0033	carotene isomerase	one	one	

Supplemental Table 2. Continued

Locus ID	Annotation	Continuous Light	Fluctuating Light	All samples?
slr0038	hypothetical protein	**BOTH**	**BOTH**	**Yes**
slr0039	hypothetical protein	**BOTH**	0	
slr0042	probable porin; major outer membrane protein	one	0	
slr0044	bicarbonate transport system ATP-binding protein	one	0	
sll0518	unknown protein	**BOTH**	**BOTH**	**Yes**
slr0525	Mg-protoporphyrin IX methyl transferase	**BOTH**	0	
slr0528	UDP-N-acetylmuramoylalanyl-D-glutamate--2, 6-diaminopimelate ligase	**BOTH**	**BOTH**	**Yes**
sll0513	hypothetical protein	one	0	
slr0535	protease	0	one	
slr0536	uroporphyrinogen decarboxylase	**BOTH**	**BOTH**	**Yes**
slr0537	putative sugar kinase	**BOTH**	**BOTH**	**Yes**
sll0504	diaminopimelate decarboxylase	**BOTH**	**BOTH**	**Yes**
sll0502	arginyl-tRNA-synthetase	**BOTH**	one	
slr0542	ATP-dependent protease ClpP	**BOTH**	**BOTH**	**Yes**
slr0543	tryptophan synthase beta subunit	**BOTH**	**BOTH**	**Yes**
sll0499	hypothetical protein	0	one	
sll0495	asparaginyl-tRNA synthetase	**BOTH**	0	
sll0902	ornithine carbamoyltransferase	**BOTH**	0	
slr0925	single-stranded DNA-binding protein	**BOTH**	**BOTH**	**Yes**
slr0927	photosystem II reaction center D2 protein	**BOTH**	**BOTH**	**Yes**
sll0900	ATP phosphoribosyltransferase	**BOTH**	0	
sll0899	UDP-N-acetylglucosamine pyrophosphorylase	**BOTH**	0	
ssl1707	hypothetical protein	**BOTH**	**BOTH**	**Yes**
sll0897	DnaJ protein, heat shock protein 40, molecular chaperone	**BOTH**	**BOTH**	**Yes**
slr0546	indole-3-glycerol phosphate synthase	one	0	
sll0534	ATP-dependent Clp protease proteolytic subunit 2	**BOTH**	**BOTH**	**Yes**
sll0533	trigger factor	**BOTH**	**BOTH**	**Yes**
slr0549	aspartate beta-semialdehyde dehydrogenese	**BOTH**	one	
slr0550	dihydrodipicolinate synthase	one	**BOTH**	
slr0551	hypothetical protein	**BOTH**	one	
slr0552	hypothetical protein	**BOTH**	**BOTH**	**Yes**
sll0529	hypothetical protein	**BOTH**	**BOTH**	**Yes**
slr0557	valyl-tRNA synthetase	**BOTH**	**BOTH**	**Yes**

Supplemental Table 2. Continued

Locus ID	Annotation	Continuous Light	Fluctuating Light	All samples?
sll0522	NADH dehydrogenase subunit 4L	**BOTH**	one	
sll0521	NADH dehydrogenase subunit 6	one	0	
sll0520	NADH dehydrogenase subunit NdhI	**BOTH**	**BOTH**	**Yes**
sll0519	NADH dehydrogenase subunit 1	**BOTH**	one	
sll1343	aminopeptidase	**BOTH**	0	
sll1342	NAD(P)-dependent glyceraldehyde-3-phosphate dehydrogenase	**BOTH**	**BOTH**	**Yes**
slr1423	UDP-N-acetylmuramate-alanine ligase	**BOTH**	0	
sll1341	bacterioferritin	**BOTH**	**BOTH**	**Yes**
sll1338	unknown protein	**BOTH**	one	
sll1336	hypothetical protein	**BOTH**	**BOTH**	**Yes**
slr1431	hypothetical protein	0	one	
sll1367	hypothetical protein	one	0	
slr1459	phycobilisome core component	**BOTH**	**BOTH**	**Yes**
sll1365	unknown protein	0	one	
slr1463	elongation factor EF-G	**BOTH**	**BOTH**	**Yes**
ssl2667	an assembly factor for iron-sulfur culsters	**BOTH**	**BOTH**	**Yes**
sll1363	ketol-acid reductoisomerase	**BOTH**	**BOTH**	**Yes**
slr0651	hypothetical protein	**BOTH**	**BOTH**	**Yes**
slr0652	phosphorybosilformimino-5-amino- phosphorybosil-4-imidazolecarboxamideisomerase	**BOTH**	**BOTH**	**Yes**
sll0629	alternative photosystem I reaction center subunit X	**BOTH**	**BOTH**	**Yes**
slr0653	principal RNA polymerase sigma factor SigA	**BOTH**	**BOTH**	**Yes**
slr0657	aspartate kinase	**BOTH**	0	
slr0659	oligopeptidase A	**BOTH**	0	
slr0662	arginine decarboxylase	one	0	
sll0623	unknown protein	one	**BOTH**	
sll0622	quinolinate synthetase	one	0	
slr0665	aconitate hydratase	**BOTH**	**BOTH**	**Yes**
sll1499	ferredoxin-dependent glutamate synthase	**BOTH**	**BOTH**	**Yes**
sll1498	carbamoyl-phosphate synthase small chain	**BOTH**	**BOTH**	**Yes**
slr1557	hypothetical protein	one	0	
sll1496	mannose-1-phosphate guanyltransferase	0	one	
slr1559	shikimate 5-dehydrogenase	one	one	
slr1560	histidyl tRNA synthetase	**BOTH**	0	

Supplemental Table 2. Continued

Locus ID	Annotation	Continuous Light	Fluctuating Light	All samples?
ssl2891	unknown protein	**BOTH**	one	
slr1566	hypothetical protein	0	one	
sll1491	periplasmic WD-repeat protein	**BOTH**	one	
slr1567	unknown protein	0	one	
slr1571	unknown protein	one	0	
ssl2874	hypothetical protein	one	0	
sll1483	periplasmic protein, similar to transforming growth factor induced protein	**BOTH**	**BOTH**	**Yes**
sll1471	phycobilisome rod-core linker polypeptide	**BOTH**	0	
sll1470	3-isopropylmalate dehydratase large subunit	**BOTH**	**BOTH**	**Yes**
slr0746	glucosylglycerolphosphate phosphatase	0	one	
sll0735	hypothetical protein	**BOTH**	one	
slr0752	enolase	**BOTH**	**BOTH**	**Yes**
sll0728	acetyl-CoA carboxylase alpha subunit	**BOTH**	0	
sll0726	phosphoglucomutase	**BOTH**	**BOTH**	**Yes**
slr0758	circadian clock protein KaiC homolog	0	one	
sll1550	probable porin; major outer membrane protein	0	**BOTH**	
slr1655	photosystem I subunit XI	**BOTH**	**BOTH**	**Yes**
slr1658	unknown protein	one	0	
sll1547	hypothetical protein	one	0	
sll1545	glutathione S-transferase	**BOTH**	one	
slr1665	diaminopimelate epimerase	**BOTH**	**BOTH**	**Yes**
slr1666	pleiotropic regulatory protein homolog	**BOTH**	0	
ssr2781	hypothetical protein	0	one	
slr1667	hypothetical protein (target gene of sycrp1)	one	one	
slr1668	periplasmic protein, function unknown (target gene of sycrp1)	one	0	
sll0448	unknown protein	one	**BOTH**	
sll0446	unknown protein	one	0	
slr0452	dihydroxyacid dehydratase	**BOTH**	**BOTH**	**Yes**
slr0453	hypothetical protein	one	0	
ssl0832	hypothetical protein	0	**BOTH**	
slr0455	hypothetical protein	**BOTH**	**BOTH**	**Yes**
slr0458	unknown protein	one	0	
sll0430	HtpG, heat shock protein 90, molecular chaperone	**BOTH**	**BOTH**	**Yes**

Supplemental Table 2. Continued

Locus ID	Annotation	Continuous Light	Fluctuating Light	All samples?
slr1176	glucose-1-phosphate adenylyltransferase	**BOTH**	**BOTH**	**Yes**
sll1110	peptide chain release factor 1	**BOTH**	**BOTH**	**Yes**
sll1109	hypothetical protein	one	one	
slr1181	photosystem II D1 protein	0	one	
slr1183	hypothetical protein	one	**BOTH**	
sll1106	hypothetical protein	**BOTH**	**BOTH**	**Yes**
slr0585	argininosuccinate synthetase	**BOTH**	**BOTH**	**Yes**
slr0586	hypothetical protein	one	0	
sll0577	hypothetical protein	**BOTH**	**BOTH**	**Yes**
slr0590	hypothetical protein	0	one	
sll0576	putative sugar-nucleotide epimerase/dehydratease	**BOTH**	**BOTH**	**Yes**
sll0569	RecA gene product	**BOTH**	0	
slr0597	phosphoribosyl aminoimidazole carboxy formyl formyltransferase/inosinemonophosphate cyclohydrolase (PUR-H(J))	**BOTH**	one	
slr0600	NADP-thioredoxin reductase	**BOTH**	**BOTH**	**Yes**
sll0563	unknown protein	0	one	
slr0604	GTP-binding protein	one	0	
slr0605	hypothetical protein	**BOTH**	0	
slr0606	hypothetical protein	**BOTH**	0	
slr0607	hypothetical protein	**BOTH**	one	
slr0609	hypothetical protein	**BOTH**	**BOTH**	**Yes**
slr5023	hypothetical protein	0	one	
sll5026	hypothetical protein	**BOTH**	one	
sll5034	hypothetical protein	0	one	
slr5038	chromate transporter	**BOTH**	0	
slr5051	unknown protein	**BOTH**	0	
slr5082	hypothetical protein	**BOTH**	**BOTH**	**Yes**
sll5104	arsenate reductase	one	0	
slr5112	unknown protein	0	one	
slr5118	hypothetical protein	**BOTH**	**BOTH**	**Yes**
slr5119	hypothetical protein	one	**BOTH**	
sll5122	SOS mutagenesis and repair, UmuC protein homolog	one	0	
slr5124	hypothetical protein	**BOTH**	**BOTH**	**Yes**
sll6017	hypothetical protein	**BOTH**	**BOTH**	**Yes**

Supplemental Table 2. Continued

Locus ID	Annotation	Continuous Light	Fluctuating Light	All samples?
slr6037	arsenate reductase	one	0	
slr6040	two-component response regulator	one	0	
slr6043	probable cation efflux system protein, czcA homolog	0	one	
slr6057	hypothetical protein	0	**BOTH**	
sll6076	hypothetical protein	**BOTH**	**BOTH**	**Yes**
slr6095	type I restriction-modification system, M subunit (fragment)	0	one	
slr7023	hypothetical protein	0	one	
slr7024	hypothetical protein	**BOTH**	one	
slr7049	resolvase	one	0	
sll7066	unknown protein	one	0	
slr7080	unknown protein	0	one	
slr7099	unknown protein	one	one	
slr7100	unknown protein	0	**BOTH**	
sll8006	type I restriction-modification system, S subunit	0	one	
slr9201	unknown protein [ORF2]	**BOTH**	0	
slr9002	unknown protein [ORF-A]	0	one	
slr9003	hypothetical protein [ORF-B]	one	0	
ssr9004	hypothetical protein [ORF-C]	0	one	

APPENDIX:

ADDITIONAL OBSERVATIONS ABOUT SLR1719

1. Introduction

In chapter two I described an experiment we conducted that uses physiology and proteomics to compare the response of the cyanobacterium *Synechocystis sp.* PCC6803 in fluctuating vs continuous light. Our hope was that by improving our understanding of the response to fluctuating light, we would provide useful information that could be used to identify genetic targets for engineering strains to perform better in industrial production environments. In that experiment we found ~100 proteins had a significantly different abundance between the two conditions, and about $1/5^{th}$ of them were hypothetical, or poorly characterized. We reasoned that these proteins may have important roles in the response to fluctuating light that are not currently understood. To further explore the function of some of these hypothetical proteins and gain a better understanding of the response to fluctuating light as a whole, we created several mutant lines by disrupting the open reading frames that code for these proteins.

The set of hypothetical/poorly characterized proteins that we chose to knock out was based on a dataset generated from the same experiment, but the protein identification and quantification used an older version of the Peaks software. This older version, Peaks 6.0, uses a different algorithm for feature matching and alignment than the improved version in Peaks 7.0, which was used to generate the dataset analyzed in chapter two. From the Peaks 6.0 dataset, five proteins were selected to knock out: slr1533, slr0642, sll1003, sll1866, and slr1719. The first four of these showed no phenotypic difference from WT, and/or we could not get a complete

knock out. This section will describe our preliminary characterization of the fifth protein that we disrupted, slr1719. After a brief review of previous studies on this protein in the literature, I will describe an experiment we performed that found that the growth rate of a Δslr1719 mutant line is significantly lower than a control strain in low CO_2 conditions, regardless of light intensity, but showed no growth rate difference in replete CO_2 regardless of light intensity. In conjunction with what is known about the role of this protein from the literature, we propose that this suggests a role in cyclic electron flow. I also describe a method used to quantify the total organic carbon accumulation of Δslr1719, which will require further method development, but shows promising results that under certain conditions the Δslr1719 mutant accumulates more total organic carbon than WT.

In the Peaks 6.0 dataset, slr1719 had an abundance 3x lower in fluctuating light compared to continuous light that was statistically different using a student's t-test ($p<0.05$). However, when Peaks 7.0 was used to process the same data set, the improved algorithm for peptide recognition gave a lower -10logP peptide significance score (2.74) for slr1719 than our threshold of 13.01, so it was not considered in the analysis in chapter two.

1.1 slr1719 is an NAD(P)H:quinone reductase with a suggested role in cyclic electron flow or in the transition from photo-autotrophic growth to respiration

The protein coded by slr1719 was originally discovered by Elanskaya et al. (1998) [1]. Their group mutagenized Synechocystis and selected strains having mutations which conferred resistance to the PSII inhibitor dinoseb (2-*sec*-butyl-4,6-dinitrophenol). They discovered that three resistant lines had mutations in the same open reading frame: slr1719. They subsequently named the protein coded by this gene "drgA" for drug resistance. They discovered that dinoseb is non-toxic until it is reduced. In the process of reduction a superoxide anion is generated, which

leads to inhibition of PSII. The drgA protein is apparently responsible for reducing dinoseb in WT cells, because the slr1719 mutants were unable to reduce dinoseb, and so showed resistance to the toxic effects of this herbicide [1].

That same year the slr1719 protein was independently discovered through an unrelated study looking for NAD(P)H dehydrogenases. Matsuo et al. (1998) ran a protein extract from Synechocystis on a native polyacrylamide gel electrophoresis (PAGE), and then stained for NAD(P)H dehydrogenase activity using nitroblue tetrazolium [2]. These salts are colorless and soluble, but form a blue precipitant called formazan upon reduction [3, 4]. By adding nitroblue tetrazolium and providing either NADPH or NADH as a substrate for potential NAD(P)H dehydrogenase enzymes, the authors discovered four protein bands with NADPH or NADH dehydrogenase activity or both. One of these bands, with both NADPH and NADH dehydrogenase activity, was found to be the slr1719 gene product by protein sequencing.

The protein coded by slr1719 is soluble and is able to reduce several different classes of molecules using electrons derived from NAD(P)H [2, 5, 6]. In all three *in vitro* activity studies performed on purified slr1719, the enzyme showed the highest activity when reducing quinones, but also was able to reduce flavins, nitrofurazone, and ferricyanide, though at reduced activity levels [2, 5, 6]. For all molecules tested, it showed a ~25-50% higher activity with NADPH as a substrate than NADH [2, 5, 6]. Because of the strong NADPH: Quinone Reductase activity, the protein coded by slr1719 is sometimes referred to as NQR rather than drgA [7]. NADPH: quinone reductase activity was verified *in vivo* by demonstrating a slower $p700^+$ re-reduction after a light pulse in the Δslr1719 compared to WT [8]. A similar finding was made using isolated thylakoid membrane extracts. Re-reduction rate was lower in the mutant, but was restored by the addition of recombinant DrgA and NADPH [5]. This demonstrates the enzyme's

ability to donate electrons from NADPH to the quinone pool, which re-reduces p700 after oxidation.

There are two dominant, but not necessarily mutually exclusive theories on the role of slr1719. One theory is that it is involved in the transition of light to dark by oxidizing NAD(P)H to $NAD(P)^+$, and allowing the TCA cycle to function [8]. The other theory is that it is involved in cyclic electron flow [7].

1.2 Role of slr1719 in activating the TCA cycle for the catabolism of glucose

Several key findings point to an involvement of glucose in the role of slr1719. The expression of slr1719 was enhanced by glucose in the light or dark, but not enhanced by the dark alone when cultivated in a 12 hr light dark cycle [9, 10].

Elanskaya (2004) argued that slr1719 was responsible for regulating the $NADP^+/NAD^+$ oxidation state, which is key in activation of the tricarboxylic acid (TCA) cycle and Oxidative Pentose Phosphate pathway (OPP) [8, 11]. In Synechocystis glucose is metabolized to fructose-6-phosphate and glucose-3-phosphate by OPP, and then through glycolytic enzymes is converted into pyruvate [12]. Pyruvate can be further metabolized in the TCA cycle [12]. Thus the oxidation state of the NAD(P)H pool is critical for glucose metabolism.

Cooley et al. (2001) put forward a similar argument that found that deletion of the NAD(P)H dehydrogenase-1 (NDH-1) complex, or NADH dehydrogenase-2 (NDH-2), which can oxidize NAD(P)H by transferring electrons to the plastoquinone pool, caused reduced activity of the TCA cycle. Two key steps of the TCA cycle require oxidized $NADP^+$ or NAD^+ to function. The conversion of isocitrate to oxoglutarate requires the availability of oxidized $NADP^+$, and the conversion of malate to oxaloacetate requires oxidized NAD^+ [13]. Their argument was that deletion of NDH-1 and NDH-2, as the primary dehydrogenases for NADPH and NADH

respectively, led to a higher NAD(P)H/NAD(P)$^+$ ratio, which prevented these key enzymatic steps of the TCA cycle to occur. They demonstrate enzymatic bottlenecks from the accumulation of malate and isocitrate in various dehydrogenase mutants [13]. Elanskaya extended this argument saying that slr1719 is also involved in the oxidation of NADPH and NADH to allow glucose metabolism.

1.3 slr1719 is involved in cyclic electron flow

The other key theory on the role of slr1719 is that through its role as an NAD(P)H:quinone reductase it can participate in cyclic electron flow similarly to the NDH-1 complex [14]. Cyclic electron flow occurs when NADPH or ferredoxin is instead used to re-reduce the plastoquinone pool, or the b6/f complex directly, rather than donate electrons to the Calvin cycle as in linear electron transport (See Chapter 1 for an overview) [15]. Because electron transport creates a proton gradient that leads to ATP production, cyclic electron flow results in a higher ATP/NADPH ratio [15]. A higher amount of ATP is required in conditions such as high salt, or low CO_2, to energize transporters for the removal of salt, or intake of inorganic carbon [7].

The main route for cyclic electron flow in Synechocystis is the NDH-1 complex. This complex is critical for survival in high ATP requiring conditions. For example, when the NDH-1 complex is knocked out, cells cannot grow unless they are in a 3% CO_2 environment [16]. Because slr1719 can perform the reaction necessary for cyclic electron flow, authors have speculated that may be its function *in vivo* [5, 7].

The most direct evidence for the participation of slr1719 in cyclic electron flow *in vivo* comes from Ooyabu et al. (2008) [7]. This group ran native PAGE gels of protein extracts after various treatments. They then measured NADPH reductase activity with nitroblue-tetrazolium by

gauging the size of the resulting formazan band. As in Matsuo (1998) they found a band corresponding to slr1719 [2]. Ooyabu et al found that the activity level of slr1719 was increased when cyclic electron flow was induced with high salt, or low CO_2 [7]. Additionally, they found when cultures were treated with the NDH-1 inhibitor $HgCl_2$ that the activity level of slr1719 increased, suggesting it was compensating for the lack of NDH-1 [7].

1.4 Experimental overview to test if Δslr1719 grows poorly in low CO_2

We speculated that if slr1719 has a role in cyclic electron flow, then like the NDH-1 complex knock-outs, deletion of slr1719 should cause reduced growth in low CO_2 environments [16]. To test this we generated a knock-out of slr1719. However, we were unable to completely knock out all copies of the gene (See screening procedure below). So rather than compare Δslr1719 to a WT strain, we also constructed a strain with a kanamycin cassette in a neutral site to compare to. We call this "WT-Kan" as it should show no phenotype other than its ability to grow on kanamycin.

Considering that high light intensities can exacerbate CO_2 stress, it can be difficult to distinguish between high/low CO_2 phenotypes and high light/low light phenotypes. To clarify if slr1719 had a CO_2 related phenotype, or a light level phenotype, we performed a 2 x 2 x 2 comparison of WT-Kan and Δslr1719 using high/low CO_2, and saturating/sub-saturating light levels. We measured growth rate, chlorophyll/phycobilisome fluorescence per cell, and the forward scatter pulse area, which is an indicator of size [17].

2 Methods

2.1 Mutant strain construction

Both the Δslr1719 strain and the WT-Kan strain were constructed by interupting either the slr1719 or slr0168 ORF respectively with a kanamycin cassette derived from the pIGA4

vector. slr0168 is a commonly used “neutral” site in the Synechocystis genome, and disruption of this gene has not shown any phenotype [18, 19]. Genomic integration of the kanamycin cassette occurred by homologous recombination. Knock out vectors with homologous regions bordering the kanamycin cassette were constructed using standard cloning techniques.

The transformation procedure used was based on recommendations in Zang et al. [20]. *Synechocystis sp.* PCC6803 WT cells (Peers WT strain) were harvested in exponential growth, and concentrated to 1*10^9 cells/ml. Cells were divided into 100µl aliquots and 2ug of the uncut knock out vector was added to each aliquot. Cells were incubated at 50uE, and 30ºC for 5 hours. Cells were then plated on BG-11 plates with 25µg/ml kanamycin, or diluted with 5ml BG-11with 10mM bicarbonate. Diluted cells were incubated overnight in 50uE, 30ºC and the next morning cells were spun down, re-suspended in 500µl. 100µl of the concentrated cells were plated onto BG-11 plates with 25µg/ml kanamycin.

Transformed cells were incubated on the BG-11 plates at 50µE, 28ºC ± 1. Individual colonies appeared after ~5-6 days, and were patched onto a new BG-11 plate with a concentration of 50-100 µg/ml kanamycin. After these patched colonies had filled in, 4 colonies were streaked for isolation on separate BG-11 plates with 50-100µg/ml kanamycin. Individual colonies appeared after 5-6 days and were patched onto a new plate. Once these patched colonies had filled in, a PCR screen (details below) was performed to test for presence of the native gene. The WT-Kan strain was completely segregated after 1 iteration of this cycle (Figure 1). The Δslr1719, however, never achieved segregation to homoplasmy, even after several iterations of streaking for isolation on increasing concentrations of kanamycin, and patching isolated colonies (Figure 2).

2.2 Screening Procedure

Because *Synechocystis sp.* PCC6803 has many copies of its genome [21], it is possible that not all copies of the genome will have the kanamycin cassette interrupting the gene of interest [22]. To determine if the strain is fully segregated to homoplasmy, or if some copies of the native gene persist, I have developed a sensitive PCR screen. The screen amplifies the native gene if present, but is unable to amplify the knocked out copies of the gene, because the amplicon is too long for the extension time used. Thus, presence of a band in this screen signifies persistence of the native gene, which means the strain is not fully knocked out. Absence of a band indicates the strain is segregated to homoplasmy.

All PCR reactions were prepared with 0.2-0.24 μM final concentration of each primer, 3% DMSO, and 1X RedTaq Ready Mix. Total volume was brought to 25μl with DI water. Primers used for Δslr1719: MTY82, and MTY83. Primers used for WT-Kan: MTY44, and MTY132. See Table 1 for PCR conditions used.

2.3 Growth conditions/experimental overview

The goal was to create a high CO_2 condition, and a low CO_2 condition to compare WT-Kan and Δslr1719. The high CO_2 condition in short was provided by constantly bubbling air into the cultures, while the low CO_2 condition was achieved by growth in Erlenmeyer flasks with gentle shaking. Because CO_2 in the media is only exchanged with air at the air/liquid interface in the shake flasks, the cultures quickly became carbon limited. Carbon limitation can be measured by changes in pH [23]. As cultures begin to fix more CO_2 than can be returned to the un-buffered media, the pH begins to increase. Figure 3 demonstrates that this approach was successful at creating a condition without CO_2 limitation when cultures were bubbled with air (high CO_2), or a

condition that quickly became CO_2 limited when cultures were grown in Erlenmeyer flasks (low CO_2).

2.3.1 High CO_2 cultures

Synechocystis was grown in 450ml of BG-11 media in glass Roux flasks. Sampling port and air supply were provided by a homemade stopper as described in Chapter 2. The cultures were bubbled with air filtered by a 0.45μm polyethersulfone membrane (28145-505 VWR) at a volumetric flow rate of 1 liter of air per minute per liter of liquid culture, as measured from the outlet. Cultures were incubated in a custom Percival incubator that was held at 30ºC. The two light levels used, 150 μmol photons$\cdot m^{-2} \cdot s^{-1}$ and 50 μmol photons$\cdot m^{-2} \cdot s^{-1}$ were accomplished by cutting off power to one of the door panels, and only turning on set 2 of the bulbs. Mesh and spacing from the light source were then used to get the precise light intensity ± 5%. Light intensity was measured with a US-SQS/L quantum sensor (Walz). All media was supplemented with 100ug/ml Kanamycin. Cultures were maintained in exponential growth for at least 5 doublings before analysis.

2.3.2 Low CO_2 cultures

Low CO_2 cultures were grown in 250ml Erlenmeyer flasks in 50ml of BG-11 supplemented with 100ug/ml Kanamycin, and 10mM bicarbonate. Cultures were grown in an incubator set to 28.5ºC, which due to the arrangement and heat from growing lights resulted in a temperature of 31º C± 0.5 for 150uE cultures, and 29.5º C ± 0.5 for 50uE cultures. Light was provided by 2 or 4 overhead T5 cool-white fluorescent bulbs (GE Lighting) for 50uE and 150uE conditions respectively. Precise light intensity was achieved by culture placement, and height of the bulbs. Light intensity was measured with a US-SQS/L quantum sensor (Walz). Cultures were maintained in exponential growth for at least 5 doublings before analysis.

2.4 Growth rate determination

Growth rate was tracked by measuring cell density 1-3 times per day. At each timepoint a 1ml aliquot was removed and filtered through a 30um filter. The cell concentration was then measured on a BD Accuri C6 flow cytometer. The natural log of the cell density was plotted against time in days. The slope of the resulting curve gave the exponential growth rate. With each cell density measurement, the flow cytometer simultaneously measured the forward scatter pulse area (FSC-A) and the chlorophyll/phycobilisome relative fluorescence per cell using an excitation laser of 640nm and an emission filter of 675nm ± 25nm.

3 Results

3.1 Growth rate when Δslr1719 is cultivated without kanamycin

Because Δslr1719 is unsegregated, it is possible for it to genetically revert to having more native gene copies of the slr1719 loci, and alter its phenotype. While we have not demonstrated this reversion genetically, phenotypically we see a rapid change in the growth rate of Δslr1719 if it is removed from the selection pressure of kanamycin (Figure 4).

This finding emphasized that any physiology performed on this unsegregated strain needed to occur with kanamycin present in the growth media. In order to eliminate the possibility that the phenotype is from the presence of kanamycin in the media rather than from the reduced functional copies of slr1719, a strain was constructed that was essentially the WT strain, but with a kanamycin cassette added to a neutral site (called WT-Kan). All comparisons were made to this strain rather than to WT.

3.2 Growth Rate

There was no statistical difference in growth rate between Δslr1719 and WT-Kan strains in high CO_2 regardless of light intensity. In low CO_2 however Δslr1719 grew at a statistically slower rate for both light intensities (Figure 5).

3.3 Forward scatter pulse area

Forward scatter pulse area, or FSC-A is a measurement performed by the flow cytometer, and has been correlated to dry weight biomass and size [17]. In Figure 6 we see that in both light conditions the cultures have a higher FSC-A in low CO_2 compared to high CO_2. It appears that in low CO_2 150uE cultures the Δslr1719 culture has a slightly higher average FSC-A than WT-Kan, especially at the beginning of the growth curve.

3.4 FL4-A normalized to size

FL4-A is a measure of the fluorescence that occurs upon excitation of a red laser. In *Synechocystis* this includes both chlorophyll A fluorescence, and phycobilisome fluorescence. Because fluorescence should increase with cell size (bigger cell, more pigments) a narrow window for size was drawn to normalize fluorescence. Note that because of the FSC-A difference between low and high CO_2 (Figure 6) different normalization windows had to be drawn, so the resulting Fl4-A cannot be compared between each other.

For high and low CO_2 we see a fairly flat trend in the normalized FL4-A signal with 50uE samples (Figure 7). In the 150uE samples we see a gradual increase in normalized FL4-A, which could indicate more pigments are being added as the culture becomes more cell shaded. Δslr1719 has a slightly higher normalized FL4-A value compared to WT-Kan in the high CO_2, 150uE growth condition (Figure 7).

4. Discussion

The experiment performed here shows that there are no growth rate difference between WT-Kan and Δslr1719 in high CO_2 conditions, but in low CO_2 conditions, regardless of light intensity, there is a reduction in growth rate. This shows that Δslr1719 primarily has a high CO_2/ low CO_2 growth rate phenotype, rather than a light intensity phenotype. It is possible that light intensity exacerbates low CO_2 conditions, but is not the primary phenotype. This finding supports the hypothesis that slr1719 is involved in cyclic electron flow. Because cyclic electron flow provides additional ATP to energize CO_2 transport, removing a protein involved with cyclic electron flow would be expected to show a phenotype in low CO_2 conditions, but not in high CO_2 conditions.

An unexpected observation was that in both WT-Kan and Δslr1719, low CO_2 growth conditions were correlated with bigger cells (as indicated by higher FSC-A values, and supported by organic carbon/cell). It is possible that an increase in cell size is a response to a low CO_2 environment.

5. Conclusion

The results presented here support the hypothesis that the putative NADPH-quinone reductase slr1719 may be involved in cyclic electron flow. Partial knock outs of this gene result in poor growth exclusively in low CO_2 conditions, with no growth rate reduction in high CO_2 conditions. Because of the central role cyclic electron flow has in providing the ATP necessary for CO_2 transport in carbon stressed conditions, this supports the hypothesis that slr1719 is involved in cyclic electron flow, but still does not explain how slr1719's role is different from the NDH-1 complex, and does not eliminate the hypothesis about involvement in glucose metabolism.

Future experiments could use more *in vivo* studies of p700 re-reduction under different growth conditions to show that the capacity for cyclic electron flow changes based on whether cyclic electron transport is induced. We would expect more rapid re-reduction of p700 under conditions such as high salt, or low CO_2. Additionally, it would be interesting to see if there is a phenotypic difference of the Δslr1719 strain in fluctuating light. If slr1719 is involved in oxidation of NADPH during light transitions to activate glucose metabolism, then deletion of slr1719 could help prevent unnecessary activation of the TCA cycle and OPP cycle, which we suggested was possible in chapter 2 in the fluctuating light condition.

REFERENCES

[1] I.V. Elanskaya, E.A. Chesnavichene, C. Vernotte, C. Astier, Resistance to nitrophenolic herbicides and metronidazole in the cyanobacterium Synechocystis sp. PCC 6803 as a result of the inactivation of a nitroreductase-like protein encoded by drgA gene, FEBS letters, 428 (1998) 188-192.

[2] M. Matsuo, T. Endo, K. Asada, Isolation of a Novel NAD(P)H-Quinone Oxidoreductase from the Cyanobacterium Synechocystis PCC6803, Plant Cell Physiol., 39 (1998) 751-755.

[3] B.H. Park, S.M. Fikrig, E.M. Smithwick, Infection and Nitroblue-Tetrazolium Reduction by Neutrophils: A Diagnostic Aid, The Lancet, 292 (1968) 532-534.

[4] M. Matsuo, T. Endo, K. Asada, Properties of the respiratory NAD(P)H dehydrogenase isolated from the cyanobacterium Synechocystis PCC6803, Plant & cell physiology, 39 (1998) 263-267.

[5] I.V. Elanskaya, V.A. Toporova, V.G. Grivennikova, E.M. Muronets, E.P. Lukashev, K.N. Timofeev, Reduction of photosystem I reaction center by recombinant DrgA protein in isolated thylakoid membranes of the cyanobacterium Synechocystis sp. PCC 6803, Biochemistry (Moscow), 74 (2009) 1080-1087.

[6] K. Takeda, M. Iizuka, T. Watanabe, J. Nakagawa, S. Kawasaki, Y. Niimura, Synechocystis DrgA protein functioning as nitroreductase and ferric reductase is capable of catalyzing the Fenton reaction, The FEBS journal, 274 (2007) 1318-1327.

[7] J. Ooyabu, M. Ohtsuka, Y. Kashino, H. Koike, K. Satoh, The expression pattern of NAD(P)H oxidases and the cyclic electron transport pathway around photosystem I of Synechocystis sp. PCC6803 depend on growth conditions, Bioscience, biotechnology, and biochemistry, 72 (2008) 3180-3188.

[8] I.V. Elanskaya, K.N. Timofeev, V.G. Grivennikova, G.V. Kuznetsova, L.N. Davletshina, E.P. Lukashev, F.V. Yaminsky, Reduction of photosystem I reaction center in DrgA mutant of the cyanobacterium Synechocystis sp. PCC 6803 lacking soluble NAD(P)H:quinone oxidoreductase, Biochemistry. Biokhimiia, 69 (2004) 445-454.

[9] I.V. Karandashova, M.E. Semina, E.M. Muronets, I.V. Elanskaya, Expression of drgA gene encoding NAD(P)H:quinone-oxidoreductase in the cyanobacterium Synechocystis sp. PCC 6803, Russian Journal of Genetics, 42 (2006) 872-876.

[10] M.E. Semina, E.D. Abramenko, E.M. Muronetz, Y.V. Titaeva, K.N. Timofeev, I.V. Elanskaya, The molecular mechanism of menadione resistance in the Synechocystis sp. PCC 6803 cyanobacterium, Moscow University Biological Sciences Bulletin, 62 (2007) 7-10.

[11] A. Grossman, R.E. McGowan, Regulation of glucose 6-phosphate dehydrogenase in blue-green algae, Plant physiology, 55 (1975) 658-662.

[12] K. Yoshikawa, T. Hirasawa, K. Ogawa, Y. Hidaka, T. Nakajima, C. Furusawa, H. Shimizu, Integrated transcriptomic and metabolomic analysis of the central metabolism of Synechocystis sp. PCC 6803 under different trophic conditions, Biotechnology Journal, 8 (2013) 571-580.

[13] J.W. Cooley, W.F. Vermaas, Succinate dehydrogenase and other respiratory pathways in thylakoid membranes of Synechocystis sp. strain PCC 6803: capacity comparisons and physiological function, Journal of bacteriology, 183 (2001) 4251-4258.

[14] N. Battchikova, M. Eisenhut, E.M. Aro, Cyanobacterial NDH-1 complexes: novel insights and remaining puzzles, Biochimica et biophysica acta, 1807 (2011) 935-944.

[15] P.G. Falkowski, J.A. Raven, Aquatic Photosynthesis, 2nd ed., Princeton University Press, Princeton, 2007.

[16] P. Zhang, N. Battchikova, T. Jansen, J. Appel, T. Ogawa, E.M. Aro, Expression and functional roles of the two distinct NDH-1 complexes and the carbon acquisition complex NdhD3/NdhF3/CupA/Sll1735 in Synechocystis sp PCC 6803, The Plant cell, 16 (2004) 3326-3340.

[17] B.R. Robertson, D.K. Button, A.L. Koch, Determination of the Biomasses of Small Bacteria at Low Concentrations in a Mixture of Species with Forward Light Scatter Measurements by Flow Cytometry, Appl. Environ. Microbiol., 64 (1998) 3900-3909.

[18] J. Williams, Construction of specific mutations in photosystem II photosynthetic reaction center by genetic engineering methods in Synechocystis 6803, Cyanobacteria1988, pp. 766-778.

[19] A. Kunert, M. Hagemann, N. Erdmann, Construction of promoter probe vectors for Synechocystis sp. PCC 6803 using the light-emitting reporter systems Gfp and LuxAB, Journal of Microbiological Methods, 41 (2000) 185-194.

[20] X. Zang, B. Liu, S. Liu, K.K.I.U. Arunakumara, X. Zhang, Optimum conditions for transformation of Synechocystis sp. PCC 6803.pdf, The Journal of Microbiology, 45 (2007) 241-245.

[21] M. Griese, C. Lange, J. Soppa, Ploidy in cyanobacteria, FEMS microbiology letters, 323 (2011) 124-131.

[22] J.J. Eaton-Rye, The construction of gene knockouts in the cyanobacterium Synechocystis sp. PCC 6803.pdf, Methods in Molecular Biology, 274 (2004) 309-324.

[23] J.C. Goldman, Bioengineering aspects of inorganic carbon supply to mass algal cultures, Third Ann. Biomass Conf. Energy Biomass, Golden Colorado, SERI/TP-33-285, US Dept Energy, 1979, pp. 25-32.

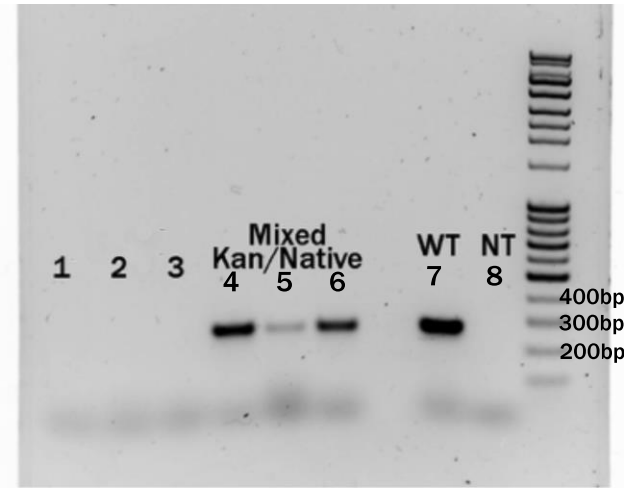

Figure 1: PCR result shows that WT-Kan is fully segregated. Lanes 1-3 show no band, indicating that there is no native (undisrupted by kanamycin cassette insertion) gene present. Lanes 4-6 were inoculated with unsegregated strains. Because the native gene still persists, the 369bp native fragment was amplified. WT control confirms the PCR works, and the No Template NT lane shows that the reagents are not contaminated with genomic DNA.

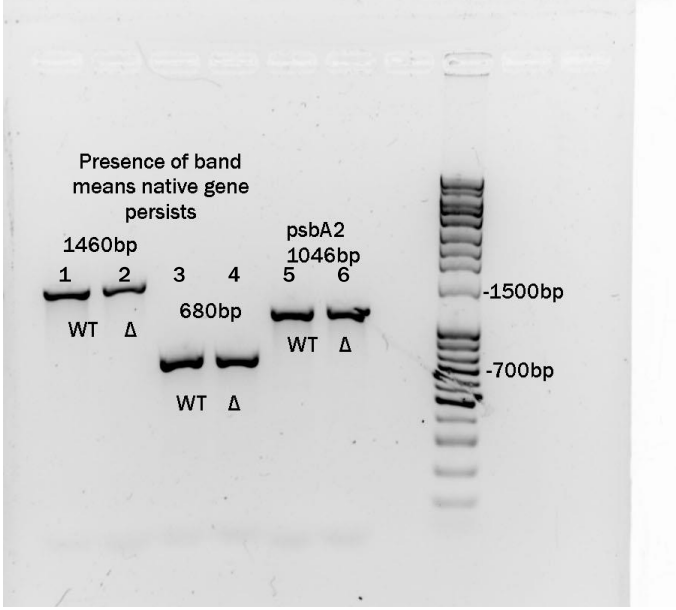

Figure 2: PCR result shows that Δslr1719 is not fully segregated. Lanes 1 and 2 use primers that are outside of the kanamycin interrupted area. These primers can amplify the native gene if it is present. As can be seen in the first two lanes the WT band, and the Δslr1719 band both amplified the 1460bp native gene. The center two lanes use an alternative screening technique that uses a primer outside the kanamycin interrupted region, and another primer that binds to the juncture where the kanamycin cassette is added. In a fully segregated mutant, this juncture would be interrupted by kanamycin, and thus the primer would not have a template to anneal with, and no product would amplify.

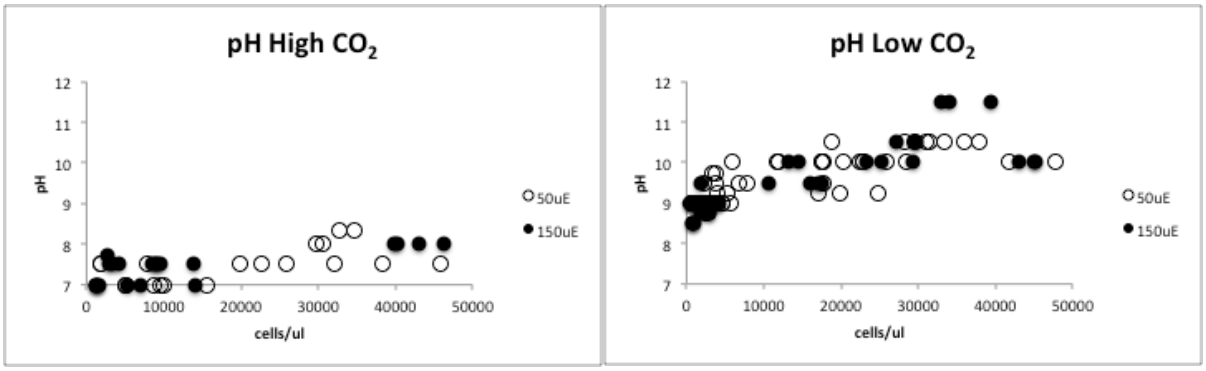

Figure 3: Shows pH measured across multiple biological replicates in the four conditions: High CO_2 50uE, High CO_2 150uE, Low CO_2 50uE, Low CO_2 150uE. WT-Kan and Δslr1719 cultures are combined, as they showed no difference in their pH changes over time. Cell density is used as a proxy for culture age. At higher densities, later in the growth curve, the culture as a whole is consuming more CO_2. Thus, if not enough gas exchange is available the pH increases, which indicates a low CO_2 environment. In the High CO_2 environment pH remains relatively constant at all cell densities, but in the low CO_2 condition pH increases with cell density.

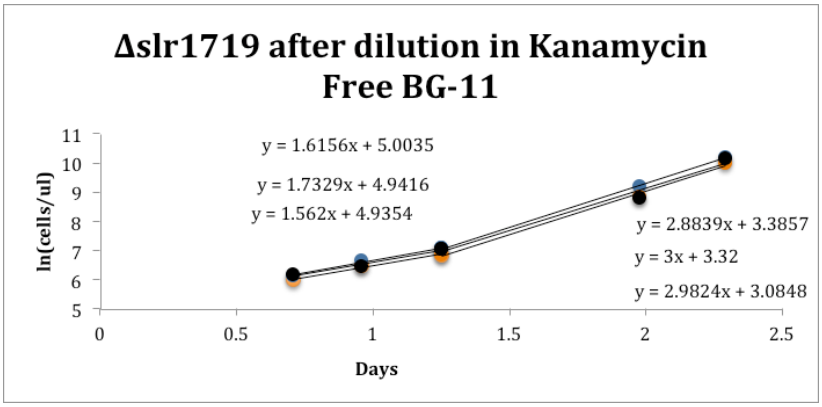

Figure 4: A culture of Δslr1719 that was being constantly maintained on 100ug/ml Kanamycin, and had a growth rate of ~1.5/day in 150uE in shake flasks. This culture was split and diluted into three biological replicates in BG-11 without Kanamycin. The graph above shows that after about 1.25 days the growth rate increased from ~1.6/day to ~3/day, which is similar to the growth rate of WT.

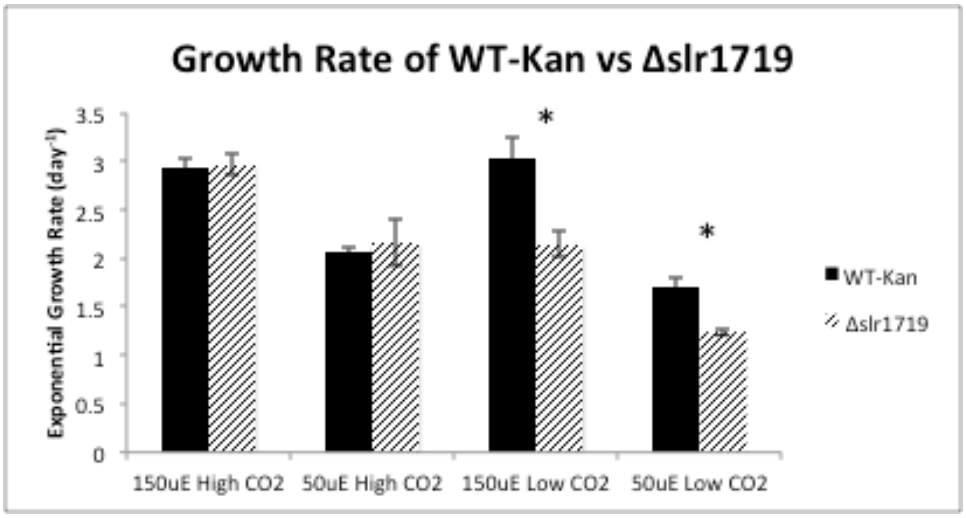

Figure 5: Shows average growth rates of WT-Kan and Δslr1719 in High CO_2 50uE, High CO_2 150uE, Low CO_2 50uE, and Low CO_2 150uE. Results indicate that there is no difference in growth rate between the two strains in high CO_2, but there is a significant decrease in growth rate in low CO_2 when slr1719 is knocked out. Error bars are ± 1 standard deviation from the mean, n=4 to 9. * Indicates statistical significance $p<0.05$ students t. test.

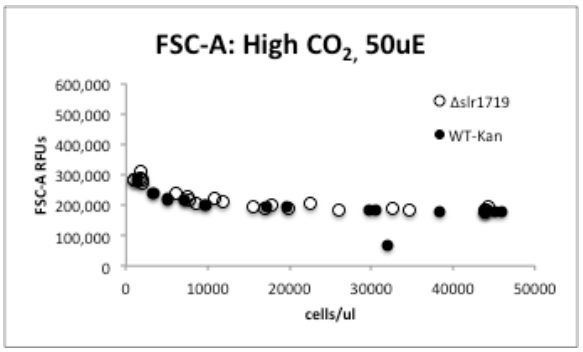

A.

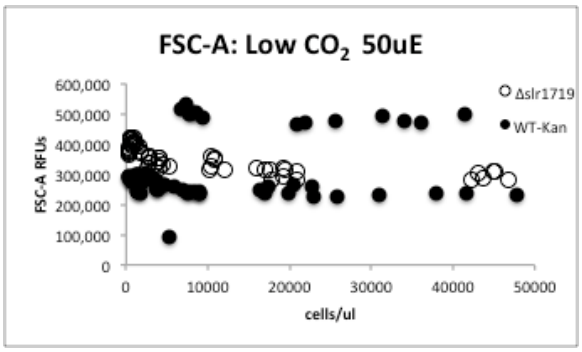

B.

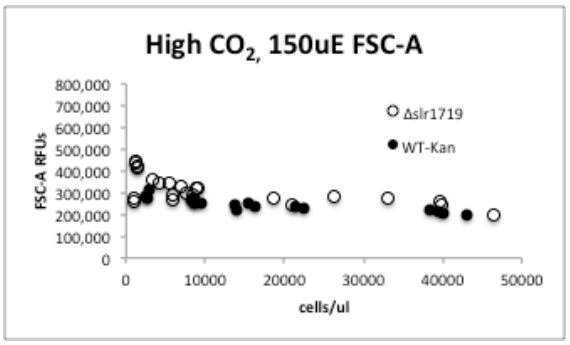

C.

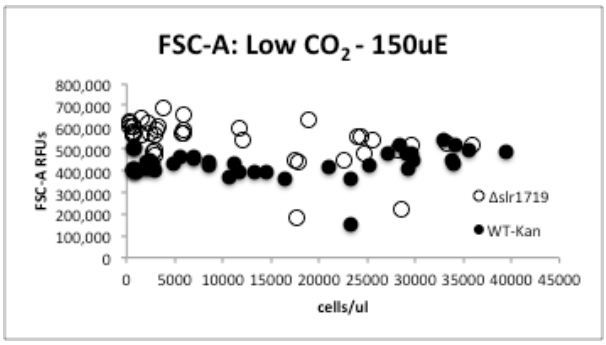

D.

Figure 6: Shows FSC-A measurements for High CO_2 50uE (A) Low CO_2 50uE (B) High CO_2 150uE (C) and Low CO_2 150uE (D). Cell density is used an indicator of culture age.

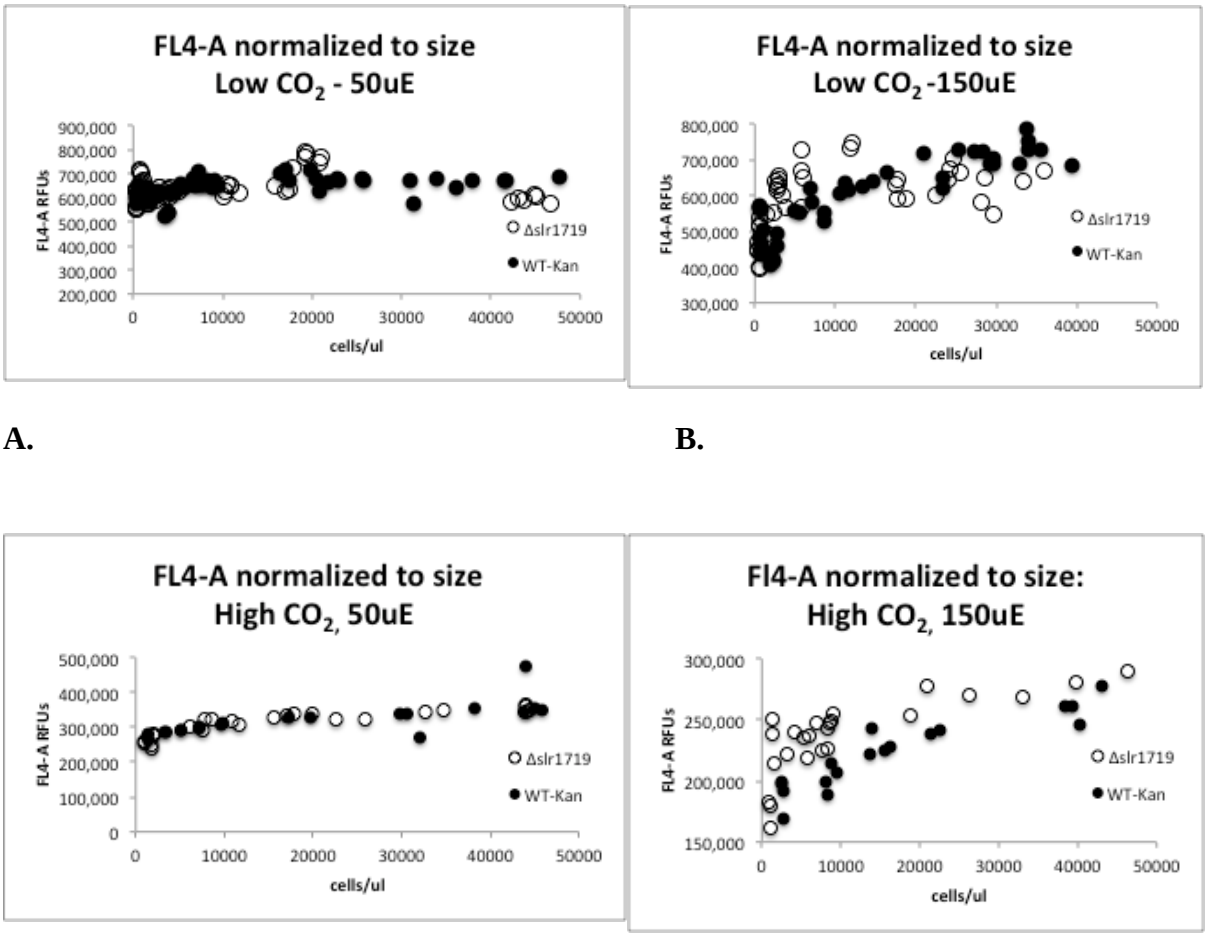

Figure 7: Shows FL4-A normalized to a narrow FSC-A window for Low CO_2 50uE (A) Low CO_2 150uE (B) High CO_2 50uE (C) and High CO_2 150uE (D). Cell density is used an indicator of culture age.

Table 1: PCR conditions used to determine if WT-Kan and Δslr1719 are fully segregated.

	Temp Cº	Time (s)
	95	180
{	95	30
30X {	48	30
{	72	10
	72	60
	4	∞

WT-Kan Native Gene PCR

369bp = native gene

	Temp Cº	Time (s)
	95	300
{	95	30
30X {	47	30
{	72	60
	72	180
	4	∞

Δslr1719 Native Gene PCR

1424bp = native gene